

# POLITECNICO DI MILANO

School of Industrial and Information Engineering

Master of Science in  
Chemical Engineering



Archimede Concentrated Solar Power Plant Dynamic Simulation: Control systems,  
Heat Transfer Fluids and Thermal Energy Storage

Supervisor: Prof. Flavio MANENTI

Master of Science Thesis by:

Georgios Rekkas Ventiris Matr. 895969

Academic Year 2018-2019

Georgios Rekkas Ventiris | Master of Science Thesis in Chemical Engineering,  
Politecnico di Milano.  
© Copyright 2019.

---

Politecnico di Milano:  
[www.polimi.it](http://www.polimi.it)

Scuola di Ingegneria Industriale e dell'Informazione:  
[www.ingindinf.polimi.it](http://www.ingindinf.polimi.it)

# Acknowledgments

I would like to express my appreciation to Mr. Prof. Manenti and his lab team for giving me the opportunity to work with them on this thesis. We had an excellent collaboration and they helped me expand my knowledge on the really interesting topic of dynamic simulation.

These two years in Milan have been great. I was really lucky to make good friends who helped and supported me a lot, throughout this experience. I thank each and every one of them.

Last but not least I would like to thank my family. Of course, a small paragraph is not enough to express my gratitude, but I hope they know that their love and support was priceless.

*Milano, 2019*

G. R. V.



*To my family.*



# Contents

<b>Introduction</b>	<b>1</b>
<b>1 Concentrated Solar Power</b>	<b>5</b>
1.1 The Present and the Future in numbers . . . . .	5
1.2 State of the Art . . . . .	8
1.2.1 Solar Power Tower . . . . .	9
1.2.2 Linear Fresnel Reflector . . . . .	11
1.2.3 Parabolic Dish Collector . . . . .	12
1.2.4 Parabolic Trough Collector . . . . .	13
1.3 Thermal Energy Storage . . . . .	16
1.3.1 Two-tank Storage . . . . .	22
1.3.2 Single-tank Storage . . . . .	25
1.4 Heat Transfer Fluid . . . . .	29
1.4.1 Thermal Oil . . . . .	29
1.4.2 Molten Salt . . . . .	30
1.4.3 Innovative materials . . . . .	31
<b>2 The Archimede Concentrating Solar Power Plant</b>	<b>35</b>
<b>3 Dynamic Simulation with DYNsIM</b>	<b>43</b>
3.1 ACSP plant with two-tank direct TES . . . . .	48
3.1.1 Control System . . . . .	48
3.1.2 Solar Salt as HTF . . . . .	52
3.1.3 Therminol VP-1 as HTF . . . . .	63
3.2 ACSP plant with two-tank indirect TES . . . . .	66
3.2.1 Control System . . . . .	69
3.2.2 Performance . . . . .	71
3.3 An innovative design . . . . .	79
<b>Conclusions and Future Development</b>	<b>81</b>
<b>Acronyms</b>	<b>83</b>
<b>Symbols</b>	<b>85</b>
<b>Bibliography</b>	<b>87</b>





# List of Figures

1.1	CSP global capacity, by Country and Region, 2008-2018 . . . . .	6
1.2	Purpose of CSP plants and their respective percentage . . . . .	6
1.3	Growth of CSP production by Region . . . . .	7
1.4	The major components of a Concentrated Solar Energy plant . . . . .	9
1.5	The Solar Power Tower . . . . .	11
1.6	Profile of a Fresnel Lens . . . . .	12
1.7	The Linear Fresnel Reflector . . . . .	12
1.8	The Parabolic Dish Collector . . . . .	13
1.9	The Parabolic Trough Collector . . . . .	14
1.10	SEGS: A Parabolic Trough Collector CSP plant . . . . .	15
1.11	Percentage of TES system in CSP plants . . . . .	17
1.12	Scheme of an oil plant with integrated TES and FBS . . . . .	17
1.13	Scheme of a CSP plant with 2-tank direct TES . . . . .	22
1.14	Dynamic behavior of the level of the tanks in the two-tank direct storage . . . . .	23
1.15	Scheme of a CSP plant with 2-tank indirect TES . . . . .	24
1.16	Scheme of a CSP plant with single-tank (thermocline) TES . . . . .	25
1.17	Dynamic behavior of the temperature of inlet and outlet stream of a thermocline during charging phase . . . . .	26
1.18	Dynamic behavior of the temperature of inlet and outlet stream of a thermocline during discharging phase . . . . .	26
1.19	Temperature distribution of different HTFs in a single-tank storage . . . . .	27
2.1	Scheme of the Archimede Concentrating Solar Power (ACSP) plant . . . . .	36
2.2	Scheme of the power block of the ACSP plant . . . . .	38
2.3	A digital maquette of the ACSP plant . . . . .	41
2.4	A picture of the two tanks and the solar field of the ACSP plant . . . . .	41
3.1	Comparison of Steady State and Dynamic model scopes . . . . .	44
3.2	Flowsheet of DYNOSIM Dynamic Simulation . . . . .	46
3.3	Description of a chemical process . . . . .	48
3.4	General structure of feedback and feedforward control systems . . . . .	50
3.5	The control system of the ACSP plant . . . . .	51
3.6	The behavior of the controller PID2 during the first minutes of the simulation . . . . .	55
3.7	The behavior of the controller PID3 during the first minutes of the simulation . . . . .	55

3.8	The power output of the plant during the first minutes of the simulation	56
3.9	The levels of the two tanks of the plant during the first minutes of the simulation . . . . .	57
3.10	Operation of the plant during the night: flowsheet . . . . .	58
3.11	Solar Field input/output temperatures and DNI during sunrise . . .	59
3.12	The behavior of the controller PID2 during sunrise . . . . .	60
3.13	The behavior of the controller PID3 during sunrise . . . . .	60
3.14	The power output of the plant during sunrise . . . . .	61
3.15	Operation of the plant during the day: flowsheet . . . . .	62
3.16	Operation of the plant during the night with Therminol VP-1: flowsheet	64
3.17	Scheme of the ACSP plant with two-tank indirect TES . . . . .	66
3.18	The control system of the ACSP plant with two-tank direct TES . .	70
3.19	The behavior of the controller PID4 during the first 30 minutes of the simulation . . . . .	72
3.20	The behavior of the controller PID3 during the first 30 minutes of the simulation . . . . .	72
3.21	The power output of the plant with two-tank indirect TES during the first minutes of the simulation . . . . .	73
3.22	Operation of the ACSP plant with two-tank indirect storage during the night: flowsheet . . . . .	74
3.23	Indirect TES: Solar Field input/output temperatures and DNI during sunrise . . . . .	76
3.24	Indirect TES: The behavior of the controller PID3 during sunrise . .	76
3.25	Indirect TES: The power output of the plant during sunrise . . . .	77
3.26	Indirect TES: Operation of the plant during the day: flowsheet . . .	78
3.27	Indirect TES: An innovative design: flowsheet . . . . .	79

# List of Tables

1.1	Electricity from CSP plants as shares of total electricity consumption.	7
1.2	Representative features of the different CSP technologies.	10
1.3	Comparison between TES and FBS for different PTC plant configurations.	16
1.4	Design criteria for a TES of a CSP plant.	19
1.5	Review of the two-tank TES.	24
1.6	Review of the single-tank (thermocline) TES.	28
1.7	Molten Salt as HTF: comparison with Thermal Oil.	31
1.8	Thermal and physical properties of common HTFs.	33
2.1	Main design parameters of the ACSP plant.	39
2.2	Temperature of the solar salt at various parts of the ACSP plant.	41
3.1	An overview of the controllers used in the ACSP two-tank direct TES plant.	52
3.2	Parameters for the motors.	52
3.3	Parameters for the valves.	52
3.4	Parameters for the controllers.	57
3.5	Temperature of the HTFs at various parts of the ACSP plant with two-tank indirect storage.	68
3.6	Main design parameters of the ACSP plant with two-tank indirect TES.	69
3.7	Parameters for the controllers (ACSP with two-tank indirect TES).	70



# Sommario

Negli ultimi due decenni, ci sono stati molti sforzi verso la disintossicazione delle società moderne da combustibili fossili. Sono state applicate politiche ambientali più rigorose e fonti alternative di energia sono state esaminate e introdotte nella nostra vita quotidiana. Una di quelle fonti è il sole, che fornisce enormi quantità di energia alla terra. Un modo per approfittare e raccogliere una parte di questa energia è via la Energia Solare Concentrata. È al giorno d'oggi una tecnologia matura e promettente.

In questa tesi, il caso specifico del impianto di Energia Solare Concentrata Archimede in Sicilia è ricercato. A cause della natura discontinua di energia solare, la tesi si concentra su la simulazione dinamica del impianto in modo da trovare un sistema di controllo ragionevole e valutare la sua prestazione. Inoltre, alcuni cambiamenti strutturali e operativi sono state apportati. Un nuovo Fluido Termovettore è stato introdotto e testato con simulazioni dinamiche. Il accumulo di energia termica a due serbatoi indiretti con un nuovo sistema di controllo è valutato per l'impianto. L'obiettivo è produrre risultati per le diverse configurazioni che saranno confrontati per ottenere alcuni conclusioni utili per quanto riguarda la funzione generale dei Fluidi Termovettori e dei Sistemi di Accumulo.

**Parole chiave:** Energia Solare Concentrata, Impianto di Energia Solare Concentrata Archimede, DYNMIM Dynamic Simulation, Fluido Termovettore, Sistema di Accumulo di Energia Termica

# Abstract

During the last two decades there have been many efforts towards the detoxification of the modern societies from fossil fuels. Stricter environmental polices have been applied and alternative sources of energy have been examined and introduced in our everyday lives. One of these sources is the sun, which provides enormous amounts of energy to the earth. A way to take advantage and harvest a part of this energy is through the Concentrated Solar Power. It is nowadays a really mature and promising technology.

In this thesis work the specific case of the Archimede concentrating solar power plant located in Sicily, Italy is investigated. Due to the discontinuous nature of solar energy, the present thesis focuses on the dynamic simulation of the plant in order to find a reasonable control system for the plant and characterize its performance. In addition, some operational and structural changes are made to the plant. A new Heat Transfer Fluid is introduced and tested through dynamic simulations. Also, the case of the two-tank indirect thermal energy storage with a new control system is investigated for the specific plant. The goal is to produce results for the different configurations that will be compared in order to get some useful conclusions regarding the general function of the different Heat Transfer Fluids and Thermal Energy Storage systems used.

**Keywords:** Concentrated Solar Power, Archimede Concentrated Solar Power Plant, DYNOSIM Dynamic Simulation, Heat Transfer Fluid, Thermal Energy Storage

# Introduction

In the modern world, quality of life and human development are strongly connected to energy [1]. As societies become denser and more active, more energy is needed to cover their needs. Annual reports show that the global energy consumption has not stopped increasing during the last 20 years [2], but so did the CO<sub>2</sub> emissions related to energy generation [3]. The link between these two phenomena is known: fossil fuels. The dependence of the energy sector to fossil fuels, such as coal, natural gas and oil, was always strong and it still is. But being the dominant source of local air pollution and emitter of CO<sub>2</sub> and other greenhouse gases [4], fossil fuels have been the target of many of the environmental policies that were imposed around the world during the last years [5]. So, facing the diptych challenge of more energy production but less emissions, governments have to use cleaner and more sustainable energy sources in order to meet the demands.

Sunlight is the largest available carbon-neutral energy source and it provides the Earth with more energy in 1 hour than it is consumed globally in an entire year [6]. Indeed, there has been a lot of research towards the ways to harvest solar energy for power generation. Solar energy still accounts, though, for a small portion of the global energy production [3]. One of the technologies that has been under investigation for several years and is now really mature, is the concentrated solar power (CSP). The principle of the CSP is simple: mirrors focus the sunlight -and consequently transfer energy- to a carrier fluid: the Heat Transfer Fluid (HTF). The HTF, with its increased temperature, can be used to power a turbine or a heat engine to generate electricity. One of the biggest advantages of the CSP technologies is that it can be coupled with Thermal Energy Storage (TES), in order to store energy and produce a sufficient and constant power output during the night or when the solar irradiation is not enough [7].

A CSP plant includes many different components and parameters that have to be taken into consideration in order to function properly and achieve the expected performance. First of all, various CSP technologies exist that differ on the way that the solar irradiation is directed to the receiver. The most widely used is the Parabolic Through Collector (PTC) [8, 9], which consists of several troughs placed in parallel, forming the solar field. The choice of the HTF is, also, crucial. For most of the industrial applications water is the suitable HTF [10] but in the CSP systems thermal oils, organics and molten salts can be introduced, every one with their own characteristics and advantages. Depending on the desired power output of the plant, the use or not of a TES system should be decided. Different configurations exist: single tank or two-tank storage with direct or indirect heat exchange can be used. Of course, another really important part of the function of the plant is the

control system: the correct choice and tuning of the controllers will reassure the smooth operation of the process and a steady output, which is vital, especially in the case of electricity production.

In this thesis work, an effort was made to investigate the dynamic behavior of an existing CSP plant, under different TES systems, HTFs as well as control schemes. The said plant is the Archimede CSP plant, located in Siracusa, Italy. It uses PTCs, a two-tank direct TES and molten salts (eutectic mixture of KNO<sub>3</sub> and NaNO<sub>3</sub>) as HTF and it is designed to produce an output of 4.8MW. The dynamic evaluation was carried out using a dynamic process simulator program called DYNMOS Dynamic Simulation<sup>©</sup>, which is used by over 100 plants worldwide to satisfy their process design, operator training and operational analysis requirements [11]. Initially, a control system was developed and tested for the plant. Then, the performance of the plant was simulated with a different HTF: Therminol VP-1<sup>©</sup>, which is an organic HTF with high thermal stability. A different TES system consisting of 2 tanks but indirect heating was, also, tested. The results of all the above simulations are discussed, always with respect to the original scheme and function of the Archimede CSP plant.



## Outline

This thesis work is structured in the following way:

**In the first chapter** an introduction to the Concentrated Solar Power is made. Some statistics are presented that reveal the current situation and the future trend of this field. The main categories of Concentrated Solar Power Plants are analyzed, focusing on their current applicability. Then, the Thermal Energy Storage is discussed into details, the theoretical advantages and disadvantages of the different Thermal Energy Storage systems are presented. The same procedure is followed in the presentation of the main Heat Transfer Fluids that are used in the Concentrated Solar Energy Plants.

**In the second chapter** the Archimede Concentrated Solar Plant is introduced. This is the plant on which the dynamic simulations will be performed in the following chapter. Its everyday way of operation is analyzed, along with the characteristics of its equipment. The main parameters of the plant that will be included in the simulations are summed up in useful tables.

**The third chapter** includes the results of the dynamic simulations. Firstly, a control system for the Archimede Concentrated Solar Power Plant is presented. Its performance is tested via dynamic simulations and the results are cited in the form of graphs. The graphs are analyzed thoroughly. The results of another dynamic simulation are commented, where a new Heat Transfer Fluid is introduced into the system. Lastly, the configuration of the plant is changed. A new Thermal Energy Storage System is tested. A control system is developed for this new configuration and the results of the dynamic simulation are presented and compared to the results of the original Archimede Concentrated Solar Power Plant. Also, a completely new configuration for the plant is presented as an idea for future research and development.



# Chapter 1

## Concentrated Solar Power

Within the general discussion about ways to harvest solar energy for power production, CSP stands as one of the most promising technologies, as it offers high efficiency, low operating costs and a good scale-up potential [9]. The number of patents related to CSP technologies keep increasing, depicting the progress being made in the specific field. [12]. Indeed, the International Energy Agency (IEA) has set an electricity generation target of 630GW for CSP technologies by 2050 [13], showing that the trust in CSP is profound. In the key findings of the CSP Roadmap published by IEA, it is highlighted that CSP offers firm, flexible electrical production capacity to utilities and grid operators while, also, enabling effective management of greater share of variable energy from renewable sources. It can produce significant amounts of high temperature heat for industrial processes. One of the biggest advantages of this technology is that it can help toward reaching a balance between demand and offer generation. Thanks to the possible coupling with a TES system, power can be produced during all time, in spite of weather conditions [8].

### 1.1 The Present and the Future in numbers

The first initiatives towards the use of CSP were taken in the period of 1984-1991, but then the price of oil dropped and the progress of CSP collapsed. New efforts started from 2006 onwards, mainly in Spain and USA, in response to government policies such as feed-in tariffs [14]. This is clear in the Figure 1.1 on the following page presented in an article, published by HELIOSCSP [15]. The graph, also, shows that there are new "players" in the market of CSP, such as China, United Arab Emirates, South Africa, Saudi Arabia and Morocco. Generally, countries that are situated at the- so called- "Sun Belt" are suitable for CSP technology implementation . This area includes the Mediterranean, Middle East and some areas of the USA. Of course, the Direct Normal Irradiation (DNI) is the most important factor that determines the capability of an area to produce energy from CSP. Commercially viable CSP plants should maintain a DNI of at least 2000-2800 kWh/m<sup>2</sup>/yr [12]. As of March 2015, the CSP market had a total capacity of 5500MW worldwide, among which 4800MW was already operational and the rest under construction [16].

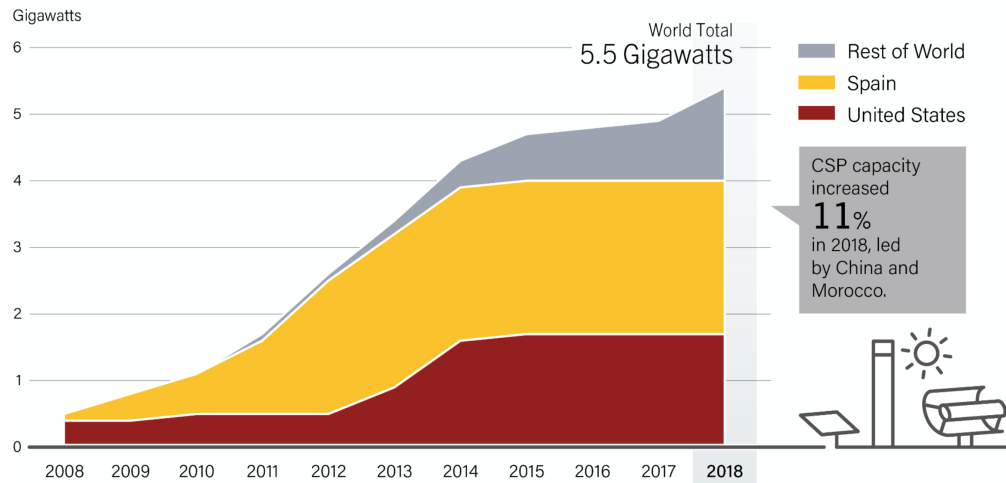


**Figure 1.1:** CSP global capacity, by Country and Region, 2008-2018 [15]

The fact that CSP is now a mature and proven technology is evident from the increasing percentage of the CSP plants that are planned to be used commercially and not just as demonstration or R&D purposes. U. Pelay et al. recently published an interesting article where 267 CSP plants all around the world are categorized according to different characteristics [9]. One of them is the purpose of the CSP plants as it can be seen in the following figure.

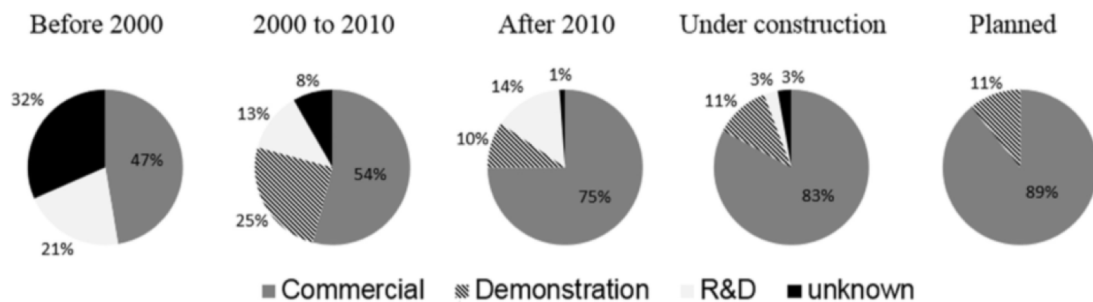


**Figure 1.2:** Purpose of CSP plants and their respective percentage [9]

The number of the commercial CSP plants has been constantly increasing, indicating that this technology has become more mature and readily available for commercialization. This, also, resulted to an increased average power of the plants, which will be over 120MW in the projects under construction.

The future of the CSP technology is really promising. Governments are relying more and more to renewable sources of energy, investing money to make them part of our everyday lives. It is calculated that renewables, in general, will contribute to an overall CO<sub>2</sub> reduction of 30% by 2050, compared to 2012 [17]. CSP plants are predicted to produce a global electricity contribution of 7% by the year 2030 and 25% by the year 2050. CSP could meet up to 6% of the world's power demand by 2030 and 12% by 2050. Even in the least optimistic scenarios, 5% to 12% of the global electricity demand will be satisfied by the CSP plants by 2050 [18]. In the following years it is expected that CSP will be an economically competitive source of bulk power generation for base-load power. The CSP Roadmap, published by the

International Energy Agency (IEA) features some interesting statistics related to the predicted future growth of the CSP technology around the world [14]. As it can be seen in the Table 1.1, in some regions, 40% of the total electricity consumption will come from CSP plants by 2050.

**Table 1.1:** Electricity from CSP plants as shares of total electricity consumption.

Countries	2020	2030	2040	2050
Australia, Central Asia <sup>1</sup> , Chile, India <sup>2</sup> Mexico, Middle East, North Africa Peru, South Africa, USA(Southwest)	5%	12%	30%	40%
USA (remainder)	3%	6%	15%	20%
Europe(imports), Turkey	3%	6%	10%	15%
Africa(remainder), Argentina, Brazil	1%	5%	8%	15%
China, Russia	0.5%	1.5%	3%	4%

1: *Afghanistan, Kazakhstan, Pakistan, Kyrgyzstan  
Tajikistan, Uzbekistan*

2: *Gujarat, Rajasthan*

The following figure, also taken from the CSP Roadmap, depicts the potential growth of CSP around the world till 2050, in terms of TWh per year.

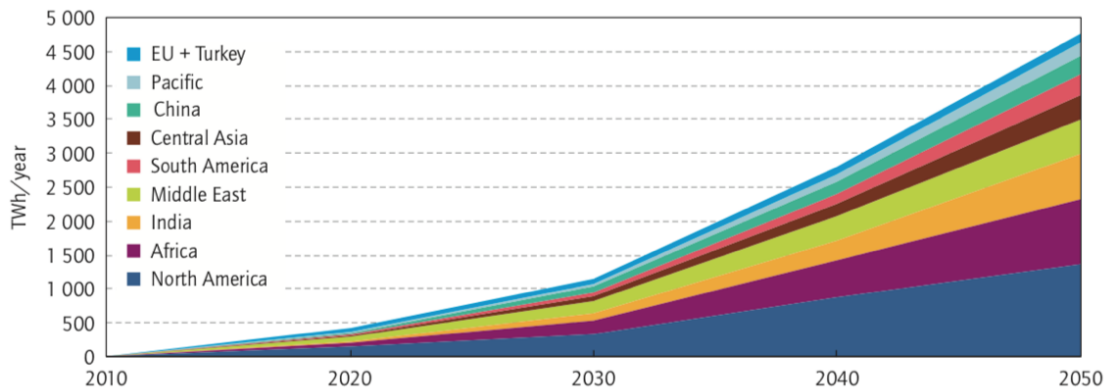


**Figure 1.3:** Growth of CSP production by Region [14]

An important factor which can increase the achievable potential of CSP is the long range transportation of electricity. If an efficient way is found in order to transfer electricity from CSP plants to regions of low DNI, then much more people will have access to electricity from renewable sources. This would promote the transfer of large amounts of solar energy from desert areas to population centers. The DESERTEC Industry Initiative aims to establish a framework for investments to supply the Middle East, North Africa and Europe with solar and wind power. The long-term goal is to satisfy a substantial part of the energy needs of the Middle East and North Africa, and meet as much as 15% of Europe's electricity demand by 2050 [14].

## 1.2 State of the Art

The technologies used in the CSP plants, basically differ on the way in which the sun irradiation is concentrated, by the focusing device, which is usually a series of mirrors, to the receiver, which contains the HTF to be heated up. A possible first level categorization can be made based on the focus type and the receiver type. The focus can be "line focus" or "point focus". The first means that the collectors track the sun along a single axis and focus irradiance on a linear/tubular receiver. In the latter, the collectors track the sun along two axes and focus irradiance at a single point receiver. This allows for higher temperature. As for the receiver, it can be "fixed", meaning that it is a stationary device that remains independent of the plant's focusing device, or "mobile", where the receiver moves together with the focusing device. Mobile receivers are generally able to collect higher amounts of energy [14].

The CSP plants currently in use or designed, have the same three major components [8]:

1. The **Solar Field**, which includes the solar concentrators that reflect and focus the direct sunlight onto the relative small area of the receiver, through which the HTF passes. It includes mirrors, receivers, support structures, the HTF, collectors, heat exchangers, pumps and piping.
2. The **Power Block**, where the heat energy received by the HTF is converted into electricity, through conventional thermodynamic cycle, such as the Rankine or Brayton Cycle. Brayton cycle engines require higher working temperatures but they can provide higher efficiency. Rankine cycle engines have an important advantage over the Brayton cycle: the heat transfer coefficients in the generator are high, allowing the use of high-energy densities and smaller receivers [19]. The hot HTF exchanges energy with water (working fluid) in multiple heat exchangers, with the ultimate goal being to turn water into steam, through a boiler. In some cases, though, the same mixture/substance can be used as both HTF and working fluid. The steam which is then superheated, can be expanded through a turbine to produce mechanical power. An electric generator converts the mechanical power into electrical power. The Power Block usually consists of the turbine, the generator, a condenser, superheater(s), pump(s), a boiler and heat exchangers.
3. The **Storage System**, where the hot and cold storage fluid is stored in order for the plant to be able to function and produce energy even in cloudy days or during the night. The Storage media, tanks and heat exchangers constitute the Storage System.

The following Figure 1.4 on the facing page illustrates the three major components of a CSP plant mentioned above, all connected together:

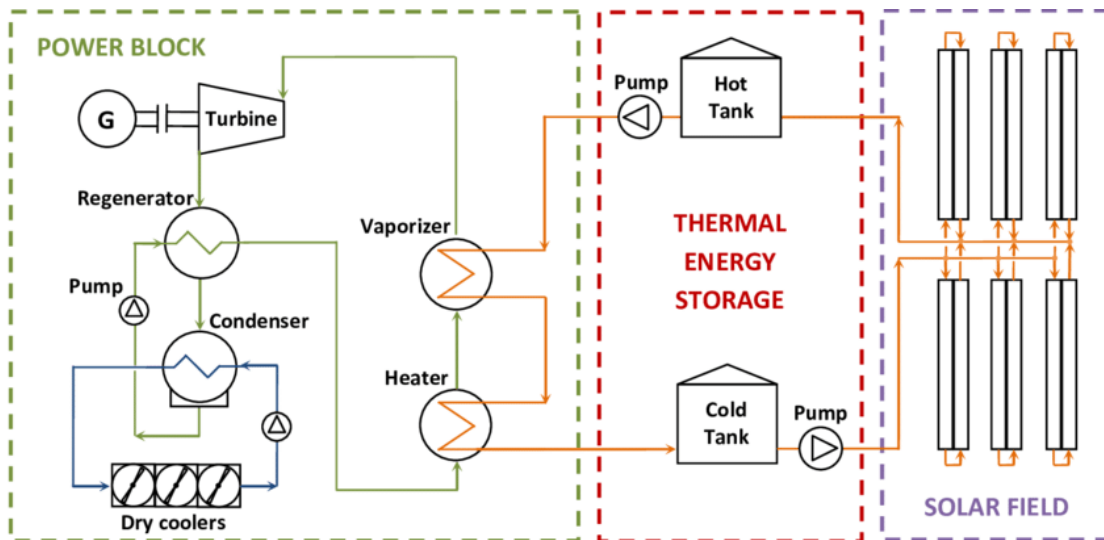


Figure 1.4: A typical scheme of a CSP plant [20]

Before starting analyzing the main technologies used for power production in CSP plants, Table 1.2 on the next page is presented that summarizes their main characteristics. Information was gathered from various different sources [7, 9, 12, 16, 19, 21–23].

The state of the art technologies in the Solar Field of CSP plants are the following [9, 12, 21, 24] :

### 1.2.1 Solar Power Tower

A Solar Power Tower (SPT) consists of an array of large flat tracking mirrors (heliostats), which are properly placed to avoid shadowing and reflect the direct beams of sunlight to a central receiver placed in an elevated support. The solar flux reaching the receiver can be as high as  $1000\text{kW}/\text{m}^2$ , providing an opportunity to achieve really high working temperatures [25].

The mirrors are the major capital investment in a SPT plant [26]. They are computer-controlled and they move to maintain a focus from dawn to dusk.

Figure 1.5 on page 11 presents a typical scheme of a SPT and a real life application of the Gemasolar SPT plant located in Sevilla, Spain. The specific plant has a capacity of 19.9MW and consists of an array of 2650 heliostats that aim solar radiation at a 140m height central tower. It can supply electricity to about 27,500 households in the south of Spain [27].

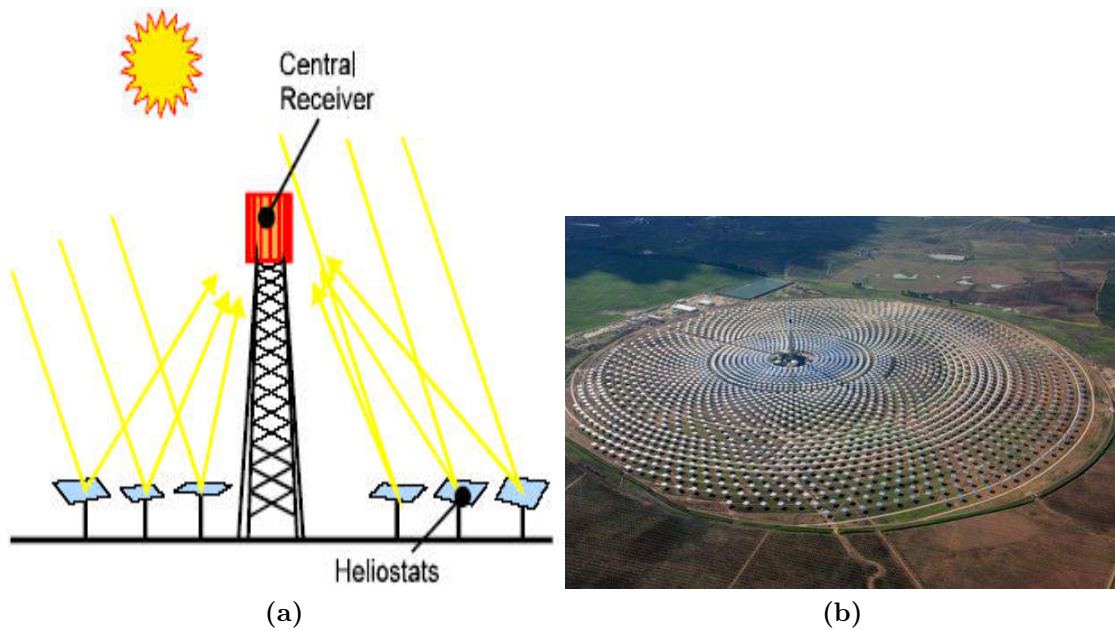
The central receiver usually contains water, which is heated up by the concentrated solar radiation. Some of the hot steam produced can be stored, while most of it goes to the power block in order to be turned into high-pressure superheated steam, able to spin the turbine and produce electricity. The power block is located at the bottom of the tower. Usually for larger heliostats, Rankine cycle engines are installed. Brayton cycle engines are, also, a good alternative leading to higher efficiency, but they require higher operating temperature. [19].

Table 1.2: Representative features of the different CSP technologies.

	Power Tower	Linear Fresnel	Parabolic Dish	Parabolic Trough
<b>Maturity</b>	Medium	Medium, pilot plants	Low, demo plants	High, commercially proven
<b>Collector sun tracking</b>	Two-axis	Single-axis	Two-axis	Single-axis
<b>Absorber type</b>	Point	Tubular	Point	Tubular
<b>Concentration ratio</b>	150-1500	10-60	100-1000 or >1000 w/ Stirling engine	10-85 290-550
<b>Operating temperature (°C)</b>	250-650	250-390	800	4-6
<b>Area requirement (m<sup>2</sup>/MWh)</b>	8-12	6-8	30-40	13-15%
<b>Annual solar-to-electric efficiency</b>	14-20%	9-13%	22-25%	30-40%
<b>Thermal efficiency</b>	30-40%	-	30-40%	14-21%
<b>Plant peak efficiency</b>	20-25%	20%	29%	424
<b>Capital cost (US\$/m<sup>2</sup>)</b>	476	234	-	0.26-0.30
<b>LCOE<sup>1</sup> without TES (US\$/kWh)</b>	>0.29	>0.35	-	

<sup>1</sup>LCOE: Levelized Cost of Electricity.





**Figure 1.5:** (a) A typical scheme of a SPT (b) Gemasolar power plant in Spain [24]

Molten salt can be used, instead, as working fluid. In this case the molten salt is heated up by the solar radiation and it transfers heat to water through a heat exchanger, in order to produce steam. SPT technology is not "mature", yet. It is mainly applied to pilot plants, with some commercial projects under construction. To reduce the financial risk and to lower the cost of electricity production, often SPT plants are advised to hybridize with a natural gas combined-cycle [28]. One of the strong advantages of SPT is that it can reach high thermodynamic efficiency thanks to the high operating temperature. On the other hand, it requires large space area and relatively high installation costs. The largest plant using such technology was established in 2014 and it is located in the United States, named Ivanpah Solar Electric Generating System, with a turbine capacity of 392MW [29].

### 1.2.2 Linear Fresnel Reflector

A Linear Fresnel Reflector (LFR) CSP plant consists of linear mirror strips as reflectors, with receivers, tracking system, steam turbine and generator. Also in this case, the reflectors are the most important component of the system and they work the same way as the Fresnel lens. A Fresnel lens replaces the curved surface of a conventional optical lens with a series of concentric grooves. These contours act as individual refracting surfaces, bending parallel light rays to a common focal length. As a result, a Fresnel lens, while physically narrow in profile, is capable of focusing light similar to a conventional optical lens but has several advantages over its thicker counterpart [30].

In the Figure 1.6 on the next page the profile of a Fresnel lens is shown. Generally, using a Fresnel lens for light collection is ideal for concentrating light onto a photovoltaic (PV) cell or to heat a surface. The overall surface area of the lens determines the amount of collected light. The Figure 1.7 on the following page presents a typical scheme of a LFR and a real life application of the LFR CSP

plant located in Sicily, Italy.

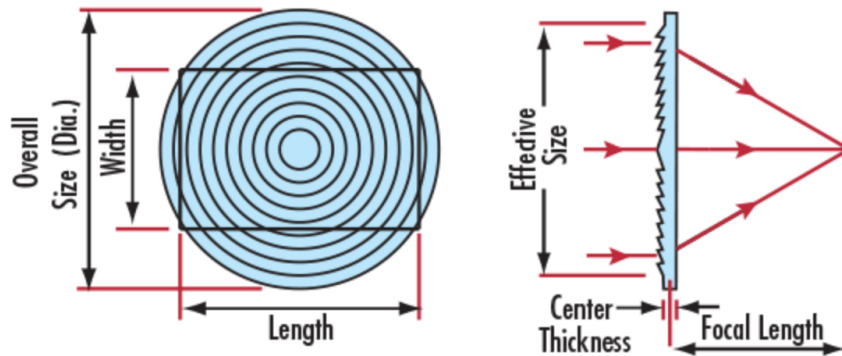


**Figure 1.6:** Profile of a Fresnel lens [31]

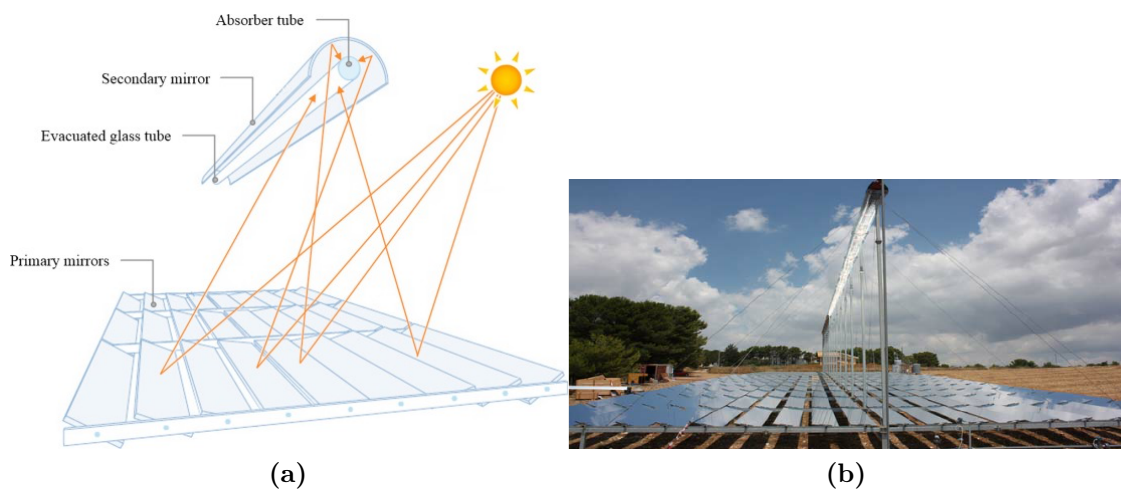


**Figure 1.7:** (a) A typical scheme of a LFR (b) LFR CSP power plant in Italy [32]

So, in the particular case of a LFR CSP plant, the sun's rays are reflected by the big surface of Fresnel lens and focused at one point, generally on to a permanent receiver on a linear tower, shaped like a long cylinder that contains a number of tubes filled with water [33]. The idea for the power generation remains the same: the water evaporates to steam which is then superheated in order to spin a turbine and generate electricity. This technology is not commercially proven, it is still used mainly for demo purposes. In 2014 the largest operational LFR CSP plant was installed in India, with a capacity of 125MW.

LFR CSP technology offers a relatively low installation cost, a more stable design compared to the SPT but it is not able to reach high operating temperatures, due to its high thermal loss coefficient.

### 1.2.3 Parabolic Dish Collector

In the plants using the Parabolic Dish Collector (PDC) technology, a parabolic concentrator in the form of a dish is used to reflect solar radiation onto a receiver

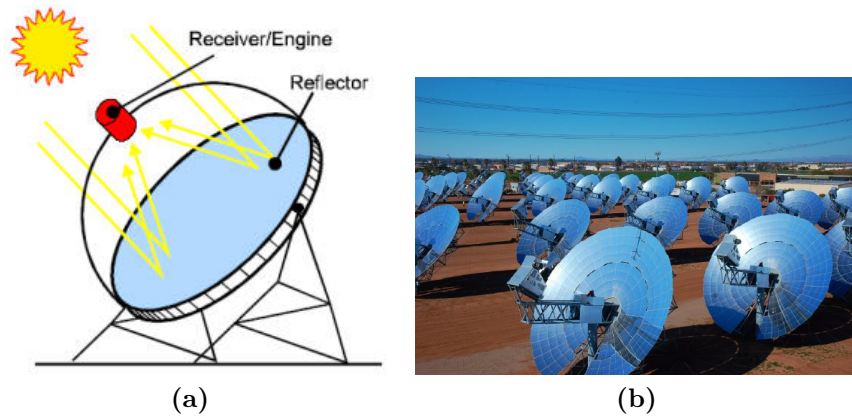


**Figure 1.8:** (a) A typical scheme of a PDC (b) Small PDC CSP plant in the USA [34]

at the focal point, above the dish. The concentrator is "point focus", meaning that it uses a two-axis tracking system to follow the movement of the sun. This makes the collector system really efficient, as it constantly tracks the sun.

The thermal energy can be either transported to a central generator for conversion or converted directly into electricity at a local generator coupled to the receiver. A dish-engine system, for example, is a stand-alone unit composed of a collector, a receiver and an engine. Its dish produces 5-25kW of electricity. The Stirling-engine systems are generally used instead of the traditional Rankine or Brayton cycle engines in this case. Microturbines and concentrating photovoltaics are being evaluated for future applications.[19].

PDCs are still only in demonstrative phase with a weak experimental feedback. But, the fact that they can achieve high operating temperature leading to high thermodynamic efficiency makes it a promising technology for CSP applications. Figure 1.8 presents a typical scheme of a PDC and a picture of one of the few commercial and operational PDC plants worldwide, in Utah, USA. The plant has a capacity of 1.5MW and consists of 429 solar dishes with a Stirling engine.

### 1.2.4 Parabolic Trough Collector

Parabolic Trough Collector (PTC) is the most common CSP technology, with a major data availability. PTCs are linear focus mobile collectors, with parabolic shaped concentrators. As it can be seen in Figure 1.9 on the following page the receiver is a black metal tube, covered with a glass tube to reduce heat losses and it is placed along the focal line of the receiver.

"Linear focus" indicates that a single-axis tracking system is used to follow the movement of the sun. The collector can be oriented in an east-west direction, tracking the sun from north to south or in a north-south direction, tracking the sun from east to west. The advantages of the former tracking mode is that little collector adjustment is required during the day and the full aperture always faces the sun at noon but the collector performance during the early and late hours of the day is greatly reduced, due to large incidence angles (cosine loss). North-south oriented troughs have their highest cosine loss at noon and the lowest in the mornings and evenings, when the sun is due east or due west. Over a period of one year, a

horizontal north–south trough field usually collects slightly more energy than a horizontal east–west one. However, the north–south field collects a lot of energy in summer and much less in winter. The east–west field collects more energy in winter than a north–south field and less in summer, providing a more constant annual output. Therefore, the choice of orientation usually depends on the application and whether more energy is needed during summer or winter [19].

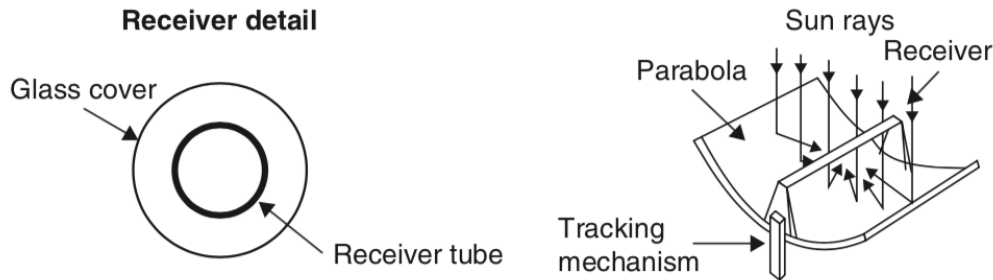


**Figure 1.9:** A typical scheme of a PTC and its receiver [19]

In a Solar Field using PTCs, there are several hundred of troughs, placed in parallel rows. When the sun’s heat is reflected off the mirrors of the troughs, most of the heat is sent on to the tubular receiver. The receiver is filled with the HTF, which is heated up. It is, then, used to increase the temperature of water through a heat exchanger and produce steam. The produced steam enters a conventional steam turbine thermodynamic cycle to produce electricity. The used steam can be cooled, condensed and recycled again to repeat the process. And the same goes for the HTF: after being used in the thermodynamic cycle, it is recycled back to the solar field to increase its temperature and repeat the cycle.[14]. It is common that a natural gas system hybridizes the PTC CSP plants and contributes to 25% of their output.

The most expensive project so far undertaken based on this technology was the Solana Generating Station, installed in 2013 with a cost of approximately 2 billion US\$. The planned electricity generation is estimated at 944,000 MWh/year (capacity of 107.7 MW). [35]. While, one of the biggest applications of this type of system is the nine southern California power plants known as solar electric generating systems (SEGS), which have a total capacity of 354 MW [36]. A picture of SEGS is shown in the following figure.

This is the most mature, proven and widely-used CPS technology, with several plants operating and being constructed all around the world. Of course, there is still research and development aiming to further reduce the cost in the following years. Some of the main goals are [19]:

- Higher-reflectivity mirrors.
- More sophisticated sun tracking systems.
- Better receiver selective coatings, with higher absorption and lower emittance.
- Better heat transfer techniques.

PTC technology offers a large experimental feedback and a relatively low installation cost. It, also, produces the lowest cost solar-generated electricity, compared to the other existing technologies. On the other hand, parabolic trough plants require a considerable amount of land and large amounts of water. Water availability can be a serious issue in the dry regions where these plants are usually situated.



**Figure 1.10:** Photograph of SEGS: a PTC CSP plant in the USA [37]

### 1.3 Thermal Energy Storage

The biggest disadvantage of using Solar Energy to produce electricity is its intermittent behavior. The solar radiation reaching a CSP plant, for example, is not constant every day, it even changes within a single day. This happens due to weather conditions and due to the direction and intensity of the sun seasonally. Households and businesses need a constant power supply and their everyday activities strongly depend on this fact. So, when a CSP plant provides electricity to them, variability of the power output is not an option.

There are two main solutions to overcome intermittency in a CSP plant [9]:

1. Use a Fuel Backup System (FBS) that burns fossil fuel or biomass
2. Use a Thermal Energy Storage (TES) system

In both cases the idea is to dispatch heat during periods of weak or no solar irradiation (during the night), in order to maintain stable the power output of the plant. The option of the hybridization with a FBS manages to increase the plant's global efficiency [38], but it produces pollutants from combustion and it is, also, expensive as it requires feeding of a fuel.

TES on the other hand, is an integrated part of a CSP plant, consisting of tank(s) that act as reservoir of energy that collect thermal concentrated energy during the normal operation of the plant and dispatch it to the power block whenever is needed. It is a less pollutant solution, with lower capital costs but higher LCOE [16].

In 2015, an interesting paper was published by T.E. Boukelia et al. [39], in which a 4E(energy-exergy-environmental-economic) comparative study was performed in 8 different configurations of PTC solar thermal power plants, with two different HTFs, with or without FBS or/and TES present. A constant net power of 50MWe was generated by all the configurations. The same TES capacity and solar field layout was considered in every case. Focusing on the four configurations using molten salt or Therminol VP-1 as HTF, the two with TES only and the other two with FBS only, the following results\* were obtained, related to the environmental and economic aspect:

**Table 1.3:** Comparison between TES and FBS for different PTC plant configurations.

	Therminol TES	Therminol FBS	Salt TES	Salt FBS
<b>Land use (acres)</b>	360	359	326	326
<b>Annual water usage (m<sup>3</sup>)</b>	540,089	538,553	431,510	452,389
<b>Annual CO<sub>2</sub> emissions (ton)</b>	9114	23,782	7571	21,326
<b>Total capital cost(million \$)</b>	337	232	231	198
<b>LCOE (£/kWh)</b>	11.62	7.58	10.29	7.74

\*Table adjusted from [39]

It can be observed that there is not a big difference neither at the land occupied nor at the annual water usage between the two technologies of TES and FBS. The

strong disadvantage of the FBS is evident in the numbers: the annual emissions of carbon dioxide are greatly higher compared to the emissions of the TES. As it was mentioned earlier though, the total capital cost as well as the LCOE are lower for the case of FBS.

Another interesting fact is that more than 70% of the CSP plant currently under construction and almost 80% of those already planned, will be integrated with a TES system [9], as it can be seen in the following fFigure 1.11.

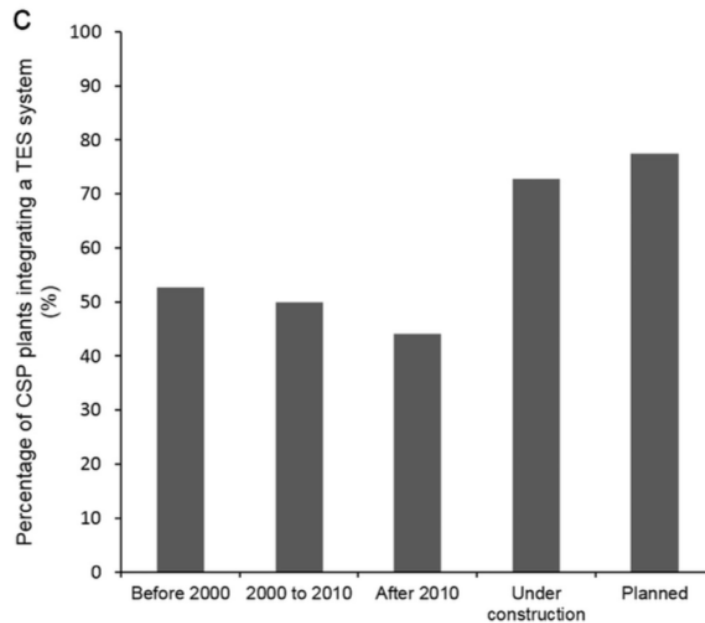


**Figure 1.11:** Percentage of TES systems in CSP plants [9]

There is, also, the option of combining a TES and a FBS in a single plant, thus achieving a tradeoff between total capital cost, efficiency and LCOE. Indeed, as shown in the paper of T.E. Boukelia et al. [39], a configuration consisting of both TES and FBS, achieves the lowest LCOE, a lower capital cost than the FBS alone but the highest CO<sub>2</sub> emissions compared to the values of the other configurations of the Table 1.3 on the facing page. A simplified scheme of an oil plant with integrated both systems is shown in Figure 1.12.

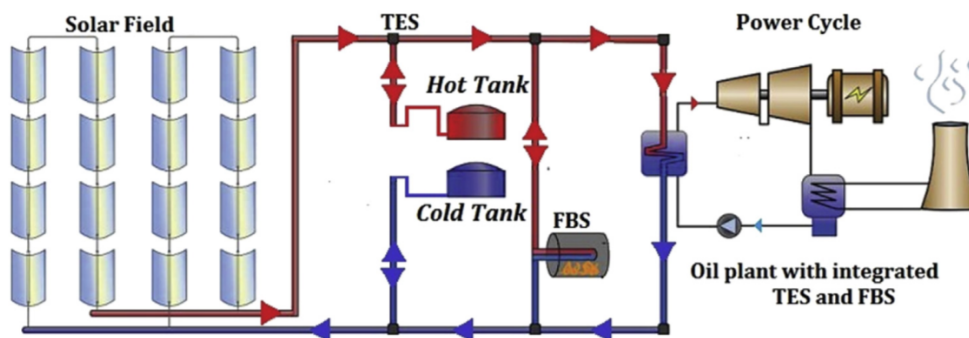


**Figure 1.12:** Scheme of an oil plant with integrated TES and FBS [39]

Focusing on the TES technology, it may offer the following functions [16, 21, 40]:

- Mitigating short fluctuations during transient weather conditions. Without TES, solar power is an intermittent power source, dependent on when the sun shines. The ability to store energy and dispatch solar power when is needed helps to make solar power plants a more reliable and firm power source.
- Shifting the power generation period from peak hours of solar irradiation to peak hours of demand, solving in this way, the time mismatch between solar energy supply and electricity peak demand. In some cases, utilities have greater need for power at night. Without TES, it is impossible for a CSP plant to deliver electricity during the night, when it is needed the most. It should, also, be considered that the power produced during the peak hours is usually valued higher than during the periods of low demand. This provides an economic benefit for the addition of a TES system, that extends the generation period even during the night.
- Reducing the number of start-ups of the plant. Starting up a power plant takes time, energy, causes additional corrosion on equipment, and is often the time when systems are most susceptible to failure. Solar power plants without thermal storage, during partially cloudy days, are forced to start-up every time sufficient solar energy is available. Multiple plant start-ups in a single day are not unusual. The addition of thermal storage allows solar energy to be collected during short sunny periods and stored for later use when sufficient energy has been collected to run the power plant for a sustained period.
- Improving the annual capacity factor. This is a performance parameter that compares the net electricity delivered by the plant to the energy that it could have produced under continuous full power operation during the same time period. A 7hr of storage, for example, can increase this factor from its typical value of 25% to 28% and up to 43%.
- Increasing the plant availability. A TES system provides a buffer in case of any delays caused by long start-up, faulty equipment etc. In a plant without TES, even minor delays can result in a significant loss of power generation.

Before implementing a TES in a CSP plant, there are some considerations that have to be taken into account. Firstly, the space availability has to be evaluated. This is essential for choosing the type of TES. Also, the operating T as well as the maximum load should be thought of. Another important point is to access how the increased capital costs of the TES will affect the LCOE based, always, on the available tariffs.

When the time of implementation comes, there are some important design criteria for the TES that should not be ignored. They are summed up in the Table 1.4 on the facing page [41, 42].



**Table 1.4:** Design criteria for a TES of a CSP plant.

Design Criteria	Influencing factors
<b>Technical</b>	<ol style="list-style-type: none"> <li>1. High energy thermal storage capacity</li> <li>2. Efficient heat transfer rate between HTF and storage material</li> <li>3. Good mechanical and chemical stability</li> <li>4. Compatibility between HTF, heat exchanger (if present) and storage material</li> <li>5. Complete reversibility for a large number of cycles</li> <li>6. Low thermal losses</li> <li>7. Ease of control</li> </ol>
<b>Cost-effectiveness</b>	<ol style="list-style-type: none"> <li>1. Cost of TES materials</li> <li>2. Cost of heat exchanger (if present)</li> <li>3. Cost of the land for the TES</li> </ol>
<b>Environmental</b>	<ol style="list-style-type: none"> <li>1. Operation strategy</li> <li>2. Integration of the TES in the plant</li> <li>3. Environmentally friendly materials</li> </ol>

There are generally three different ways in which thermal energy can be stored: sensible, latent and thermochemical heat storage.

**Sensible** heat storage means that thermal energy is stored/released by raising/decreasing the temperature of a storage material, in a pure physical process without any phase change. It is the most commonly used and most mature TES technology with many inexpensive materials available [16, 21, 42]. In the case of water for example, sensible is the heat required to increase its the temperature in constant pressure without changing its phase. The sensible heat storage depends strongly on the characteristics of the storage material. Its specific heat  $c_p$ , determines the energy density and the thermal diffusivity  $k/c_p$ , determines the rate at which that heat can be released or extracted. The amount of energy stored in this case is:

$$Q_{st} = m_{sm}c_p\Delta T \quad (1.1)$$

$m_{sm}$ : the mass of the storage medium

Density and specific heat of the storage material, operating T, thermal conductivity, diffusivity, chemical/thermo-chemical stability and cost of materials should be taken into account [43].

In the **latent** heat storage, thermal energy is stored/released by a material while changing its phase at a constant temperature. It is a pure physical process without any chemical reaction. In the example of water, latent heat is the heat needed to change its phase in constant temperature and pressure. Mainly solid-liquid transition is preferred and the substances used under this technology are called Phase Change Materials (PCM). PCM allow large amounts of energy to be stored

in relatively small volumes, resulting in some of the lowest storage media costs of any storage concept [42]. Latent heat storage can offer higher energy density but a poor heat transfer performance due to the very low thermal conductivity of the PCM. The heat stored in the case of a solid to liquid phase change:

$$Q_{st} = m_{sm}[c_{ps}(T_m - T_s) + h + c_{pl}(T_l - T_m)] \quad (1.2)$$

where  $h$  is the enthalpy of phase change,  $T_m$  is the melting temperature,  $T_s$ : the starting temperature of the solid and  $T_l$ : the final temperature of the liquid. It is a nearly isothermal process that can provide significantly enhanced storage quantities when compared to sensible heat storage. Isothermal storage is an important characteristic because solar field inlet and outlet T are limited due to constraints in the HTF, solar field equipment and steam turbine cycle [21].

The least investigated technology so far is the **thermochemical** storage. It is based on reversible chemical reactions which are characterized by a change in the molecular configuration of the reactants. Solar heat is used to drive an endothermic chemical reaction and then stored in the form of chemical potential. During the discharge, the stored heat can be released by the reversed exothermic reaction, sometimes by adding a catalyst [44]. It has been receiving the attention of the scientific community because it can potentially store more energy than sensible or latent heat systems thanks to the heat of reaction. The heat stored:

$$Q_{st} = \alpha m \Delta H \quad (1.3)$$

where  $\alpha$  is the fraction of the components that reacted and  $\Delta H$  is the heat of reaction per unit of mass.

The thermochemical heat storage offers the highest energy density (up to 19 times greater than the latent heat) and constant temperature. The dissociation reaction can be stored indefinitely at ambient temperature, thus reducing the thermal losses. On the other hand the design of the reactors can be complex and the cost high. Also, the chemical stability is still low. The performance of the system is degraded over charge and discharge and it is strongly restricted by the reaction kinetics [21, 44].

In the particular case of the CSP plants, the TES systems can be further classified as active and passive. In the **active** storage systems, the storage medium (fluid) itself flows to absorb or release heat by forced convection. The **passive** storage systems are generally dual medium storage systems: the HTF passes through the storage only for charging and discharging a solid material, carrying the energy received from the energy source (solar field). In other words, the HTF circulates through the TES system in order to heat up or cool down the (solid) storage materials that are kept inside [9, 21, 43]. Another conceptual design for TES is the **combined** system. It is a three-part storage system where a phase change material is deployed for two-phase evaporation in a Direct Steam Generation (DSG) plant, while concrete storage is used for storing sensible heat, i.e., for preheating of water and superheating of steam. A system like this will be used in the 1 MW Dahan DSG power tower plant in China. The low temperature stage consists of a

steam accumulator that will store saturated steam at 2.35 MPa, 220.7 oC. During discharging, the saturated steam will be converted to superheated steam via a storage system which uses oil as the storage medium [21].

Another way to diversify the type of TES in CSP plants is based on the number of storage tanks used.

### 1.3.1 Two-tank Storage

It has been successfully commercialized in the solar field with many applications in the CSP plants. It uses two tanks to store the storage medium: the "hot tank" where the storage medium with increased temperature is stored and the "cold tank" which contains the storage medium of low temperature.

#### Direct Storage

In the case of the direct two-tank storage, the energy storage mechanism is placed on the main process streams and it is directly fed by energy, without any utility/process/heat exchanger. The energy storage linearly increases/decreases according to the inflow and outflow of the tanks [45]. An example of a simplified scheme for a CSP plant working with a two-tank TES is presented in Figure 1.13.

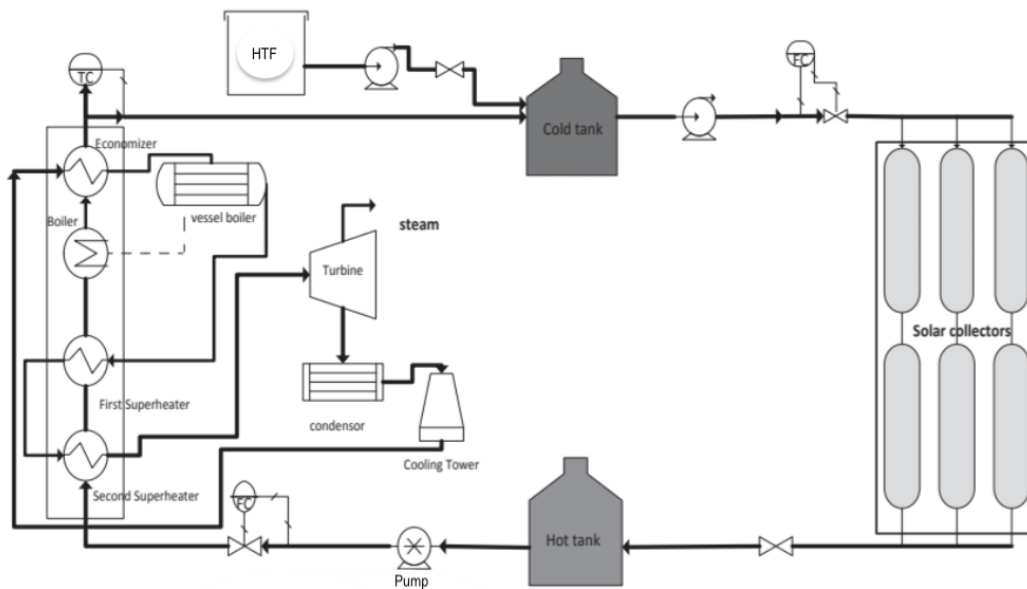
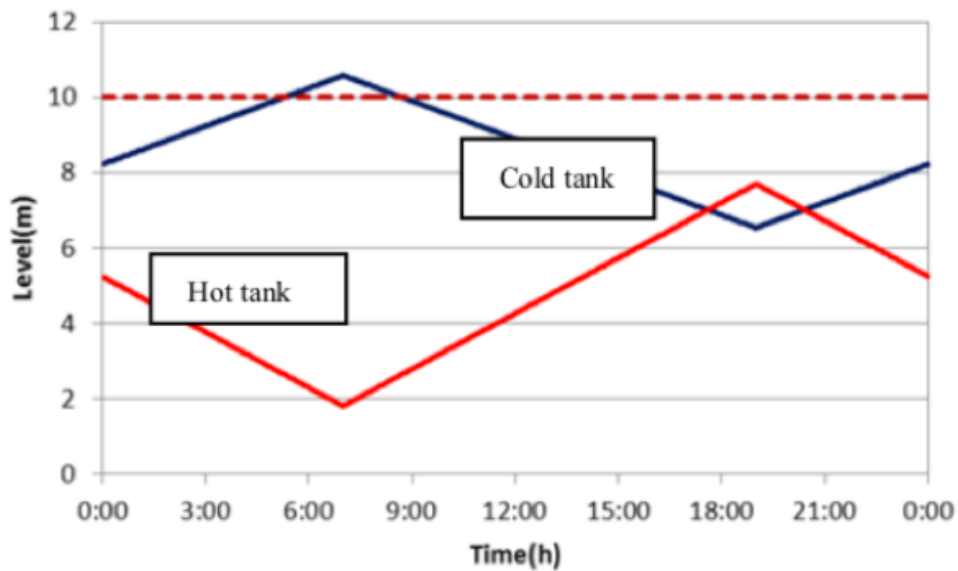


Figure 1.13: The two-tank direct TES [46]

The working principle of the system above is the following. At the startup of the plant the HTF is loaded in the cold tank at a low temperature. During the day, when the sun provides enough radiation, the cold HTF is pumped out of the cold tank and into the solar field (here: solar collectors). There, the temperature of the HTF rises. Some of the hot HTF is now sent for storage at the hot tank while another part passes to the heat exchanger train at the power block in order to produce electricity. This procedure goes on till the sunset, when the radiation of the sun is not anymore enough to heat up the cold HTF at the solar field. At that point the level inside the hot tank has reached a certain predicted value. During the night, the hot HTF is pumped out of the hot tank and enters the power block to continue producing electricity. It is cooled down because it passes from a series of heat exchangers and then, at a low temperature it enters the cold tank. The solar field is not active. When the next day comes, the cold tank has been filled up with cold HTF and the hot tank is either empty or has a low level of hot HTF.

The process is repeated all over again.

In the direct TES configuration, the HTF acts as both the transfer fluid and the storage medium. The liquid holdup for the hot and cold tank have linear behavior during the day. During the charging period, the content of hot tank gradually increases and conversely through the discharging period, the harvested energy is consumed and consequently the levels of the stored liquid decreases with a similar slope of the harvesting one [47]. This behavior is depicted in the following figure.



**Figure 1.14:** Dynamic behavior of the level of the tanks in the two-tank direct storage [47]

It can be observed that at night and early in the morning, the level of the hot tank decreases linearly. The hot HTF is flowing out of the hot tank in order for the plant to be able to produce constant power output. During the day, at the charging period, the cold HTF is flowing through the solar field and into the hot tank, thus the level of the former is decreasing and the level of the latter is increasing. The sum of the two levels of the tank remains constant throughout the 24h (dotted horizontal line). For each tank, at any point of operation, the accumulation is practically always non zero:

$$\frac{dm}{dt} = \dot{m}_{in} - \dot{m}_{out} \quad (1.4)$$

Where  $\dot{m}$  is the mass flow rate.

### Indirect Storage

The indirect two-tank storage is the most installed TES technology in the PTC CSP plants [48]. In this technology the storage medium from the cold storage tank is heated up in a heat exchanger by a HTF coming from the solar field. Then the heated storage medium is stored in the hot tank. In contrast to the direct two-tank storage, the storage medium is different from the transfer fluid. This is sometimes

inevitable because the circulating HTF is maybe too expensive or it does not have the suitable properties in order to act as a storage medium. The most important addition and the most vital part of this configuration is the heat exchanger, where the HTF and the storage medium exchange energy. The scheme of a two-tank indirect TES system is presented in the Figure 1.15.

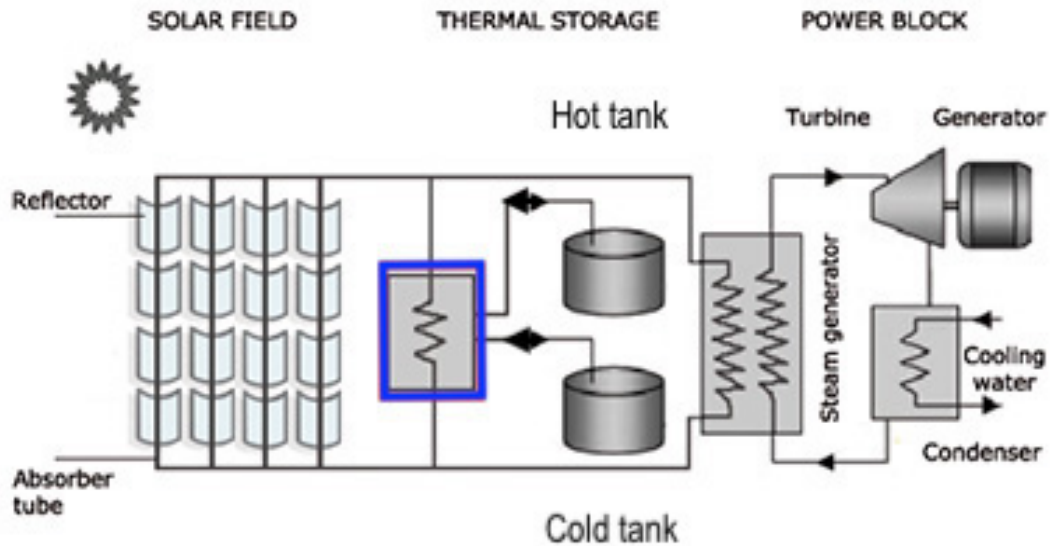


**Figure 1.15:** The two-tank indirect TES [49]

At the charging phase, HTF is pumped from the cold tank and it is heated as it passes through the heat exchanger (here inside the blue line) and flows into the hot tank. To discharge the storage system, storage fluid is pumped from the hot tank and transfers its heat through the heat exchanger to the HTF, and return to the cold tank. The hot HTF, from the output of the heat exchanger goes towards the power block for power generation.

The main advantages and disadvantages of the two-tank storage are reviewed in the Table 1.5.

**Table 1.5:** Review of the two-tank TES.

<b>Advantages</b>	<ol style="list-style-type: none"> <li>1. Low risk approach, cold and hot storage medium are stored separately</li> <li>2. Possibility to raise the solar field output temperature, rankine cycle efficiency of the power block can reach 40%</li> </ol>
<b>Disadvantages</b>	<ol style="list-style-type: none"> <li>1. High cost of material used as HTF and storage materials</li> <li>2. High cost of extra heat exchanger (if present) and 2nd tank</li> <li>3. High risk of solidification of storage fluid</li> </ol>

### 1.3.2 Single-tank Storage

In the single-tank or **thermocline** storage, one tank only contains simultaneously hot and cold HTF in stratified way by appropriately feeding them to it from the top to the bottom. This technology requires that the lower density hot fluid rests stably above the higher density cold fluid and remain essentially stratified during energy charge, resting and discharge [50]. Hot fluid is pumped into the single tank, gradually displacing the colder fluid. A thermal gradient is created within the system and it is ideally stabilized and preserved by buoyancy effects, which induce stratification leading to two isothermal regions along the vertical direction. In other words, this gradient is a narrow layer of substantial temperature gradient that grows at the interface between the hot and cold region and it is known as thermocline or heat transfer region [51]. In order to achieve a high efficiency, the temperature stratification must be maintained constant and mixing should be avoided. Usually a filler material (quartzite rock, sand, concrete, industrial waste) is added in the thermocline to enhance the thermocline effect and to reduce the needed quantity of storage materials. It aids in maintaining the gradient and reduces natural convection within the liquid. Systems using filler materials are categorized as passive because the filler acts as the primary storage material [21, 52, 53].

In the following figure, a typical scheme of a CSP plant using direct single-tank storage is presented.

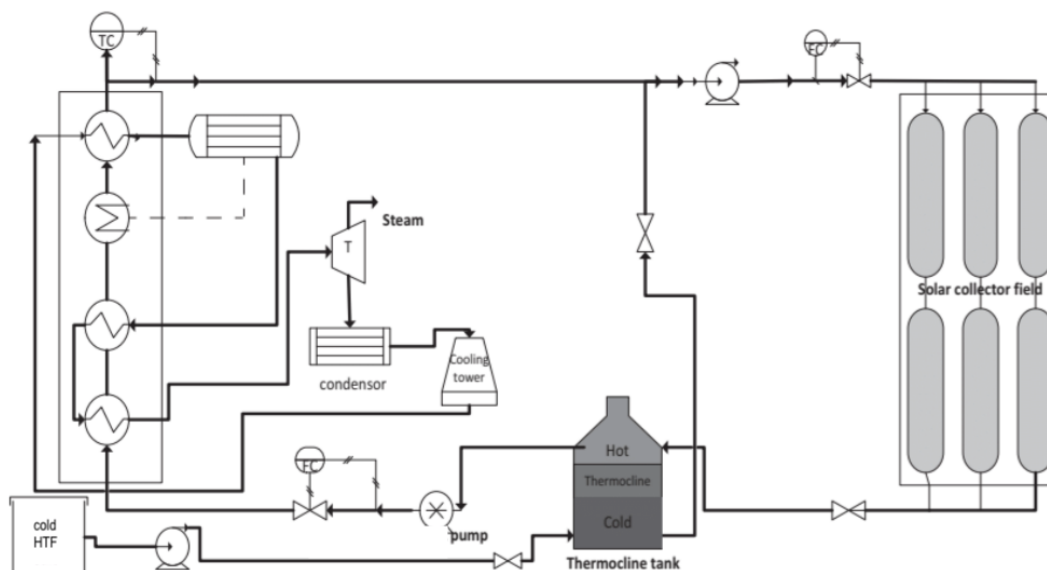


**Figure 1.16:** The single-tank (thermocline) TES [46]

The hot fluid is loaded into the tank from the top at daytime and at the same time the cold fluid is pumped out from the bottom into the solar field to harvest solar energy. During the night, the cold fluid line is off and no hot fluid is supplied to the thermocline. On the other hand, the hot fluid is continuously pumped out from the top and releases the stored heat to the plant (e.g to produce electricity) before returning back to the bottom. This process moves the thermocline region downward

daytime and increases the thermal energy potential in the storage. During this charging phase (hot HTF going in and cold HTF going out of the thermocline), the temperature of the cold HTF entering the heat exchanger is constant until the gradient reaches the bottom of the tank. At that point the temperature coming out of the bottom of the tank starts to rise, as it can be seen at the following figure:

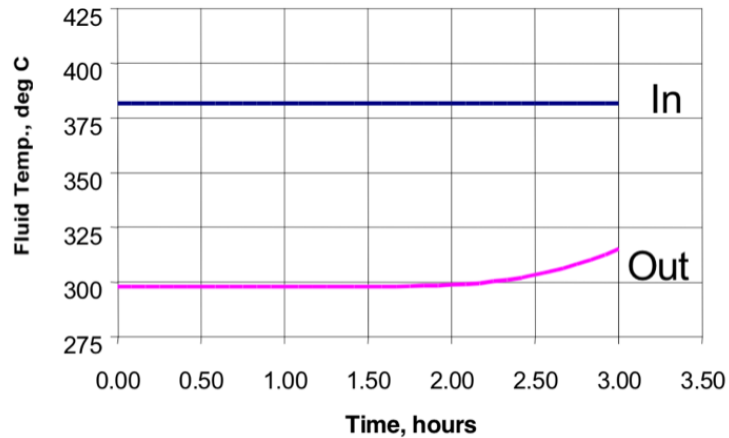


**Figure 1.17:** Dynamic behavior of the temperature of inlet and outlet stream of a thermocline during charging phase [53]

At night, reversing the flow, moves the thermocline upward and depletes the thermal energy [46, 50].

Similar behavior is observed for the temperatures of the inlet and outlet streams.

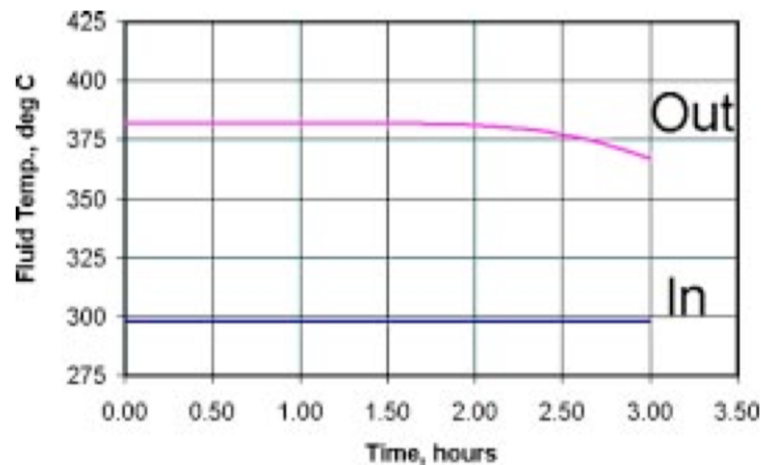


**Figure 1.18:** Dynamic behavior of the temperature of inlet and outlet stream of a thermocline during discharging phase [53]

In thermocline systems, the exergetic efficiency depends on the ability to keep the thermocline region as narrow as possible, thereby achieving the best possible temperature separation [54]. So, an ideal thermocline tank is a conceptual tank consisting of hot and cold fluid separated by a fictitious barrier without any filler



material ( $\varepsilon = 1$ ). In this way, in an ideal thermocline there is no loss in exergy during charging and discharging process.

The temperature of the filler material is always higher than the fluid within the tank since the filler material acts like a heat reservoir. As the operation time of tank increases, filler material eventually loses heat to the flowing cold fluid and attains thermal equilibrium with cold fluid after a specific operation time of tank. The operation time of tank is decided based on the outlet temperature of tank which is a function of time. In a study published by KS Reddy et al it was observed that as the operation time increases, thermocline thickness in the tank increases in the upward direction and eventually gets vanished [51]. This is depicted clearly in the Figure 1.19, where results of simulations for the temperature distribution inside a single tank, for three different HTFs, are shown.

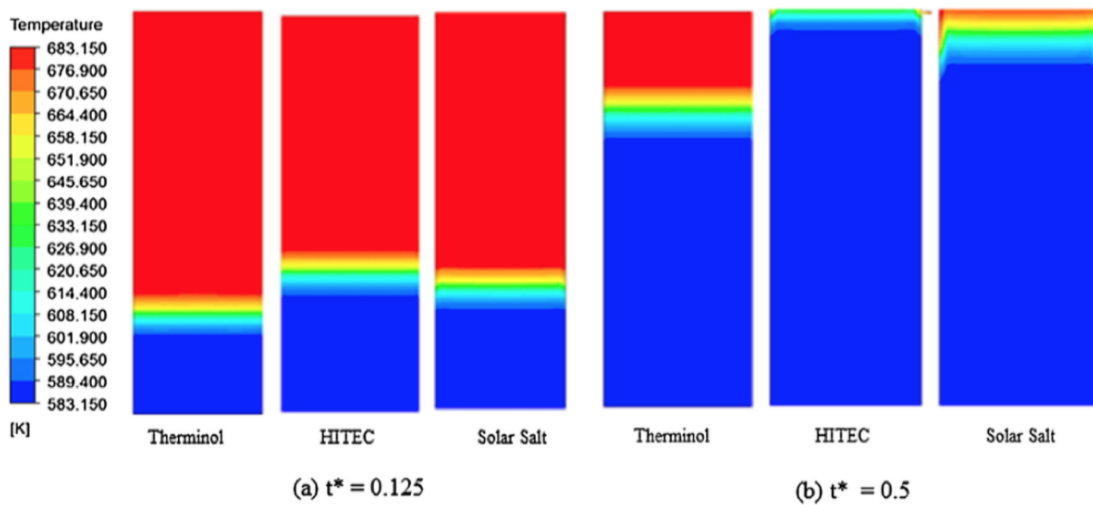


**Figure 1.19:** Temperature distribution of different HTFs in a single-tank storage [51]

Thermocline storage is designed in such a way that the velocity of the fluid is adjusted to maintain the thermocline thickness within the tank for the required operation of the tank. In reality though, as shown in Figure 1.19, the thermocline thickness increases with operation time of the tank because of the convective mixing happening between the hot and the cold fluid, which is to be retarded. The influence of the fluid properties like viscosity, thermal conductivity is responsible for maintaining thermocline thickness within the tank for the required operation of the tank.

In a paper published by Pacheco et al. [53], a comparison between different possible filler materials for single-tank storage was carried out. The ideal filler material would be inexpensive and widely available, with a high heat capacity, a low void fraction, compatible with nitrate salts and nion-hazardous. The most successful candidates were quartzite, taconite, marble, NM limestone, apatite, corundum, scheelite, and cassiterite. Because taconite, marble, NM limestone, and quartzite are available in bulk quantities for a reasonable price, the attention was focused on these materials to conduct thermal cycling tests. Quartzite rock and silica and turned out to have the best performance.

With the tank being the most important part of a thermocline storage system,

its dimensions have to be calculated correctly to guarantee the correct overall performance of the plant. Generally, because of the height required for the gradient, taller tanks with smaller diameters are favored over shorter tanks with larger diameters. It is interesting to see how the sizing of an ideal storage tank can be approached [50].

The heat storage or delivery rate for any storage tank is related to the required mass flow rate and the required period of operation of a thermal power plant. If the storage system is ideal, the heat delivery rate will be:

$$\dot{Q}_T = \dot{m}\bar{C}(T_H - T_L) \quad (1.5)$$

where  $T_H$  is the temperature of the hot fluid stored and  $T_L$ : the temperature that the fluid reaches after it gives out its thermal energy. The ideal total energy delivered for a specific time span  $t_{ref}$  :

$$Q_T = t_{ref}\dot{Q}_T \quad (1.6)$$

and the ideal volume of the fluid storage tank:

$$V_{ideal} = \frac{t_{ref}\dot{m}}{\rho_f} \quad (1.7)$$

In reality, the tank dimensions are decided based on various values of operational parameters taken directly from the power plant. The electrical power, the thermal efficiency, the period of operation, the inlet/outlet fluid temperature, the properties of the HTF and the thermal storage material including the fillers should all be taken into consideration [50, 54]. Computational Fluid Dynamics (CFD) is strongly involved in the decision.

The reasons why thermocline should be investigated more for the CSP plants, but also some of the drawbacks of this technology are listed in the Table 1.6 [16, 43, 46, 47, 52].

**Table 1.6:** Review of the single-tank (thermocline) TES.

<b>Advantages</b>	<ol style="list-style-type: none"> <li>1. Ability to dispatch thermal energy at nearly constant temperature over most of the discharge cycle</li> <li>2. Possibility to reduce 33% of the cost of TES</li> </ol>
<b>Disadvantages</b>	<ol style="list-style-type: none"> <li>1. Requires really good control to avoid mixing</li> <li>2. The design of the storage system is more complex</li> <li>3. Stability of the filler material in the hot HTF</li> <li>4. Thermo-mechanically induced ratcheting*</li> </ol>

\*In mechanics, ratcheting is a behavior in which plastic deformation accumulates due to cyclic mechanical or thermal stress. Thermal ratcheting of the tank: as the tank heats up, its internal volume increases and the fill particles settle lower to cover the additional volume created. When it cools down, it compresses, but the particles cannot physically move upwards due to gravity build-up of mechanical stress in the tank shell through repeated operational cycles.

## 1.4 Heat Transfer Fluid

Water has been the most popular HTF for most of the industrial applications thanks to its availability, high specific heat, high density and moderate viscosity [10]. The biggest drawback is the limited range of temperatures in which water can be used. In order to keep it liquid above the 100°C, high pressure is needed and high pressure equals really high costs. This is the reason why water is not generally used as HTF in the CSP plants, where high temperatures are reached, in order to create the biggest heat exchange "reservoir" possible for the HTF. There are some specific characteristics that a HTF should have in order to be suitable for use in the CSP field taking into account that the HTF is the "bond" between solar field, power block and storage system (if present). These characteristics are [13, 51, 55, 56]:

- Extended working temperature range.
- Good thermo-physical properties.
- Anti-hazard.
- High heat capacity.
- Moderate density and viscosity.
- High thermal energy storage density.
- Low corrosion with metal alloys.
- Low cost.

All of the characteristics listed above have to be combined, in order to satisfy the goal of increasing the efficiency of the cycle, reducing the costs and making the components of the process robust and compatible with each other.

The HTFs currently used in the CSP plants, can be categorized based on their chemical composition. The main ones will be analyzed and some innovations made in the area of the HTFs will, also, be presented.

### 1.4.1 Thermal Oil

Mineral, silicon and synthetic oil have been tested and used in CSP applications [13]. They can maintain their liquid phase up to 300°C and they are thermally stable up to 400°C. That is why they are not suitable for high-temperature applications in the solar field. This temperature limit is a serious barrier to increasing the power block efficiency of a CSP plant, because the temperature of the steam delivered cannot be higher than 390°C, thus limiting the steam turbine efficiency [55]. The three thermal oils mentioned above, have more or less the same (relatively low) thermal conductivity of 0.10-0.12W/mK and low density of 770-900kg/m<sup>3</sup>. This causes limitations to the rate at which the heat can be released and extracted. Oils have rather high vapor pressure which causes serious safety and environmental issues. Another problem with these thermal oils is that they are expensive [41].

Probably the most well known thermal oil in the CSP industry is the **Therminol VP-1**. It is an organic thermal oil that consists of biphenyl ( $C_{12}H_{10}$ ) and diphenyl oxide ( $C_{12}H_{10}O$ ) pair. This is an eutectic mixture of two very stable organic compounds. Therminol VP-1 is produced by Eastman Chemical Company but the same eutectic mixture is used, also, in a HTF developed by Dow Chemicals, under the name of Dowtherm A. Therminol VP-1 can be used in a wide temperature range, thanks to its low crystallization point of  $12^{\circ}\text{C}$ . It has some interesting properties as it can be used both as vapor and liquid-phase HTF. The liquid phase heating does not require any condensate return equipment and it can be managed by simpler and more easily operated systems. Vapor phase heating, on the other hand, can provide much more heat per unit mass of heat medium and it can offer an easier temperature control to the user because of the more uniform distribution of temperature. Therminol VP-1 can be used at up to  $400^{\circ}\text{C}$  with a normal boiling point of  $257^{\circ}\text{C}$ . Overheating must be avoided because it has an autoignition temperature of  $601^{\circ}\text{C}$ . It has the strong advantage of high thermal stability [57].

### 1.4.2 Molten Salt

In order to help the CSP plant achieve higher efficiency in the power block, a HTF that works at higher temperatures compared to the thermal oils, have to be used. Molten salts have become a really could candidate exactly for this reason. They are thermally stable at high temperatures, up to  $600^{\circ}\text{C}$  [13, 43]. At high temperature, they have low vapor pressure, similar to that of the water [58]. Another important advantage of molten salts is that they are suitable for TES, offering an efficient heat storage and this is why the two-tank indirect TES with molten salts is the most widely used TES configuration in CSP plants. [48, 59]. Another interesting conclusion, reported by D. Kearney et al., is that the use of molten salts as HTF makes economical sense only if the plant includes a TES system [60]. It should, also, be mentioned that the risk of fire or pollution is low when molten salts are being used, as they are non-flammable and non-toxic. Of course, the disadvantages are not absent. The higher outlet temperature of molten salts means heat losses from the solar heat, requiring more expensive piping and materials [43]. Also, their high melting point of around  $220^{\circ}\text{C}$  introduces the risk of crystallization inside the pipes during winter or night-time. A routine freeze protection operation should be carried out. During this operation, the HTF is circulated at a low flow rate through the SF during the night as required. By this means, the piping will be kept warm, thus avoiding critical thermal gradients during start up. If the HTF temperature falls below a certain value, then an auxiliary heater is used to maintain a minimum temperature [61]. A significant amount of energy is consumed during this procedure.

The main strong points and drawbacks of molten salts compared to thermal oil are highlighted in the following table [55, 61]:

An example of a molten salt HTF is the **Hitec XL**. It is a ternary mixture of sodium, potassium and calcium nitrates:  $\text{NaNO}_3(7\text{wt}\%) - \text{KNO}_3(45\text{wt}\%) - \text{Ca}(\text{NO}_3)_2(48\text{wt}\%)$ . It has a lower melting point ( $120^{\circ}\text{C}$ ) compared to the most of

**Table 1.7:** Molten Salt as HTF: comparison with Thermal Oil.

Advantages over thermal oil	Disadvantages over thermal oil
1. Efficient heat storage	1. Thermal losses overnight
2. Higher working temperature	2. Complex solar field design
3. No pollution/fire-hazard	3. Higher electricity consumption
	4. Lower mass flow leads to high $\Delta P$

the molten salts and this is its strong advantage. However, it is thermally stable only up to 500°C [13]. Many HTFs consisting of almost the same components but in different molar fractions exist: Hitec, LiNaK carbonate, Sandia Mix and Halotechnics SS-500 are some examples. **Solar Salt** is the most popular HTF used in CSP plants. It is a binary salt mixture of 60wt% NaNO<sub>3</sub> (sodium nitrate) and 40wt% KNO<sub>3</sub> (potassium nitrate). It melts at 223°C and remains thermally stable at liquid phase up to 600°C. Many reviews can be found in literature for this specific HTF, that assess its performance within the plant as well as the possible corrosion effects. It is one of the most well-studied HTFs and this is a reason why it is generally preferred in the CSP plants.

A recent paper published by A. Bonk et al. [62], compares five different molten salt systems: Solar Salt, HitecXL, LiNaK Nitrate, Hitec and CaLiNaK/NO<sub>2</sub>. Their physical properties are discussed and useful temperature-dependent data are provided. In the Table 1.8 on page 33 some of the most important thermal and physical properties of the most commonly used HTFs in the CSP plants are summed up [13, 43, 61].

### 1.4.3 Innovative materials

The search by the scientific community for even more efficient HTFs, suitable for CSP applications, still continues. A lot of papers have been published during the recent years, proposing new ideas for alternative HTFs that seem promising and could bring a revolution in the CSP field in the near future. G. Flamant et al. [56] and J. Spelling et al. [63], proposed a dense suspension of particles (solid fraction in the range of 30%-40%) in vertical adsorbing tubes submitted to concentrated solar energy. Temperatures up to 750°C are expected, thus opening new opportunities for high temperature applications and for thermodynamic cycles with higher efficiency. A study carried out by A. d'Entremont et al. [64] proposes the high temperature magnesium iron ( $Mg_2FEH_6$ ) hydride coupled with the low temperature sodium alanate ( $Na_3AlH_6$ ) hydride as a possible HTF for CSP plants. The system's operating temperature in this case varies from 450°C to 500°C, with hydrogen pressures between 30 bar and 70 bar. This makes the TES system a suitable candidate for pairing with a solar driven steam power plant. The model results obtained, showed an actual TES system volumetric energy density of about 132 KWh/m<sup>3</sup>, which is more than 5 times higher than the U.S. Department of Energy SunShot target (25KWh/m<sup>3</sup>).

Many papers in 2018, investigated the possibility of the use of **nano-fluids** in solar concentrating technologies. The term "nano-fluid" refers to a fluid which is

created by dispersing nanoparticles into a base fluid. The used nanoparticles can be metallic (Al, Fe, Cu, Ag, Au) or non-metallic ( $Al_2O_3$ ,  $Fe_2O_3$ , ZnO, CuO,  $SiO_2$ ,  $TiO_2$ ). Carbon nanotubes are, also, common. The nanoparticles are extremely small with a diameter as low as 10nm. The base fluids can be water, ethylene glycol or thermal oils. The nano-fluids have increased thermal conductivity, dynamic viscosity, density and decreased specific heat capacity compared to the base fluids. This allows them to carry higher amounts of thermal energy and offer higher thermal efficiency to the collectors. The biggest limitation that has to be taken into consideration is that the nano-fluids may increase the pressure drops. A comprehensive and complete review of this relatively new technology is given by E. Bellos et al. [65], focusing on the performance of the nano-fluids in different collector types. A. Yasinskiy et al. [66] analyzed the properties of  $TiO_2$ -based nano-fluids with a diphenyl oxide-biphenyl mixture as the base fluid and 1-octadecanethiol (ODT). They observed an improvement in the thermal properties and the efficiency. Pt-based nano-fluids with ODT were, also, tested by R. Villarejo et al. [67], showing enhanced thermophysical properties such as increased thermal conductivity and heat transfer coefficient.

There is still a long road to be covered in order for these concept ideas to reach the market. In any case, it is really encouraging that serious efforts are being made towards the improvement of the current methods used in CSP plants. It is evident, that the CSP technology has gained the trust of the scientific community and it is ready to move to new frontiers.

Table 1.8: Thermal and physical properties of common HTFs.

Heat Transfer Fluid	Synthetic Oil	Hitec	Hitec XL	Therminol VP-1	Solar Salt
Operating temperature (°C)	-20-350	142-535	120-500	12-393	220-600
Average density (kg/m <sup>3</sup> )	900	1640	1992	890	1800
Viscosity (Pa s) @ 300°C	-	0.00316	0.00631	0.000590	0.00326
Heat capacity (kJ/kg/K)	2.3	1.56	1.45	1.93	1.1
Thermal conductivity (W/m/K) @ 300°C	average value 0.11	@300°C 0.20	@300°C 0.52	@300°C 0.01	@600°C 0.55
Cost (\$/kg)	3	0.93	1.1	2.2	0.5
Storage cost (\$/kWh)	-	10.7	20.1	57.5	5.8





## Chapter 2

# The Archimede Concentrating Solar Power Plant

The Archimede Concentrating Solar Power (ACSP) plant, is an example of a combined cycle plant, located in Priolo Gargallo close to Syracuse, Sicily, Italy. The solar field was connected on 14 July 2010 to the already existing combined cycle (installed in 2003) and the plant has been in full operation since then. The plant was named after Archimedes, the ancient Greek inventor, who used a giant mirror, or a set of mirrors to concentrate the sunlight and set fire to Roman ships attacking his home city of Syracuse in 212 B.C, during the Siege of Syracuse. The technology implemented in this plant is the PTC, which is the most widely-used and most mature in the CSP field. The total area of the mirrors is 30000m<sup>2</sup> and the total length of the tubes, where the HTF circulates, is about 5400m. The solar field covers 27 acres of land. The Archimede CSP plant was the first one to use molten salts as HTF and storage fluid, in a two-tank direct TES system. It uses technology developed by ENEA and Archimede Solar Energy, a joint venture between Angelantoni Industrie and Siemens Energy. The plant is currently owned and operated by ENEL. As in most of the cases of the PTC plants, also in the Archimede plant, an Integrated Solar Combined Cycle System (ISCCS) is used. The integration of PTCs into a modern combined cycle has been first proposed by Luz Solar International [68]. In the case of the Archimede plant, the nominal power output coming from the solar energy is 4.8MW and according to the ENEL research chief Sauro Pasini, it can produce 9 million KWh per year - enough to satisfy the electricity demand of about 4.000 homes.

It is worth mentioning that the Archimede Solar Energy company launched another project in 2013; a stand-alone molten salt parabolic trough plant located in Massa Martana, Italy. The purpose of the plant was demonstrative, at least during the first year. For this first year of operation, the collected heat had been dispersed into the environment through a molten salt-to-air heat exchanger; but in the summer of 2014 a steam generating unit was realized and operated. The plant was built to show the efficiency, the manageability and the robustness of such kind of plants, that many experts consider as the most promising application in the field of CSP. It was, also, important to debunk the negative myths associated to the use of molten salts, mainly due to their relatively high freezing temperature. The results from the first demonstrative year of operation were really satisfying, even

though Massa Martana is not the most ideal place for a plant like this; from 22nd of December 2013 till the 1st of March 2014 the plant was basically stopped and all the salt was drained. During the rest of the year, a total of 4450 hours were cumulated with salt in circulation. All the draining and filling tested performed were successful. As for the freezing test, it was carried out to address the possible problem of the molten salts and their high freezing point. There is the fear that during the night, or when the ambient temperature drops, the molten salts may freeze inside the pipes of the system, thus causing some serious problems in the piping and the flexible connections of the solar field. In order to exactly reproduce the situation that might occur on the receivers installed on the solar field, the heating systems, once filled, they were switched off for several hours to produce a complete freezing of the salt inside the receivers, the flex hose and the valve. More than ten cycles were performed, without damages for any of the components of the test facility [69]. These results were encouraging, also, for the ACSP plant in Sicily, which uses the same technology and it is situated in a much better area for CSP applications, with higher annual DNI.

So, focusing on the case of the ACSP plant in Sicily, a scheme of the plant is presented in the following figure.

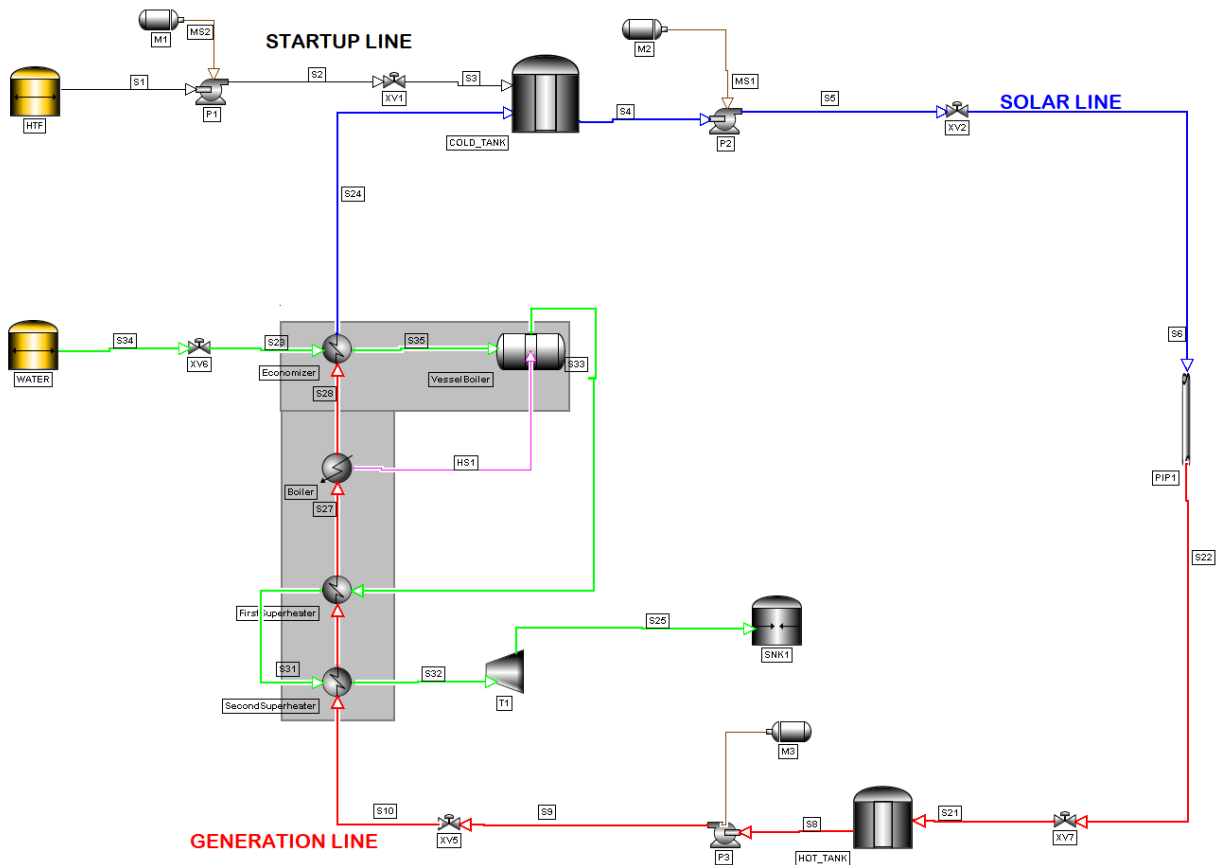


Figure 2.1: Scheme of the Archimede Concentrating Solar Power (ACSP) plant

## Thermal Energy Storage

The plant uses a two-tank direct TES system. This means that the same chemical mixture acts as both the transfer and the storage fluid, without any utility, process or heat exchanger. This plant uses molten salt and more in particular solar salt, which is a binary salt mixture of 60wt% NaNO<sub>3</sub> (sodium nitrate) and 40wt% KNO<sub>3</sub> (potassium nitrate), as it was mentioned in Chapter 2.

In the COLD\_TANK the cold solar salt is kept at a temperature of 290°C. In the HOT\_TANK the hot solar salt is stored at around 550°C. The two tanks are not identical. They have different diameters due to safety reasons; actually the COLD\_TANK has double volume with respect to the HOT\_TANK and it works as a blowdown vessel for emergency conditions [45]. It can contain the whole quantity of molten salts circulating in the solar plant plus the amount stored in the HOT\_TANK.

## Solar Field

As far as the solar field is concerned, in Figure 2.1 on the facing page it is depicted as a pipe (PIP1) and in reality it consists of receivers of 0.07m diameter and a total length of about 5400m. There are 9 strings of 6 collectors each and the length of one collector is about 100m.

## Power Block

Focusing on the third and the most complicated part of the CSP plant, the power block, it consists of the economizer, the boiler, the first and second superheater and the turbine. A close up of the scheme of the power block of the plant is shown in Figure 2.2 on the next page.

The idea behind the function of the power block is the following: along its path and in every one of the heat exchangers present, the hot HTF coming from the solar field will exchange heat with the water/steam. The hot HTF will gradually decrease its temperature while the water/steam will be increasing its temperature. The goal is to convert water to superheated steam, capable of moving the turbine and produce power.

More in details, and always based on the Figure 2.2 on the following page, the hot HTF enters the heat exchangers in the following order: second superheater, first superheater and economizer. The water follows the opposite route. At first it enters at the economizer. There, it will reach a temperature really close to its boiling temperature at the given operating pressure. It is actually a preheating phase for the water before entering the boiler, which allows to spend less energy for the boiler's operation, as the boiling temperature is, almost, already reached. This will help in the increase of the overall efficiency. It is worth mentioning that the economizer refines the lowest temperature of the HTF. In the case of molten salts, for example, their outlet temperature has to be continuously monitored in order to avoid too low temperatures that can lead to total or local crystallization [70]. In the boiler the water turns into saturated steam. In the figure, the boiler

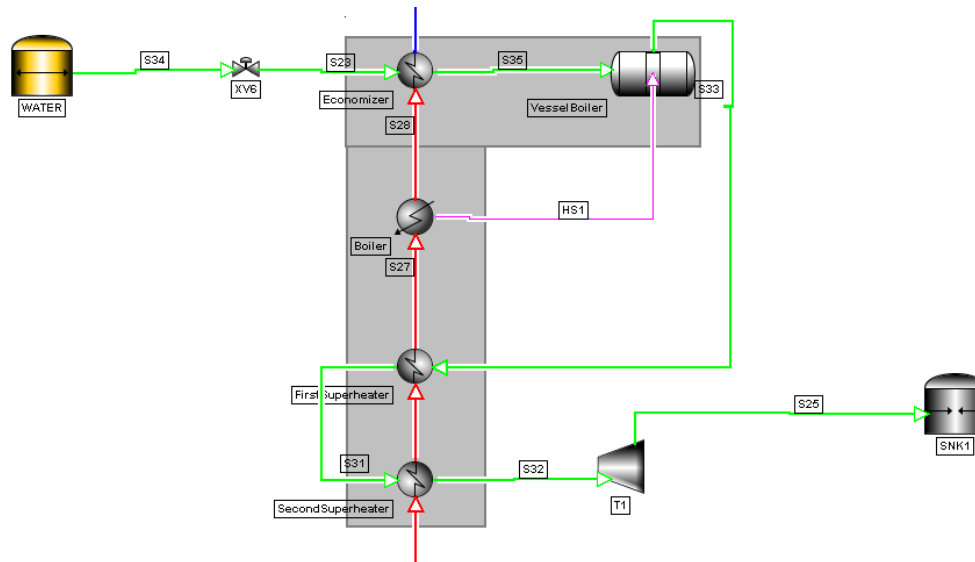


**Figure 2.2:** Scheme of the power block of the ACSP plant

is actually depicted as the VesselBoiler and the heat exchanger named Boiler is providing power to it. After the boiler, the steam has to be superheated. The extra energy that the superheated steam contains in the form of sensible heat added at the superheaters, keeps the steam from condensing inside the piping or in the turbine's nozzles. Also, the superheated steam has high thermal capacity per unit volume, offering extremely-high thermal conductivity. Moreover, the high thermal conductivity offers powerful drying capability. Last but not least, steam can be superheated without applying really high pressure and the equipment can remain simple. So, the saturated steam coming out from the boiler, enters the superheaters where it exchanges energy with the hot HTF, which is still in pretty high temperature as it just entered the power block. The temperature of the saturated steam will be furthered increased resulting to superheated steam, which will be used to turn the turbine. A steam turbine has blades (set/stages of blades) that turn when steam blows past them. The mechanical energy produced will be transformed into electricity at a generator which is connected to the turbine. It is important to underline that the steam is not a source of energy, but an energy-transporting fluid that helps to covert energy. A non-condensing steam turbine uses high-pressure steam for the rotation of blades. This steam then leaves the turbine at the atmospheric pressure or lower pressure. The pressure of outlet steam depends on the load, therefore, this turbine is also known as the back-pressure steam turbine. There are lots of benefits of this steam turbine but at the same time it has few disadvantages which are listed below.

Advantages:

- The configuration of this steam turbine is very simple.
- It is relatively inexpensive as compared to extraction steam turbine.
- It requires very less or no cooling water.
- Its efficiency is higher as it does not reject heat in the condensation process.

Disadvantages:

- The biggest disadvantage of this type of steam turbine is that it is highly inflexible.
- The output of this turbine can't be regulated as it does not allow changing the pressure and temperature of steam in the turbine, therefore, it works best with the constant load.
- The thermal load of this turbine defines the flow of steam mass which makes it difficult to change the output value.

The idea, in the ACSP plant, is for the steam coming out of the turbine to return to the economizer, after being condensed, and repeat the power cycle. This loop is not shown in Figure 2.1 on page 36.

The rest of the equipment of the plant that was not mentioned above, helps connecting the TES with the solar field and the power block and makes the plant work as a whole. For example, the motors are powering the pumps up, which are responsible for the circulation of the HTF inside the piping. The various valves are placed in different parts of the plant and they are able to regulate the flow rate of the HTF/water passing through it.

Some of the main design parameters and characteristics of the ACSP plant are summed up in the following table [45].

**Table 2.1:** Main design parameters of the ACSP plant.

Parameter	Value
HTF	Solar Salt (60wt% NaNO <sub>3</sub> + 40wt% KNO <sub>3</sub> )
TES system	Two-tank direct
Expected power output	4.7 MW
Turbine efficiency	37.5 %
DNI <sup>1</sup>	1.9 kW/m <sup>2</sup>
Solar Field total area	27 acres
Mirrors total area	30000 m <sup>2</sup>
Receivers diameter	0.07 m
Receivers total length	5400 m
HOT_TANK height	10 m
HOT_TANK diameter	24 m
COLD_TANK height	13 m
COLD_TANK diameter	29 m
Economizer heat transfer area	150 m <sup>2</sup>
Boiler heat transfer area	330 m <sup>2</sup>
First Superheater heat transfer area	16 m <sup>2</sup>
Second Superheater heat transfer area	15 m <sup>2</sup>

1: Based on the average DNI in Sicily

As far as the everyday operation of the ACSP plant is concerned, it can be divided in the following stages:

### **The Startup Line**

This line is activated only during the startup of the plant. The motor M1 is activated and the valve XV1 is open. The pump P1 directs the solar salt from the tank SALT to the COLD\_TANK at a temperature of 300°C, which is 80°C above its melting point, in order to minimize the risk of crystallization inside the pipes. This procedure will go on till a specific level of molten salts is reached inside the COLD\_TANK. It should be underlined that the startup line is not activated everyday, but only when fresh molten salts have to be introduced into the system, for example after maintenance of the plant.

### **The Solar Line**

This is actually the operation of the plant during the day. Once the desired amount of salts is reached inside the COLD\_TANK, the motor M2 is activated and the valves XV2 and XV7 are open. This allows the cold solar salt to pass through the solar field (PIP1). There, it increases its temperature up to 600°C and by passing through the valve XV7, it reaches the HOT\_TANK. Some of the hot solar salt will be stored in the HOT\_TANK for later use. The rest of it has to pass at the power block in order for electricity to be produced. So, the motor M3 is activated, along with the valve XV5. An amount of the hot solar salt can now pass through the superheaters and the economizer, exchanging energy with the water/steam. The valve XV6 is, also, open to release the water. No pump is needed in the water line, because it is able to flow naturally thanks to the difference of the pressure between the tank WATER and the SINK1. The temperature of the hot solar salt is gradually decreasing and eventually reaches its lowest value of around 290°C at the outlet of the economizer.

### **The Generation Line**

During the night, the solar line is deactivated and the DNI reaching the solar field can be considered equal to zero. The motor M2 is tuned off and the valves XV2 and XV7 are closed. Now, the HOT\_TANK has no inlet stream. Its outlet stream of hot solar salt, driven by the pump P3, enters the power block and continues the heat exchange with the water/steam. Theoretically, the power generation is driven by the market demand, which in reality is not constant, so the flow rates of the water and hot HTF should change accordingly. At the end of the night, the level of the hot solar salt in the HOT\_TANK will have reached its minimum. The solar line is activated again at sunrise.

The expected temperatures of the solar salt at some of the key parts of the ACSP plant are summed up in the following table. Also, in the two following figures, two images of the ACSP plant are presented, taken from the official website of the Archimede Solar Energy company.

**Table 2.2:** Temperature of the solar salt at various parts of the ACSP plant.

Solar Salt	Temperature(°C)
at the COLD_TANK	300
at the Solar Field outlet	~600
at the HOT_TANK	~550
at the Power Block outlet	290

**Figure 2.3:** Digital maquette of the ACSP plant [71]**Figure 2.4:** The two tanks and a part of the solar field of the ACSP plant [71]





# Chapter 3

## Dynamic Simulation with DYNSSIM

From chemical engineering to economics, the operation of all processes varies over time. For some of the cases, this variation is an inherent characteristic and for others, it is caused by external disturbances or regular operational changes. Many chemical processes are intended to run at steady state and for practical purposes they can be modeled as such [72].

Steady state models have been widely used in the industry for process conceptualization, design and evaluation. However, the steady state represents an idealistic condition, used by the engineers as a representation of design conditions which are not always accomplished in practice [73]. This type of model is typically carried out during the conceptual phase of a project, in order to gain a better understanding of how a design can be changed to get the most out of the process. So, when dealing with real-life transient conditions, standard process design approach is just a gross approximation and it may lead to poor equipment specification or even to complete failure in evaluating the design reference conditions [74]. And this is where dynamic modeling is useful. In contrast with the steady-state modeling, the dynamic one does not assume that the variables remain constant during time. A steady state model's objective is to describe the variables when they have been stabilized over time. A dynamic model's scope, on the other hand, is describing how the system, starting from an initial condition, changed during the time to reach a steady state. The Figure 3.1 on the following page depicts clearly the different scopes of these two models. A steady state model deals only with a small part of the process, "ignoring" the possible alterations that happened before the system reached its steady state.

A dynamic model, consists of several integral, partial differential and algebraic equations. This rather complex set of equations aims to approximate the real behavior of the process. With the development in the computing sciences and the improvement of processors speed, the solution of these equations is assigned to the computers. Plenty of modeling softwares exist that are able to solve large models and produce really accurate dynamic simulations, giving several possibilities and degrees of freedom to the user. The software that was used to carry out the dynamic simulations in this thesis work is called DYNSSIM Dynamic Simulation. It is a commercial dynamic and custom-modeling simulator, developed by AVEVA Group plc, a British multinational information technology company based in the UK, since 1967.

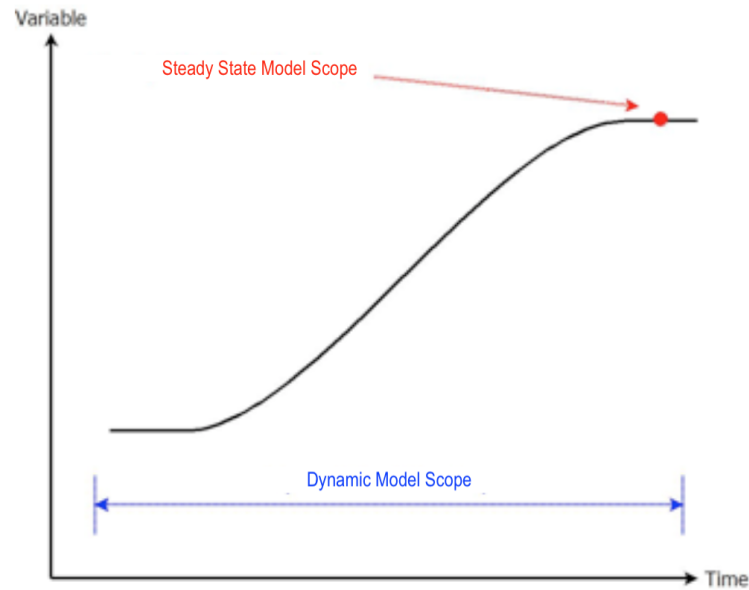


**Figure 3.1:** Comparison of Steady State and Dynamic model scopes [73]

It is important to mention some of the main applications that dynamic simulation has in the industrial sector [73, 75, 76]:

- **Process design.** In the case of a new design, an initial sizing of the equipment can be obtained by a steady state simulation and then it can be optimized based on its dynamic behavior.
- **Process evaluation.** It involves the performance evaluation of an existing piece of equipment or plant running under process conditions different from the ones initially designed. The use of different dynamic models for the same process will quickly allow the engineer to determine the optimum design as well as the limits of the process.
- **Process control.** Design and testing of regulatory control systems - selection of control structures, control algorithms and initial tuning of loops. It is one of the most important applications. Strategies can be evaluated via dynamic simulation in order to determine the best, most cost-effective control system. Process controllers can be easily pre-tuned, saving hours of expensive real-life tests performed in the plant.
- **Development of start-up and shutdown procedures.** They are both really important procedures for the plant and they can be tested and optimized with dynamic simulation. Potential hazardous conditions during these activities can be identified and tons of out-of-spec products can be avoided.
- **What-if analysis.** Run dynamic models which allow the determination of unsafe and hazardous conditions during operation. Equipment malfunction scenarios are studied.

- **Analysis of intrinsically dynamic process.** Batch, semi-continuous and periodic processes.
- **Design of relief and blowdown systems.** This is always an essential part of the safety of the plant.
- **Operator training.** Dynamic simulations give the opportunity to the operators to gain experience on the process. Complete replication of the control room can be easily installed on site to help train operators before the real plant experience. Operator Training Simulators (OTS) allow to run various scenarios related to the function of the plant, either with routine (normal operation/start-up/shutdown) or non-routine (emergency, equipment malfunction) scenarios.

So what are the advantages that a dynamic simulation software like DYNMIM Dynamic Simulation can offer to the user?

- **A risk-free environment.** A safe way to test and explore various "what-if" scenarios. The effect of changing process variables can be seen without putting production at risk. This allows making the right decisions through trial and error before implementing them in the real plant.
- **Saving money and time.** Virtual experiments with simulation models are much less expensive and take less time than experiments with real assets. Without them, all the experiments should be carried out in the real plant, thus spending valuable resources.
- **Visualization.** 2D and 3D in-software animations allow concepts and ideas to be more easily verified, communicated and understood through a user-friendly environment.
- **Increased accuracy.** Many details can be captured, providing more precise forecasting.

A CSP plant deals with some intrinsically dynamic phenomena, that need a dynamic model and simulator in order to be studied. For example, the DNI reaching the solar field is not constant throughout the day. There are rather strong transients during sunrise and sunset that affect the plant. Via the solution of the dynamic models, the simulator is able to compensate for these changes and to adjust the operation of the plant accordingly, mainly through the control system, in order to keep a constant power output. The user is then able to come to some important conclusions concerning the process that they study.

In this chapter, ACSP plant is used as a case-study, in the environment of DYNMIM Dynamic Simulation. At first, a control system is designed and tested for the plant. Then, the same system is simulated with a different HTF and its behavior is compared to the molten salt system. Different TES configurations are, also, tested. New control loops are implemented and the performance of the modified ACSP plant is compared to the original one. DYNMIM allows the user to write scenarios in a simple programming language similar to C++, that help simulating a specific process within the plant. Real-time graphs follow the changes

in variables with time, while the scenario is running, and they are a really accurate way to monitor the behavior of specific equipment or the whole plant and draw some really important conclusions. Simple yet useful live values of variables of interest can, also, be introduced in the flowsheet. Long simulations can be fast-forwarded up to 9999x.

As already mentioned before, the main goal of the simulations that follow, is to provide a useful multi-level comparison between two different widely used HTFs (molten salts and Therminol VP-1) and different TES systems in the CSP field. The fact that all of these simulations are based on the same existing CSP plant is really important, as in this way it is known a priori which goals the various configurations should accomplish, making it easier to understand whether they are feasible or not, by looking at their performance.

The following figure shows how a flowsheet of DYNsim looks like, including most of the tools it features, both for engineering and OTS purposes.

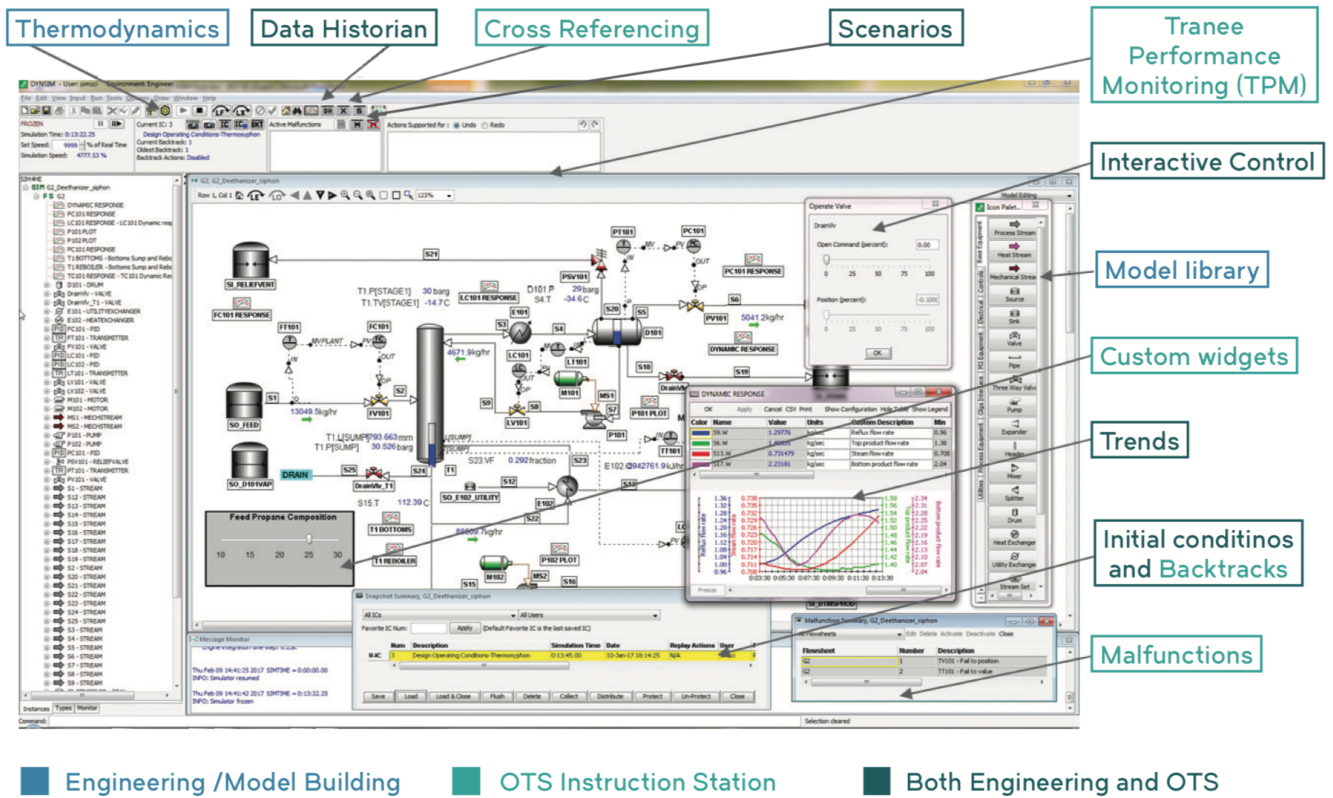


Figure 3.2: Flowsheet of DYNsim Dynamic Simulation [77]

The most important parameters of the ACSP plant are summarized in Table 2.1 on page 39. These are the standard values that guarantee the safe and correct operation of the plant and they should be respected in all of the simulations that follow.

Of course, there is a number of assumptions/approximations that were made in order to make the simulations simpler:

1. The solar field is modeled by the pipe model PIP1. The solar energy reaching

the field is provided as an external duty to the pipe. The surface area of the pipe PIP1 is equal to the total surface area of the mirrors present in the solar field.

2. The heat losses of the metal of the pipe PIP1 to the ambient are assumed to be equal to zero. Same goes for the heat losses from the fluid to the metal of the pipe.
3. The HTF is modeled as incompressible fluid.
4. The power demand of the electrical grid is constant.
5. No meteorological conditions such as clouds or dust are considered.
6. The reverse flow factor is equal to zero in every equipment.
7. The sunrise starts at 07:30am and ends at 08:30am and the sunset starts at 20:30pm and ends at 21:30pm. During this time the DNI is ramped from zero to maximum and from maximum to zero, accordingly.
8. In the power block, the condensed water turbine loop, which is recycled back as inlet water, is skipped.

### 3.1 ACSP plant with two-tank direct TES

The two tank direct TES system with solar salt (60wt%  $\text{NaNO}_3$  and 40wt%  $\text{KNO}_3$ ) as the HTF, is the original configuration of the ACSP plant. Figure 2.1 on page 36 shows the general scheme of the plant. The function of the three different lines (start-up, generation, solar) was already analyzed in the previous chapter. Just to summarize, the general idea of the operation of the plant is the following: during the day the solar line is active and the cold HTF initially stored at the COLD\_TANK (by the startup line) passes through the solar field and it is heated up. Some of the hot HTF coming out of the solar field will be stored at the HOT\_TANK. The rest goes into the power block in order to exchange heat with the water/steam and produce power output. During the night, the solar line is deactivated and the generation line is "running". The hot HTF stored in the HOT\_TANK is pumped out and enters the power block to keep the power output at the desired level. After decreasing its temperature in the power block, it re-enters the COLD\_TANK.

Solar salt and Therminol VP-1 will be tested as HTFs for the ACSP plant with two-tank direct storage in the following simulations.

#### 3.1.1 Control System

Control systems exist in many systems of engineering, sciences and in human body. In chemical engineering, a control system contributes to the smooth function of a plant. It is an interconnection of components forming a system configuration that will provide a desired system response [78].

The plant can be thought of as a black box with inputs and outputs, as shown in Figure 3.3.

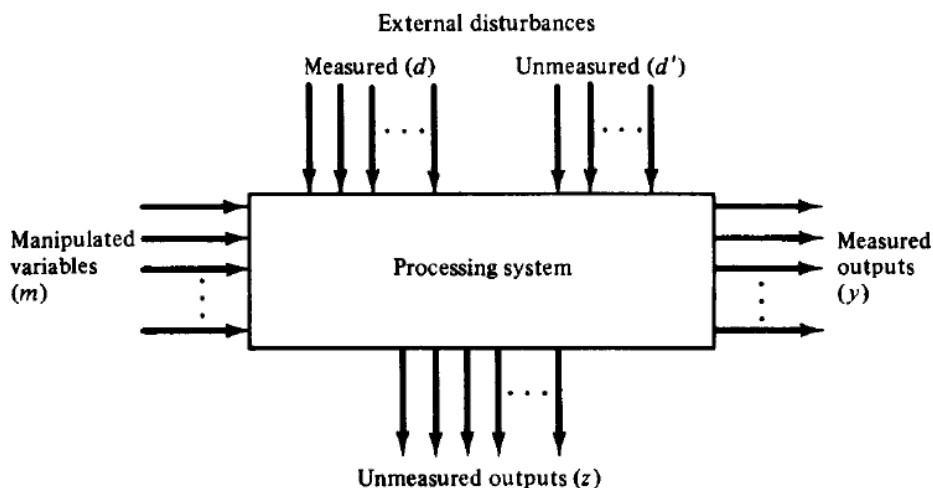


Figure 3.3: Description of a chemical process [79]

Input variables denote the effect of the surroundings on the chemical process. The output variables denote the effect of the process to the surroundings and they are

the actual response resulting from the system [80]. The input variables can be further classified into the following categories:

- Manipulated variables. Their values can be adjusted freely by the operator or the control mechanism.
- Disturbances. Their values are not the result of the adjustment by the operator or the control system.

The output variables can be, also, classified:

- Measured. Their values can be known by directly measuring them.
- Unmeasured. Their values are not or can not be measured directly.

A control system is the information structure that is used to connect the available measurements to the available manipulated variables and it can have different functions: suppress the influence of external disturbances, ensure the stability of the process or optimize the performance of the process. There are generally three types of control systems [79]:

- **Feedback control.** It uses direct measurements of the output controlled variables to adjust the values of the manipulated variables. The goal is to keep the values of the controlled variables at the desired levels (set points).
- **Feedforward control.** It uses direct measurements of disturbances to adjust the values of the manipulated variables. The objective is to keep the values of the controlled output variables at the desired levels.
- **Inferential control.** It uses secondary measurements, because the controlled variables cannot be measured, to adjust the values of the manipulated variables. The goal here is to keep the unmeasured controlled output variables at its set points.

In all of the three different control configurations described above, the controller is the active element. It receives the measurement and takes the appropriate action to adjust the manipulated variables. The most widely used type of controller in industrial automation is the PID (Proportional-Integral-Derivative). It offers the benefit of ease of use and high robustness. If  $y_m$  is the measurement reaching the controller and  $y_{sp}$  the value of the set point then the error  $e$  is the difference between them and it changes with time.

$$e = y_m - y_{sp} = f(t) \quad (3.1)$$

The goal of the controller is to minimize the value of  $e$  as much as possible. The output  $c$  of the PID controller is the sum of a proportion of the error plus its integral plus its derivative as it shown in the following equation:

$$c(t) = K_c e(t) + \frac{K_c}{\tau_I} \int_0^t e(t) dt + K_c \tau_D \frac{de}{dt} + c_s \quad (3.2)$$

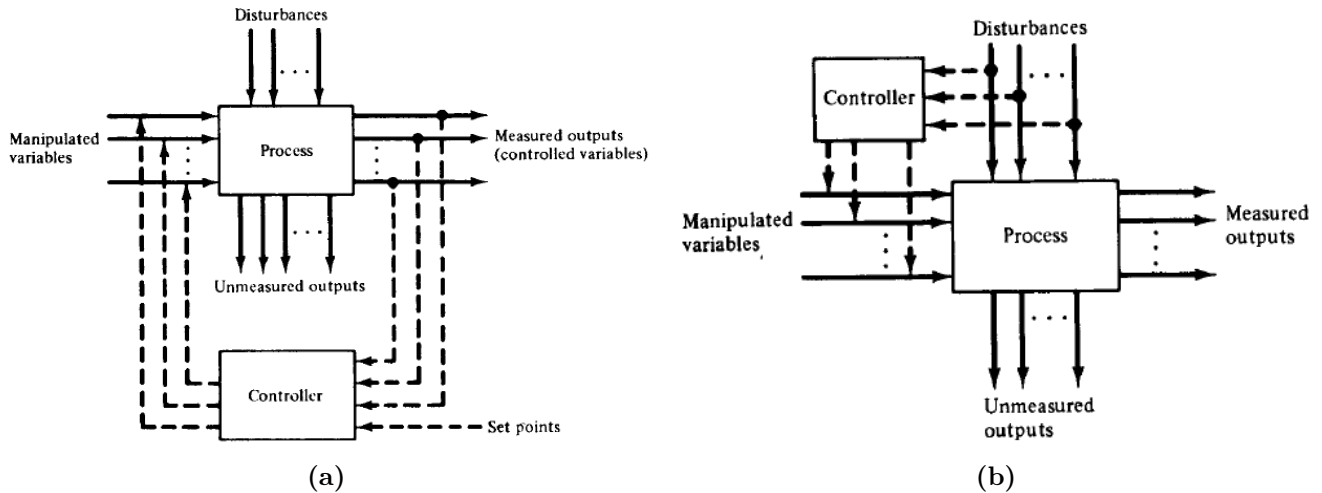


**Figure 3.4:** (a) Feedforward control system (b) Feedback control system [79]

$K_c$  is the proportional gain of the controller  
 $\tau_I$  is the integral time constant (or reset time)  
 $\tau_D$  is the derivative time constant

Each of the terms has its own advantages. The proportional term offers quick response. The integral part causes the controller output to change as long as an error exists. So, it can eliminate even small error. The derivative action permits the controller to anticipate what the error will be in the immediate future and applies a control action which is proportional to the current rate of change in the error  $\frac{de}{dt}$ . The control system that will be designed for the ACSP plant, includes PID controllers. Of course, it is much more difficult to control a complete chemical plant than a single unit. In the chemical plant there are interactions between the units that have to be taken into account. During the design phase of the control configuration it has to be decided where the controllers have to be placed, which are the most important variables to be altered, what are the set points that will be used. Generally, the simplest control configuration that works properly is the best [79].

As already mentioned, one of the biggest concerns for the operation of the ACSP plant is the possible freezing of the HTF inside the pipes. This concern has to be eliminated, especially at the point of the plant where the HTF reaches its minimum temperature: stream S24, at the output of the economizer (see Figure 2.1 on page 36). A PID controller can make sure that the temperature of the specific stream remains high enough, above the crystallization point of the HTF. Also, the set point of the controller will define the temperature at which the HTF will be stored at the COLD\_TANK, after exiting the power block. A suitable manipulated variable for this controller is the opening of the valve XV5, which is responsible for the flow rate of the HTF reaching the power block. A wide opening of the valve will allow more hot HTF to enter the heat exchanger train, thus increasing the final temperature of stream S24. Smaller opening will result to lower temperature for the specific stream.

The operation of the previous controller is much easier if the flowrate of the water



entering the power block is constant. Another PID controller can be introduced in the system for this purpose. By running several simulations, the right flow rate for the water can be found so that the BoilerVessel does not feel with liquid and a sufficient amount of superheated steam reaches the turbine for power generation. This flow rate will be used as the set point for the new PID controller that will be controlling the valve XV6.

A third PID controller will be used in order to control the flowrate in the solar line. Judging by the DNI reaching the solar field (PIP1) during the day, the flowrate of cold HTF has to have a specific value so that the desired temperature is reached at the output of the solar field (stream S22). This is an important point for the operation of the plant because if the flowrate is too low then the temperature inside PIP1 will get higher more easily, leading to a risk of vaporization of the HTF. If, on the other hand, the flow rate is too high, the DNI will not be enough to raise the temperature of the HTF at the desired value. This adjustment of the flowrate by the PID controller will be carried out by adjusting the opening of the valve XV2.

A scheme of the ACSP plant with the control system that was described above is presented in the following figure:

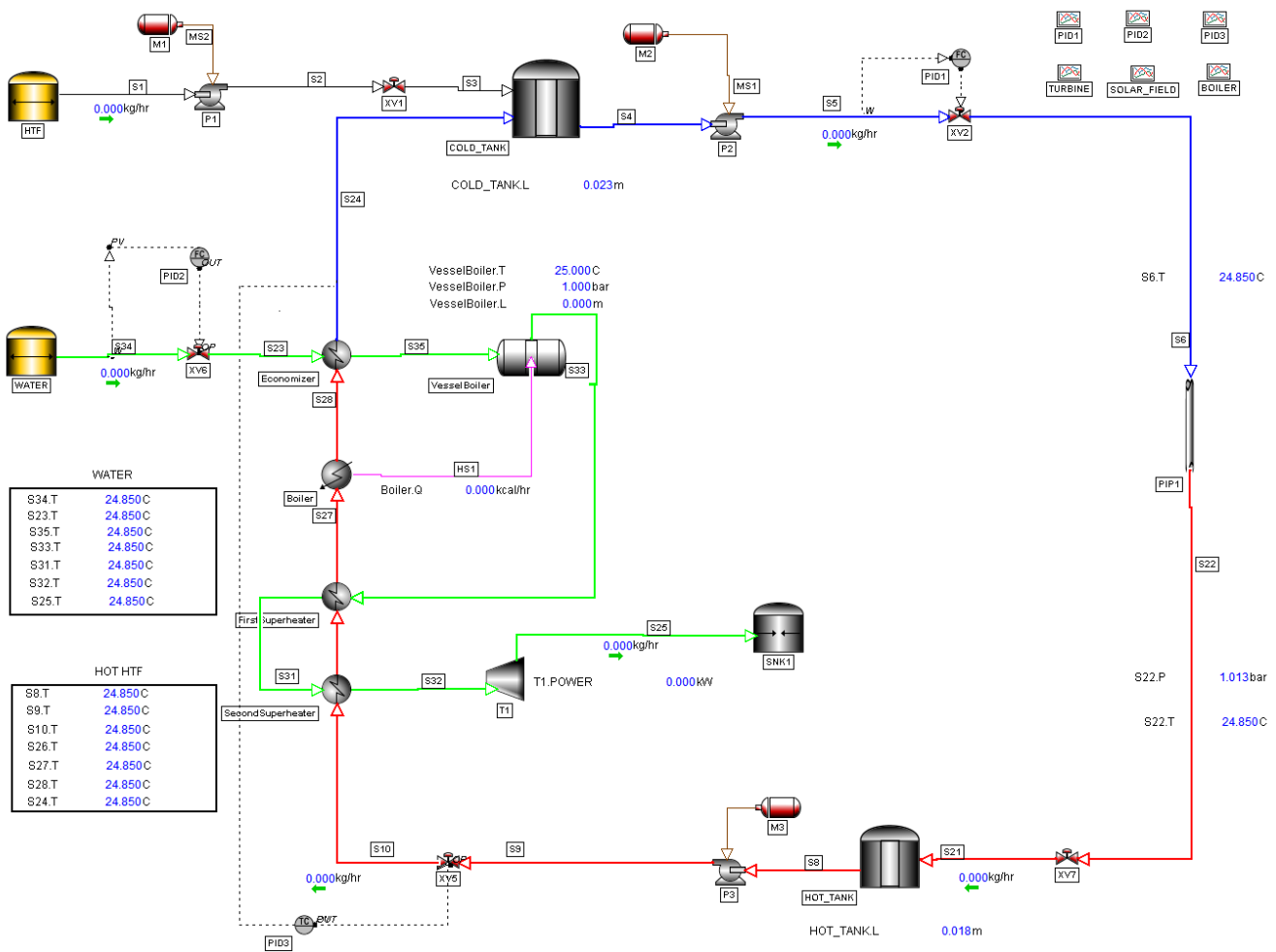


Figure 3.5: The control system of the ACSP plant

As it can be seen, DYNsIM gives the possibility to the user to introduce in the flowsheet the real time values of parameters of interest. They change during operation and this is a really good and direct way for the user to check at the same time if different parts of the plant are running smoothly. There is, also, the option to create graphs in order to study how some specific variables are changing with time. While the scenarios are running, data for the selected variables are collected and they are plotted, updating the graph as the time passes.

An overview of the controllers used in the ACSP two-tank direct TES plant is presented in the following table. The set points of the controllers depend on the HTFs used, due to their different physical and chemical properties.

**Table 3.1:** An overview of the controllers used in the ACSP two-tank direct TES plant.

Controller Name	Action	Manipulated Variable	Measured Output
<b>PID1</b>	Reverse	XV2.OP	S5.W
<b>PID2</b>	Reverse	XV5.OP	S34.W
<b>PID3</b>	Reverse	XV6.OP	S24.T

*\*OP: opening, Q: mass flow rate*

Direct action means that as the the measured output increases, then the manipulated variable increases as well. In the case that the increase of the former results to the decrease of the later then the action of the controller is reverse.

### 3.1.2 Solar Salt as HTF

Solar salt (60wt% NaNO<sub>3</sub> and 40wt% KNO<sub>3</sub>) is the HTF used in the real ACSP plant. It has actually become the most popular HTF in CSP plants thanks to its high temperature range (223°C-600°C), its efficient heat storage and its high safety. In order to build the simulation of the specific plant configuration in DYNsIM, there are some miscellaneous secondary parameters for the equipment that have to be specified. These parameters are gathered in the following tables.

**Table 3.2:** Parameters for the motors.

	M1	M2	M3
Speed (rpm)	3600	3600	3600

**Table 3.3:** Parameters for the valves.

	XV1	XV2	XV5	XV6	XV7
C <sub>v</sub>	500	500	300	120	500

C<sub>v</sub> is the valve flow coefficient and it expresses the valve's capacity for liquid or gas

to flow through it and it is connected to the pressure drop across the valve through the following equation:

$$C_V = \frac{W}{\sqrt{\frac{\Delta P}{SG}}} \quad (3.3)$$

$\Delta P$ : pressure drop

W: mass flow rate

SG: Specific gravity of the fluid (unitless)

Wherever needed as an input, the natural convection heat transfer coefficient is set equal to 0.1 kW/m<sup>2</sup>/K. This constant shows how easily the heat is transferred between the HTF and the solid surface area of the pipes, in the case that the fluid flow is caused by density differences within the fluid due to internal fluid temperature differences.

The overall heat transfer coefficient on the other hand, is used when there is a difference in temperature between the fluid and the surface. If the fluid flows due to an external force (here: pumps) then it is called forced convection. This overall heat transfer coefficient is set to 0.001 kW/m<sup>2</sup>/K for the two tanks and 1 kW/m<sup>2</sup>/K for the heat exchangers.

The total volume of the collectors at the solar field can be calculated by knowing that the field consists of 54 collectors of diameter 0.07 m and length 100 m each. Assuming cylindrical shape, the total volume is:

$$V_{collectors} = 54 \frac{\pi}{4} d^2 l \quad (3.4)$$

where d is the diameter and l is the length of a single collector. The result is 20.7 m<sup>3</sup>.

Once all of the necessary parameters have been inserted, the scenarios have to be written in order to simulate the different operations of the plant and run the main scenario, which simulates the 24-hour operation of the plant, starting from 8:30pm, when, hypothetically, the sun has just set.

### DYNSIM Scenario 1: Loading of the cold solar salt

This is for loading solar salt in the COLD\_TANK, through the startup line. It takes place at the very first run of the plant but also after maintenance (eg. anti-freezing procedure), when all of the HTF has been pumped out of the system and the plant has to restart. Valve XV1 is open and M1 is activated. Solar Salt is pumped out of the source-tank SALT at a temperature of 300°C and pressure of 1 bar. At this temperature and pressure it enters the COLD\_TANK. The scenario stops when the desired level of HTF is reached at the COLD\_TANK (11.7 m). No controllers are needed here. The valve XV1 is fully open and the motor works at its maximum velocity, so that the loading of the cold solar salt takes as less time as possible. The total time needed is about 16 hours. It is clear that this is a time-consuming and non-profitable procedure, during which the plant does not produce a power output, so it should be carried out only a few times during the year, when necessary. It introduces into the system the amount of HTF, that will be used for many cycles of heating, cooling and exchanging energy with the water/steam at the power block.

### DYN SIM Scenario 2: Loading of the hot solar salt

This scenario works as an intermediate step in order to reach the starting point of the main 24-hour simulation that follows. A sufficient amount of hot solar salt should be loaded in the HOT\_TANK so that the tank does not empty during the night operation, when there is no fresh input. This scenario, also, helps to compute the set point of PID1. By knowing that the peak DNI reaching the field PIP1 is  $1.9 \text{ kW/m}^2$  it can be found that the flow rate of cold solar salt entering the solar field should be 700000 kg/hr, in order to reach a temperature of around  $600^\circ\text{C}$  at the output of the PIP1 (stream S22). In that way, after some inevitable heat losses, the final storage temperature at the HOT\_TANK will be approximately  $555^\circ\text{C}$ . The scenario is stopped when the desired level of hot solar salt is reached inside the HOT\_TANK and it needs 6-7 hours.

### Main Scenario: 24-hour operation of the plant

This scenario simulates the operation of the plant throughout the night and day. It is a really good way to examine the strong transients present during sunrise and sunset, when the DNI is not constant, and how they affect the performance of the controllers and generally of the plant. It was decided that the simulation starts at 20:30, right after the sunset. So, at the initial point of the scenario, the DNI reaching the solar field is zero, the power output is, also, null and the level of the HOT\_TANK is 5.7m and the level of the COLD\_TANK is 4.5m.

The simulation starts by pumping hot solar salt from the HOT\_TANK to the power block. At the same time, water is pumped into the economizer at a temperature of  $210^\circ\text{C}$  and a pressure of 110 bar. After many simulations, it was found that the right flow rate for the water is 70000 kg/hr so this value is used as the set point of PID2 (S34.W). This is a value that does not let the VesselBoiler fill up with liquid and it is, also, able to produce a flowrate of superheated steam capable of giving 4.7 MW of power output. The set point of PID3 is set at  $290^\circ\text{C}$  (S24.T): this will be the temperature at which the cold solar salt enters the COLD\_TANK and, as already mentioned, it is really important for the PID3 not to let this temperature drop, due to the risk of crystallization.

- The first minutes of the simulation (20:30pm - 20:55pm)

In the following two plots, the behavior of the two active controllers (PID2 and PID3) is presented, during the first 25 minutes of the simulation. This first part of the simulation, till the desired power output is reached, is the most suitable in order for the engineer to draw conclusions for the suitability or not of the selected control system. In other words, it is the most challenging phase for the controllers, which need to quickly stabilize the system starting from scratch.

In Figure 3.6 on the next page it is evident that there is a strong oscillation of the manipulated variable (opening of the valve XV6) during the first 10 minutes. This oscillation does not seem to affect the output of the controller (flow rate of water stream S34), that follows a smoother curve with a much smaller oscillation.

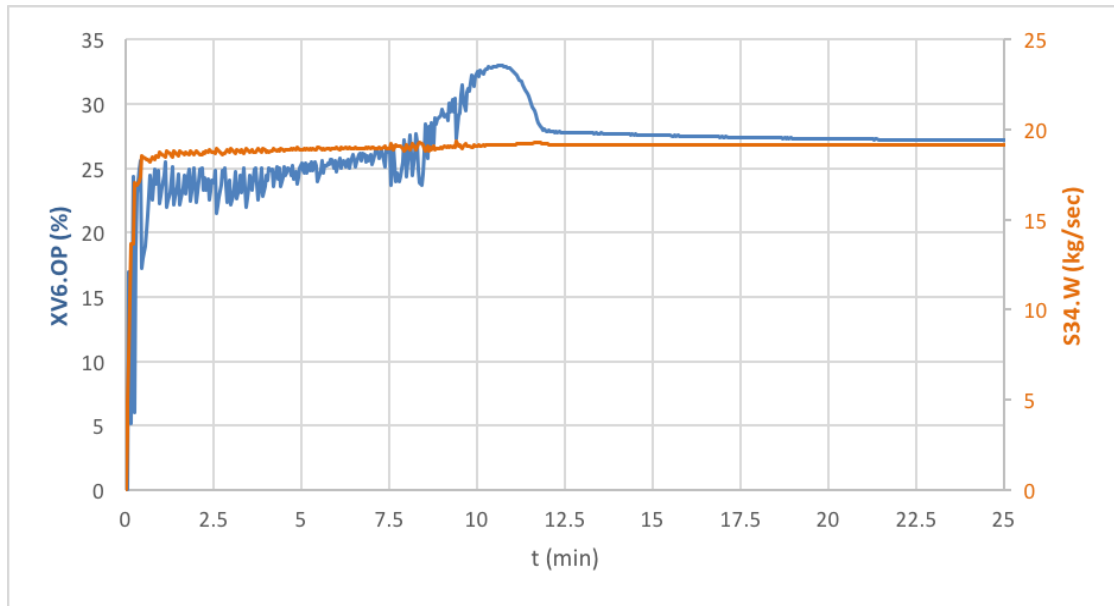


**Figure 3.6:** Controller PID2 during the first 25 minutes of the simulation

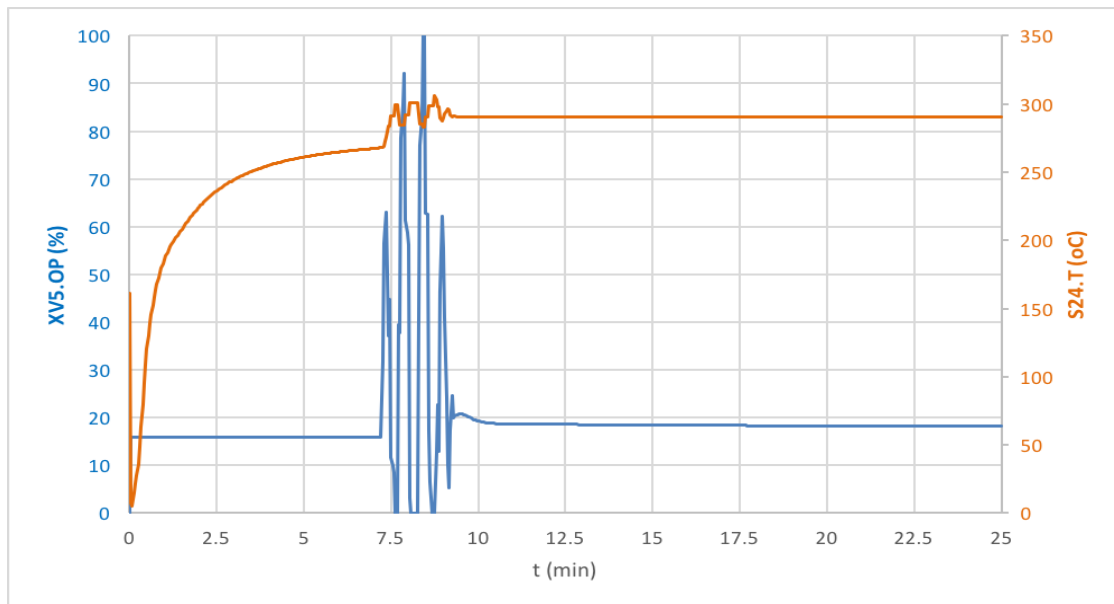


**Figure 3.7:** Controller PID3 during the first 25 minutes of the simulation

After the 10 minutes, there is a sudden pick at the opening of the valve and the stabilization follows, after 2 minutes. This behavior can be explained by looking at the Figure 3.7 of PID3. At first a constant value of 16% is selected for the opening of the valve XV5. When a certain temperature is reached (260°C), the PID3 is set to automatic mode. As it can be seen at the graph, right when the PID3 is set to auto, there is a strong but quick oscillation and the controller manages to reach its set point in less than 2 minutes.

When the PID3 is steady, the flowrate of the hot solar salt entering the power block is, also, steady. This flowrate strongly affects the flowrate of water/steam, because they are exchanging energy at multiple points within the power block. This is why

the stabilization of the two controllers comes almost at the same time (around 10 minutes).

The response of the controllers PID2 and PID3 is more than satisfying, in this first "test". They are able to overcome a fast transient and quickly reach their set points. Of course, the most important characteristic of the plant, that should always be monitored, is the power output. How long does it take for the turbine to reach the plant's specification of 4.7 MW, when starting from 0 MW in this simulation?

The power output during the first 25 minutes of the simulation is plotted:

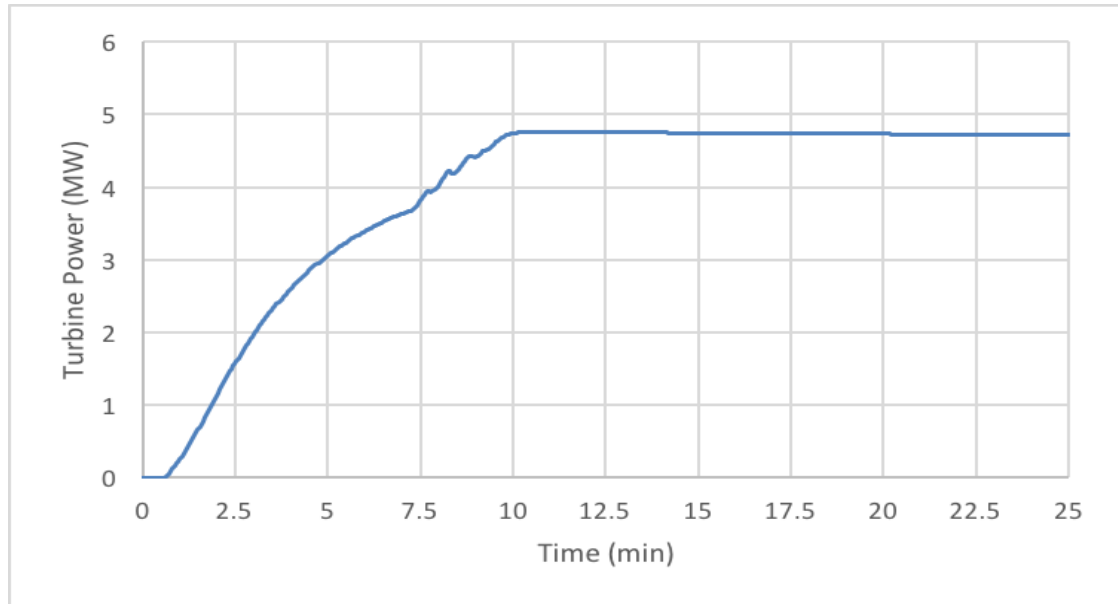


**Figure 3.8:** Power output during the first 25 minutes of the simulation

The power output keeps increasing for the first 10 minutes, because the flow rate of the superheated steam reaching the turbine's blade becomes higher and higher. When it is stabilized (around 10 minutes, as already discussed in the previous plots) the power output is stabilized as well, at 4.7MW. It is, also, important to notice that there is a small time span at the beginning of the simulation during which the power output remains zero. This is because it takes some time for the first portions of water to be vaporized at the VesselBoiler. So, for the first minute no superheated steam reaches the turbine, thus no power output is produced.

As it was mentioned in Chapter Two, in the two-tank direct storage, the levels of the tanks should increase/decrease linearly. In order to confirm this for the ACSP plant, the levels of the COLD\_TANK and HOT\_TANK are plotted, always for the first minutes of the simulation.

As it was expected, the slope in both cases is constant. The level of the HOT\_TANK is decreasing as hot HTF is pumped out and the level of the COLD\_TANK is increasing as cold HTF is entering, after the power block. The total mass balance for a single tank, since no reactions are taking place:

$$\frac{dm}{dt} = W_{in} - W_{out} \quad (3.5)$$

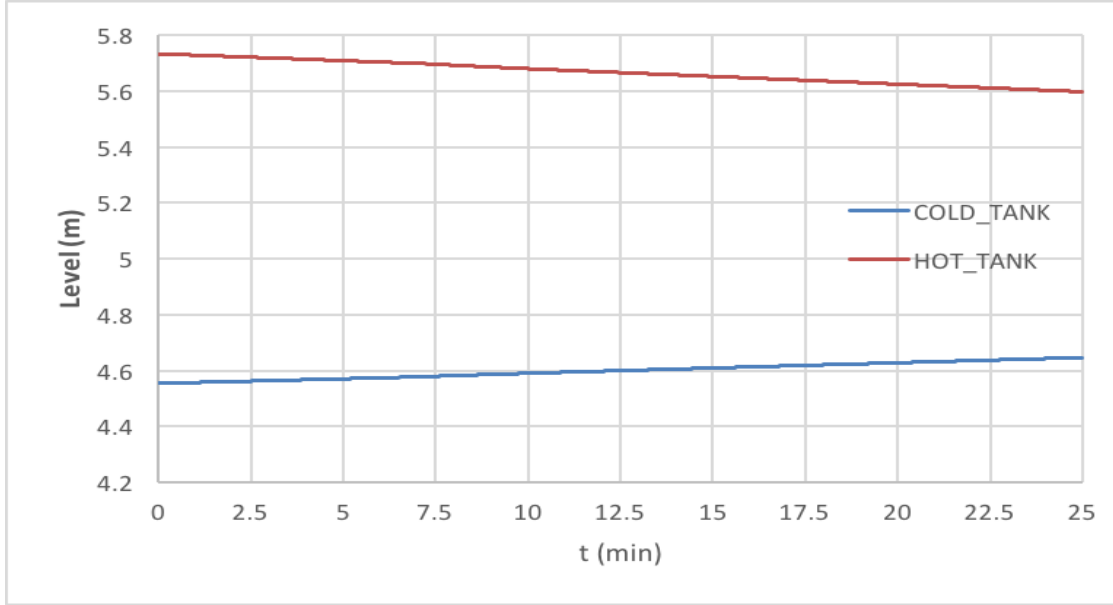


**Figure 3.9:** Level of the tanks during the first 25 minutes of the simulation

where  $m = \rho V$  is the mass of HTF in the tank and  $W$  is the mass flow rate. By assuming constant density  $\rho$ :

$$\frac{dV}{dt} = \dot{F}_{in} - \dot{F}_{out} \quad (3.6)$$

where  $\dot{F}$  is the volumetric flow rate.  $V = Al$ , where  $A$  is the horizontal section and  $l$  the level of the HTF.

$$A \frac{dl}{dt} = \dot{F}_{in} - \dot{F}_{out} \quad (3.7)$$

In both cases of the hot and cold tank, the input volumetric flow rate is never equal to the output flow rate, thus the accumulation terms are always non-zero. During the night, the input of the HOT\_TANK is zero and the output is positive. So, the accumulation will be lower than zero, resulting to a gradual decrease of the level of the HOT\_TANK. The larger variations of the level of the HOT\_TANK compared to the COLD\_TANK is due to the different diameters [45].

Now that the parameters of the controllers are known, they are summed up in the following table:

**Table 3.4:** Parameters for the controllers.

	PID1	PID2	PID3
Output	S5.W	S34.W	S24.T
Set point	700000 kg/hr	70000 kg/hr	290 °C
Proportional gain	0.1	0.1	0.05
Integral reset rate	0.1	0.1	0.1

- Night operation

It is clear from the previous Figures 4.6 - 4.8 that only after approximately 10 minutes, the most important variables of interest in the generation line are stable. The controllers do not oscillate, the flow rates along the generation line are constant and the power output has reached the desired level.

A snapshot of the flowsheet of the plant during the night (at 04:00am) is presented in the following figure.

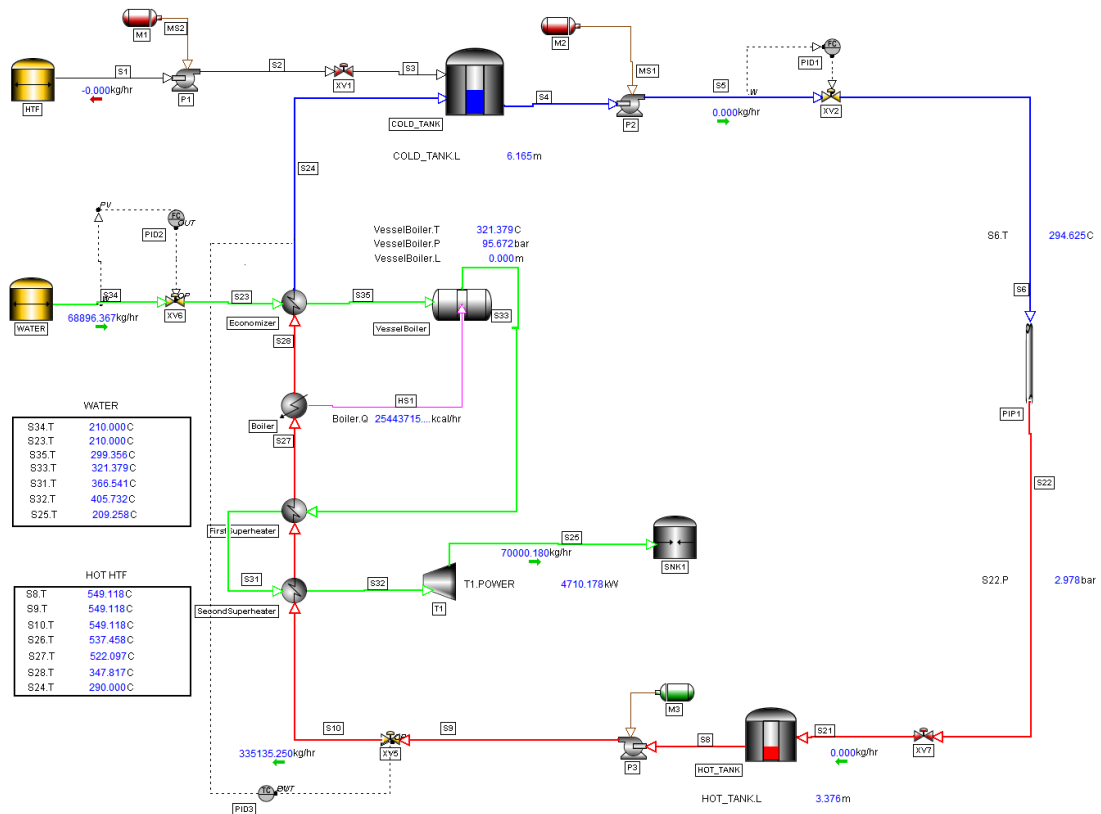


**Figure 3.10:** Operation of the plant during the night (04:00am)

Some comments:

- The power output has remained equal to 4.7 MW.
- The level of HTF of the HOT\_TANK has been further decreased and the level of the COLD\_TANK has increased as predicted by the Equation 4.6.
- The flow rates managed by PID2 and PID3 have remained constant.
- The output stream of the turbine (S25) has the same temperature (210°C) as the inlet stream of water. This is really advantageous because, in reality, the steam coming out of the turbine is condensed and it is recycled back to the economizer. When the inlet and outlet stream of the water line have similar temperatures, this procedure of condensation and recycling requires less energy.
- The VesselBoiler develops a high pressure because of the relatively low flow conductance of the steam turbine.

- Sunrise (06:30am - 07:30am)



Sunrise is probably the most difficult transient that the plant has to deal with. The reason is that right before the sunrise and right after the end of the night operation, the HOT\_TANK has reached its minimum level. Specifically for this simulation, the level of HOT\_TANK before sunrise is 2.4 m and the level of COLD\_TANK is 6.8 m. The low level of hot solar salt makes the HOT\_TANK vulnerable to temperature changes. An input stream of low temperature will easily decrease the overall temperature inside the HOT\_TANK. This will result to a lower temperature of the hot solar salt entering the power block, possibly causing problems to the stability and efficiency of the process.

The sunrise is simulated in the following way in the DYNsIM simulation: at 06:30 am the DNI starts increasing, reaching its maximum value after one hour. As already commented in the simplifications made for the simulation, by looking at the sunrise times throughout the year in Sicily, a sunrise duration of one hour starting at 06:30 am, is a good approximation for the purposes of the simulation.

As in the case of the first minutes of the simulation, also during the sunrise the values of the variables of interest were monitored and plotted. The plots are presented in the figures that follow:

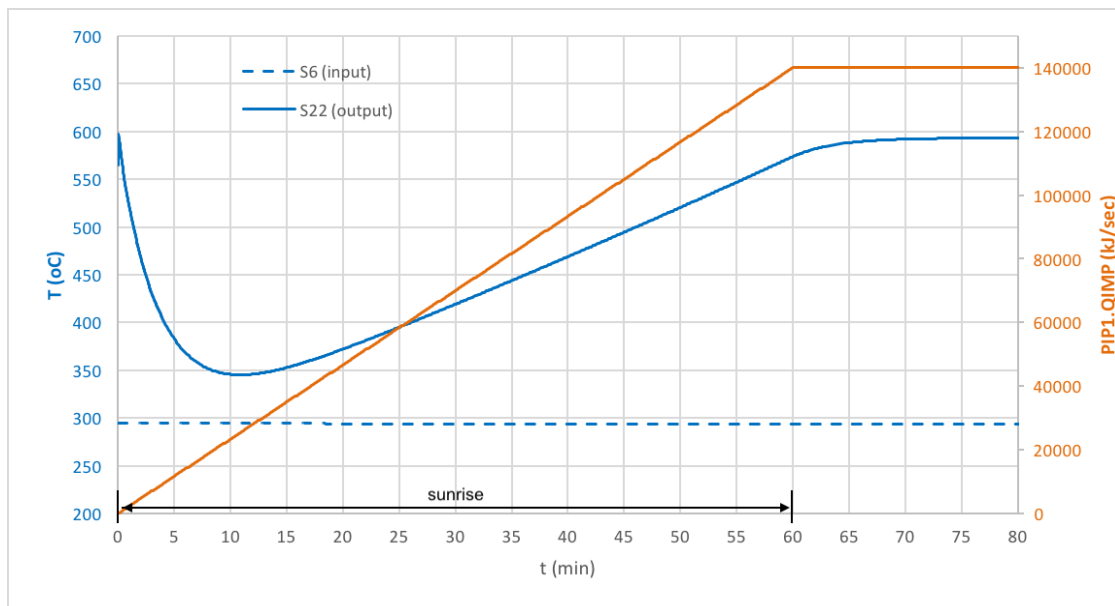


**Figure 3.11:** Solar Field temperatures and DNI during sunrise

During the first 60 minutes, the sun rises so the DNI reaching the solar field (PIP1) is increasing. Of course, in reality the increase of the radiation reaching the PIP1 is not exactly linear, but for the purposes of the simulation, linearity is a convenient and quite accurate approximation. During the first minutes of the sunrise, even if the heat imposed to the PIP1 is increasing, the output temperature is decreasing. This is because the radiation (QIMP) is still not high enough in order to maintain the output temperature of around 600°C. So, the output temperature (S22.T) keeps decreasing till the point where the QIMP has a sufficiently high value. From that point on, S22.T starts increasing. By the end of the sunrise ( $t = 60\text{min}$ ), when the

QIMP reaches its final value, S22.T is approximately 575°C. It keeps increasing for some more minutes and eventually it slowly reaches the desired output of 600°C.

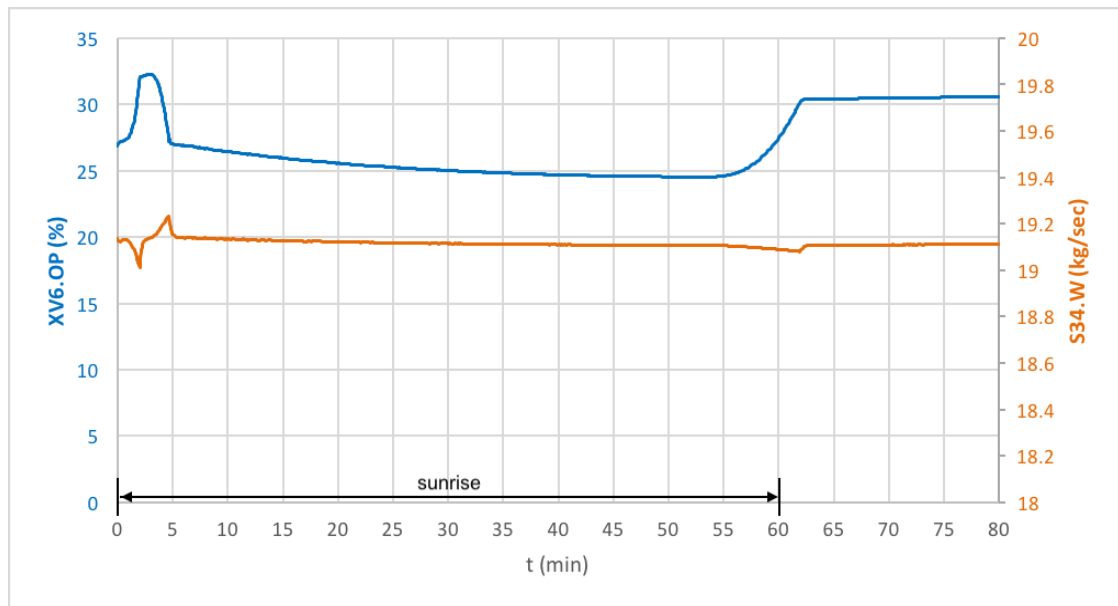


**Figure 3.12:** Controller PID2 during sunrise

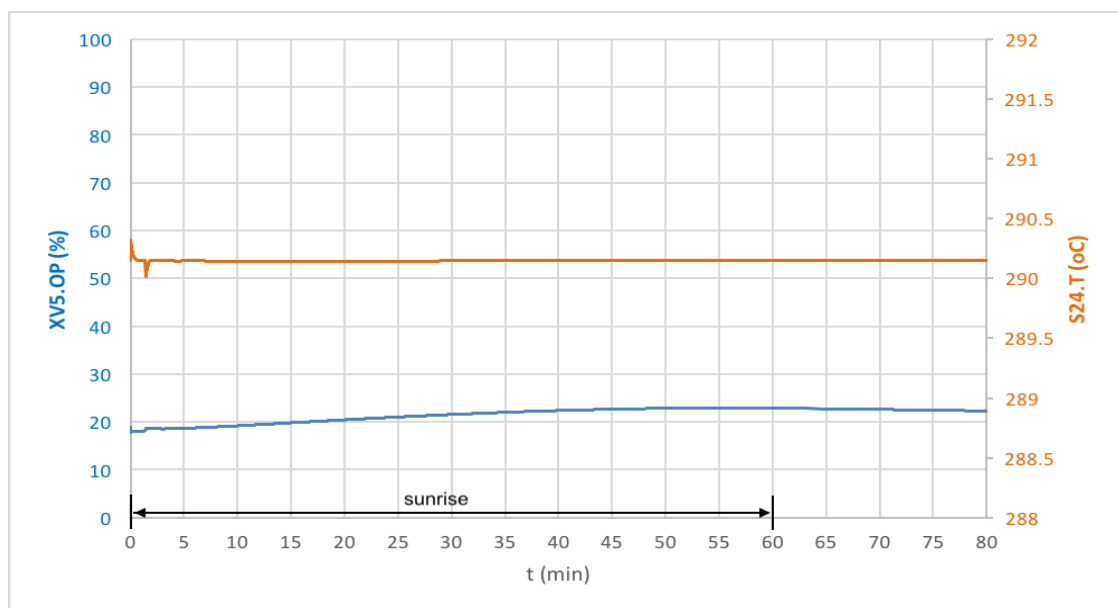


**Figure 3.13:** Controller PID3 during sunrise

In Figure 3.12 and Figure 3.13 the action of the controllers PID2 and PID3 during the sunrise is plotted. PID3 shows, once again, a really stable behavior. It manages to keep the temperature of steam S24 at the set point, by smoothly and only slightly adjusting the valve's XV5 opening. The really small oscillation at

the very beginning of the plot can be explained by looking at the Figure 3.12 on the preceding page of PID2. The strong transient introduced in the system at the beginning of the sunrise affects the controller PID3, which produces a small peak at the opening of the valve, in the first 5 minutes of the sunrise. This causes a small oscillation of the output variable (S34.W) of the controller, always around the set point. The behavior of PID1 is not plotted but it manages to keep the set point throughout the sunrise with no problems.

The sunrise is the most challenging phenomenon for the controllers of a CSP plant during the daily operation. The control system selected for the ACSP plant manages to guarantee the smooth operation of the plant, after only a short period of adjustment.

But how does the sunrise affect the power output?

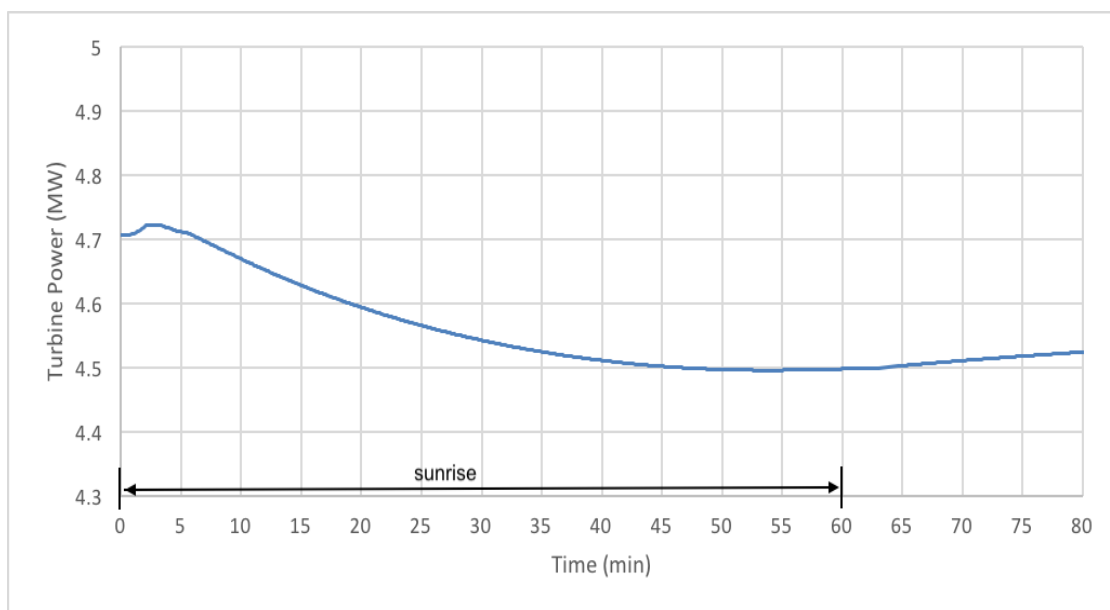


**Figure 3.14:** Power output during sunrise

Starting from the 4.7 MW reached during the night operation, firstly there is a slight increase at the value of the power output, because of the momentary increase of the flow rate of the water (S34.W), as seen in Figure 3.12 on the facing page. After that, the power output decreases 0.2 MW in total, till the end of the sunrise. This is because of the decrease in temperature of the solar salt coming out of the solar field (S22.T), as already analyzed in Figure 3.11 on page 59. This decrease means lower input solar salt temperature at the power block, thus lower power output. Only when S22.T reaches again values close to 600°C, the power output stops decreasing, it reaches the minimum of 4.5 MW and slowly starts increasing again.

It is not shown in the graph, but after reaching its minimum value, it takes for the turbine almost 1 hour to produce 4.6 MW and another 3 hours to reach the specification of 4.7 MW. Even if it is, in total, only a small decrease in the power output, it is important to mention that the time needed for the system to reach the 4.7 MW is significant. Generally during periods of decreased power generation,

it might be judged necessary to use a secondary fossil-fuel system, to boost the turbine and reach the specification output of the plant. A solution to tackle this problem in the case of the ACSP plant is to increase the set point of PID3 from 290°C to 295°C. This will allow higher flow rates of hot solar salt to enter the power block, helping with the production of more steam. The extra steam produced, will help to cover the previous losses of the power output. Indeed, a simulation run with 295°C as the set point of PID3, helped the system to reach again the 4.7 MW in less time, 2 hours quicker than before.

- Day operation

A screenshot of the flowsheet of the ACSP plant at 13:00pm is presented:

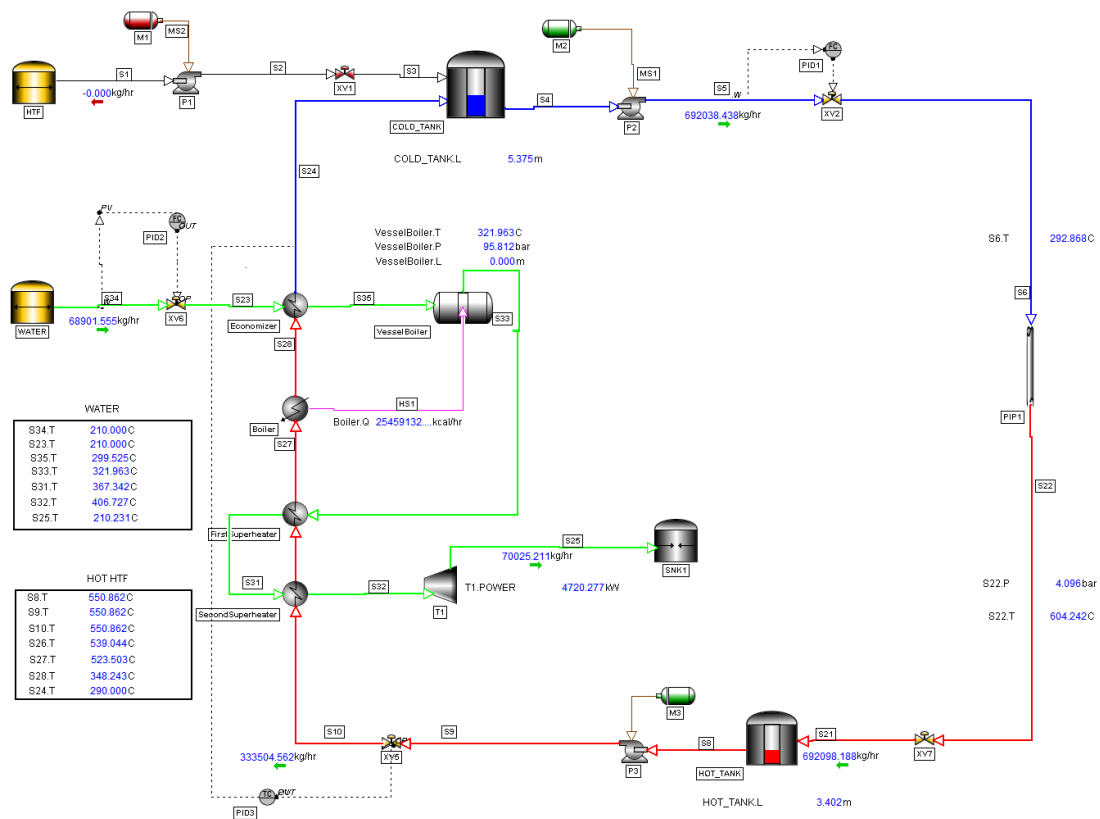


**Figure 3.15:** Operation of the plant during the day (13:00pm)

As it can be observed:

- All of the set points have been reached
- The power output is 4.7 MW
- The level of HOT\_TANK has increased to 3.4m compared to the initial level of 2.4m, before the sunrise. The input flow of the HOT\_TANK during the day is almost double compared to the output. At the end of the day operation this will result to a level high enough in order for the plant to enter to the night operation, where hot solar salt will be pumped out of the HOT\_TANK.
- Respectively, the level of the COLD\_TANK has decreased. The behavior of the increase/decrease of the levels of the tanks is always linear, as already mentioned.

### 3.1.3 Therminol VP-1 as HTF

At this point, a new simulation is carried out where the solar salt is replaced by Therminol VP-1. Therminol VP-1 is an organic thermal oil that consists of biphenyl ( $C_{12}H_{10}$ ) and diphenyl oxide ( $C_{12}H_{10}O$ ). Its main characteristics were mentioned in the previous chapters. This new simulation allows to:

1. Examine how the ACSP plant would work with a different HTF, always in comparison to the results obtained from the solar salt simulation.
2. Carry out a performance comparison between the solar salt and Therminol VP-1, as HTFs in a CSP 2-tank direct TES plant.

The suitability of the control system selected for the ACSP plant, during the strong transients imposed by the beginning of the simulation and sunrise, was already tested and discussed thoroughly. So, in the case of Therminol VP-1 it is more important to focus, for example, on the night operation of the plant and spot differences compared to the night operation with solar salt. The controllers are kept the same, but their set points may change.

- Night operation

Before starting the night operation of the plant, cold Therminol VP-1 stored in the COLD\_TANK at a temperature of 250°C (chosen based on literature [81]), passed through the solar field during peak DNI and it entered the HOT\_TANK at 400°C, which is the maximum operating temperature for the specific HTF. This is the temperature at which Therminol VP-1 will enter the power block. At the end of this procedure the level of the HOT\_TANK is 6 m and the level of the COLD\_TANK is 8.4 m. This is the initial point of the night operation. The recommended set point for PID1 is 1000000 kg/hr.

The PID3 controller manages the temperature of the HTF at the output of the power block. With Therminol VP-1 there is a bigger freedom as far as the choice of this specific temperature is concerned thanks to the low crystallization point. It freezes at 12°C so there is no risk for the pipes and there is no need for anti-freezing operation. In any case, the set point should be close to the storage temperature of the COLD\_TANK. It is set at 255°C. The optimal flow rate of water entering the power block was already computed in the case of solar salt ACSP plant. It remains the same, also, in the case of the Therminol VP-1 ACSP plant, as none of the equipments along the heat exchanger train has been changed. So, the set point of PID2 remains equal to 70000 kg/hr of water.

With this initial parametrization, the simulation of the night operation runs. The DYNsim flowsheet of the plant is presented in Figure 3.16 on the following page, after a couple of hours of operation.

There are many interesting points to be made concerning this simulation:

1. The turbine quickly manages to reach the desired power output of 4.7 MW.
2. The "water cycle" does not close. In reality the steam coming out of the turbine is condensed and it is recycled back to the economizer. So, in order

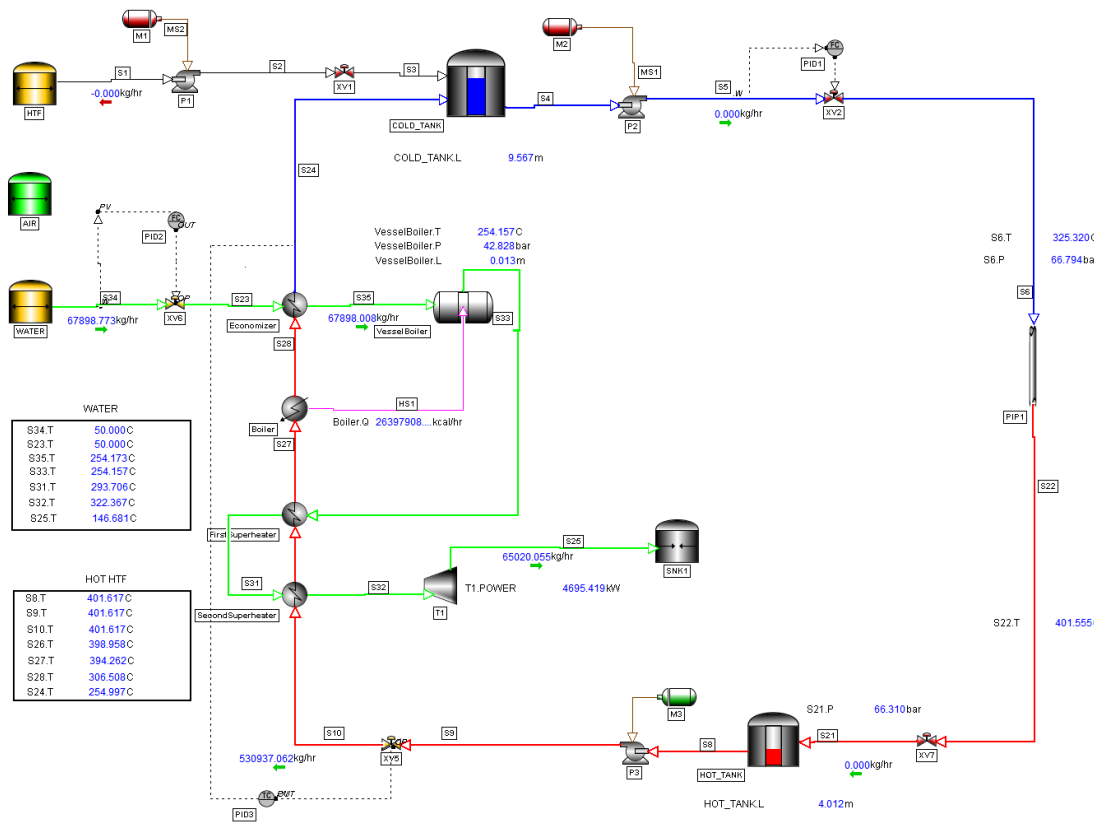


**Figure 3.16:** Therminol VP-1 as HTF. Operation of the plant during the night (00:00am)

to make the condensation less energy consuming, the starting temperature of water entering the economizer should be close to the final temperature coming out of the turbine. In the case of Therminol VP-1 a quite low temperature of water is used (50°C) in order to facilitate the heat exchange resulting to a temperature of 147°C at the end of the water line. This means that extra equipment and energy will have to be used to make the recycle feasible.

3. The set point of PID3 (S24.T=255°C) is, also, reached. But in order to do so, a really high flow rate of hot Therminol VP-1 (S10.W=530000 kg/hr) needs to enter the power block. Also, the flow rate of the cold Therminol VP-1 (S6.W=1000000 kg/hr) is much higher, compared to the corresponding flow rate of the solar salt. The higher flow rates can be explained by looking at the properties of the two HTFs (see Table 1.8 on page 33). The (much) lower thermal conductivity of Therminol VP-1 requires higher amounts to be used both in the solar field and the power block, even if the temperature rise needed in the case of Therminol VP-1 is lower than in the case of solar salt.
4. Thanks to its lower viscosity, Therminol VP-1 theoretically requires less power in order to be pumped compared to solar salt. But, in this case, as described in the previous point, due to the low thermal conductivity, bigger pumps and motors are needed in order to circulate the HTF around the plant. Indeed in the simulation, bigger pumps were used. Of course motors had to be bigger as well, spinning at 6000 rpm compared to 3600 rpm in the case of solar salt.

5. The high flow rate required to be pumped out of the HOT\_TANK during the night, actually drains the tank after almost 4 hours of operation. A bigger tank is required, containing more Therminol VP-1.

Some important conclusions are drawn from this simulation regarding the ACSP plant itself but, also, regarding the possible use of Therminol VP-1 as heat transfer and storage fluid in a CSP two-tank direct storage plant.

It is clear that Therminol VP-1 is not suitable for use in the ACSP plant. It requires changes in vital equipment such as the dimensions of the tanks, pumps and motors. All these changes, along with the bigger amounts of Therminol VP-1 that have to be purchased, increase the costs and they make the use of the specific HTF in the ACSP plant unprofitable. Also, the problem of the different temperatures at the beginning and the end of the water line would introduce extra costs. The higher pressure is an important factor, as well. ACSP plant is designed for operation under relatively low pressure, so damages can be caused to the equipment.

As far as the general use of Therminol VP-1 as a HTF in a CSP two-tank direct storage plant, it offers some important advantages that were evident in the simulation. Firstly, its low crystallization point eliminates the concerns for a possible freezing inside the pipeline of the plant. Lower temperatures can be used freely to improve the performance of the plant. Secondly, their high heat capacity and low thermal conductivity of Therminol VP-1 (see [Table 1.8 on page 33](#)) makes the heat losses negligible. In contrast to the solar salt, the output solar field temperature of Therminol VP-1 is almost equal to the final storage temperature of the HTF at the HOT\_TANK. On the other hand, some strong disadvantages can be noticed. As it was made clear, big amounts of Therminol VP-1 are generally needed to be stored in order to keep the plant running 24 hours. Its relatively high cost in the market increases a lot the cost per kWh (see [Table 1.8 on page 33](#)).

As already proved in literature, Therminol VP-1 is more suitable as a fluid for heat exchange than as a storage fluid. It, also, seems like a CSP plant with two-tank direct storage and Therminol VP-1 as both heat transfer and storage fluid requires a big investment that raises questions concerning the economic benefits of the process.

## 3.2 ACSP plant with two-tank indirect TES

When it comes to CSP plants with PTCs, the two-tank indirect TES is the most widely used. In this configuration there are two different fluids used: the transfer fluid that passes through the solar field and the storage fluid that flows in and out of the hot and the cold storage tank. In the simulations that follow, Therminol VP-1 will be the transfer fluid and solar salt will be the storage fluid. The most vital equipment of a two-tank indirect TES system is the oil-salt heat exchanger. It is where the solar salt and Therminol VP-1 will exchange energy 24 hours per day. So, it is responsible for reaching the expected output temperatures of the transfer and storage fluid.

A scheme of the ACSP plant where two-tank indirect TES is implemented, instead of the original two-tank direct, is presented in Figure 3.17. Most of the equipment is the same as in the original plant in order to be able to get a more accurate and meaningful comparison between the two TES configurations. For example, the two storage tanks, the power block and the solar field are the same, as described in Table 2.1 on page 39. Also, the desired power output is kept at 4.7 MW.

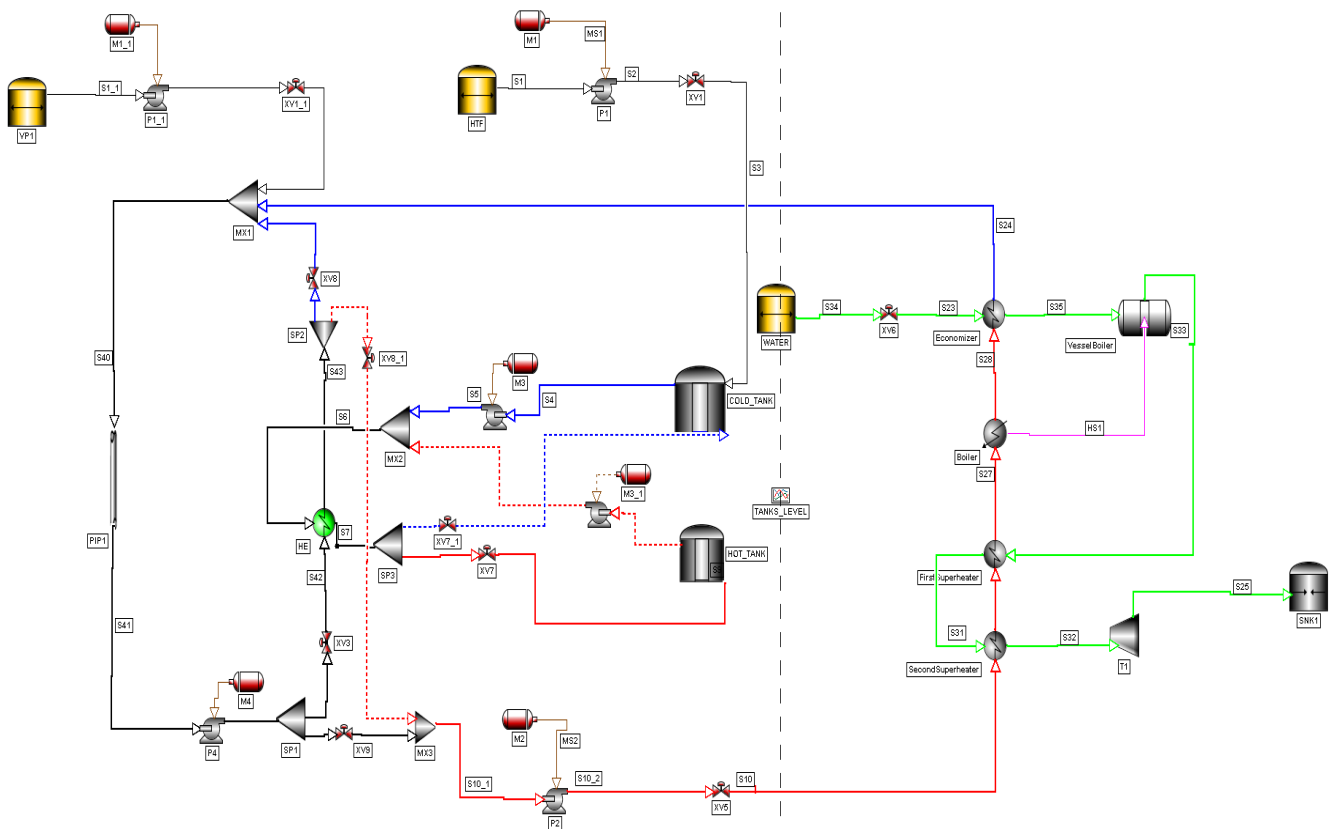


**Figure 3.17:** Scheme of the ACSP plant with two-tank indirect TES

The red and blue dotted lines are active only during the night. The general operation of this hypothetical plant can be divided in three main parts:



### Startup

During startup the two HTFs are loaded into the system. Via the one line connected to the source "HTF", cold solar salt (290°C) is pumped into the the COLD\_TANK and via the other line connected to the source "VP1", Therminol VP-1 (250°C) is loaded inside the pipeline through the mixer MX1.

Mixers have multiple streams as inlet and they produce a single outlet stream. Splitters do the opposite, they can split a single stream into two or more. Both of these equipments are useful for this simulation mainly because there are different streams that have to reach the oil-salt heat exchanger during night and day, but the heat exchanger (HE) only has single input and single output. Mixers/splitters in combination with valves help move the desired streams into the heat exchanger while blocking others.

### Day operation

During the day, the dotted lines shown in Figure 3.17 on the facing page are not active and no HTF passes through them. The cold solar salt is pumped out of the COLD\_TANK and it exchanges energy with the hot Therminol VP-1 coming out of the solar field. Hot solar salt, whose desired temperature is around 400°C), comes out of the heat exchanger and it is stored at the HOT\_TANK for later use. The other output of the heat exchanger is the cold solar salt, which will be recycled back to the inlet of the solar field at a temperature of 300°C. But only a part of the hot Therminol VP-1 reaches the oil-salt heat exchanger. When the temperature of the hot solar salt is high enough (around 400°C), the valve XV9 opens, letting it reach the power block. The motor is activated, XV5 is, also, open and water is flowing in the water line. As in the case of the original ACSP plant, there is energy exchange along the heat exchanger train, resulting to a power output. When the solar salt gets out of the power block, it has decreased its temperature and it can be mixed at the mixer MX1 with the cold solar salt coming out of the oil-salt heat exchanger. It will then go through the solar field to repeat the cycle all over again.

### Night operation

The DNI reaching the solar field is zero and the way to heat up Therminol VP-1, in order to keep the turbine running, is with the hot molten salt that is stored at the HOT\_TANK after the day operation. So, hot solar salt is pumped out of the tank and it exchanges heat with Therminol VP-1. Hot Therminol VP-1, coming out of the heat exchanger, passes through valve XV8\_1 and heads to the power block to produce energy. Then, with reduced temperature it will circulate towards the oil-salt heat exchanger in order to increase its temperature again and repeat the procedure. The cold solar salt is stored at the COLD\_TANK.

The main temperatures of the plant are summed up in the following Table 3.5 on the next page.

As mentioned before the most important equipment in this new configuration is the oil-salt heat exchanger. Its correct sizing based on the needs and specifications

**Table 3.5:** Temperature of the HTFs at various parts of the ACSP plant with two-tank indirect storage.

Temperature(°C)	
Solar Salt	
at the COLD_TANK	295
at the HOT_TANK	400
Therminol VP-1	
at the Solar Field inlet	300
at the Power Block inlet	400

of the process will guarantee the plant's smooth operation. In this simulation, the specific heat exchanger was sized as follows:

We consider the night operation of the plant, where the cold stream entering the heat exchanger is the sola salt at 292°C and the hot stream is the Therminol VP-1, entering at 393°C. The temperatures are an approximation of the temperatures expected at the upcoming simulation. The temperature of the outlet streams: 300°C for Therminol VP-1 and 386°C for molten salt. The heat from the hot stream will go to the cold stream, assuming no heat losses:

$$\dot{Q}_{hot} = \dot{Q}_{cold} \quad (3.8)$$

and

$$\dot{Q}_{hot} = W_{VP1} C_{pVP1} \Delta T_{VP1} \quad (3.9)$$

where  $W_{VP1}$  is the mass flow rate of Therminol,  $C_{pVP1}$  is its specific heat capacity and  $\Delta T_{VP1}$  is the temperature drop.

Judging from the simulation of the original ACSP plant, a reasonable value for the flow rate of the transfer fluid is around 500000 kg/hr. The specific heat capacity was computed using the following formula, for a mean value of temperature [59]:

$$C_{pVP1} = 2.414 \times T + 5.9591 \times 10^{-3} \times T^2 - 2.9879 \times 10^{-5} \times T^3 + 1498 \quad (3.10)$$

T is in K and  $C_{pVP1}$  in J/(kgK).  $\Delta T_{VP1} = -93^\circ C$

So, replacing the known values in Eq. (4.9),  $\dot{Q}_{hot}$  is found equal to  $-1.1 \times 10^{11}$  J/hr. Now that, also,  $\dot{Q}_{cold}$  is known it is easy to compute the expected flow rate for the solar salt.

The heat exchange at a heat exchanger can be also expressed as:

$$Q = U \times A \times LMTD = \dot{Q}_{hot} \quad (3.11)$$

A: exchanger area, U: heat transfer coefficient and LMTD: Logarithmic Mean Temperature Difference equal to:

$$LMTD = \frac{\Delta T_2 - \Delta T_1}{\ln \frac{\Delta T_2}{\Delta T_1}} \quad (3.12)$$

where,

$$\Delta T_2 = T_{hot_{out}} - T_{cold_{in}} \quad (3.13)$$

$$\Delta T_1 = T_{hot_{in}} - T_{cold_{out}} \quad (3.14)$$

So, the heat exchange area can be computed with Eq. (4.11). For the variables of this simulation:  $A = 4500\text{m}^2$ .

Apart of the oil-salt heat exchanger there is, also, some other new equipment used. The second startup line which loads the transfer fluid needs a pump and a valve, identical to the ones used at the startup line of the solar salt. As already mentioned, there are, also, three mixers and three splitters. Each of the outlet stream of every splitter has a valve so that it is easy to direct the HTF towards the preferred stream.

The main parameters of the new equipment, as well as some adjustments made to the variables of the parameters of the original equipment are presented in the following table:

**Table 3.6:** Main design parameters of the ACSP plant with two-tank indirect TES.

Valves	Cv	Motors	Speed (rpm)
XV3	500	M4	6000
XV9	500	M3	3600
XV7	150	M3_1	3600
XV7_1	150	M2	6000
XV8	500		
XV8_1	500		

### 3.2.1 Control System

Every time that a process is being designed, the most important variables to be controlled have to be decided. In the case of the ACSP plant with two-tank indirect TES, as presented in Figure 3.17 on page 66, one of the most important variables is the temperature of the outlet oil-salt heat exchanger stream (S43.T). During the night, this is the temperature at which Therminol VP-1 will enter the power block, so it should always be around  $400^\circ\text{C}$  (see Table 3.5 on the preceding page), in order to guarantee the production of the desired power output. So, during the night operation this specific temperature can be controlled by adjusting the opening of the valve XV7\_1.

During the day, S43.T determines the temperature at which the cold Therminol VP-1 will be recycled back to the solar field in order to be heated up again by the DNI reaching the PTCs. It can be controlled by manipulating the valve XV7.

The outlet stream of the power block (S24), also, affects the temperature of Therminol VP-1 entering the solar field. During the day it gets mixed with S43 and during the night it is the only stream reaching the solar field. So, just like in the simulation of the original ACSP plant a PID controller can open/close the valve

XV5 in order to adjust S24.T. Both S43.T and S24 should be set around 300°C. Lastly, another controller will be used in order to control the flow rate of water entering the economizer.

A scheme of the control system described above, along with the main variables that will be monitored in the simulation, is presented in the following figure.

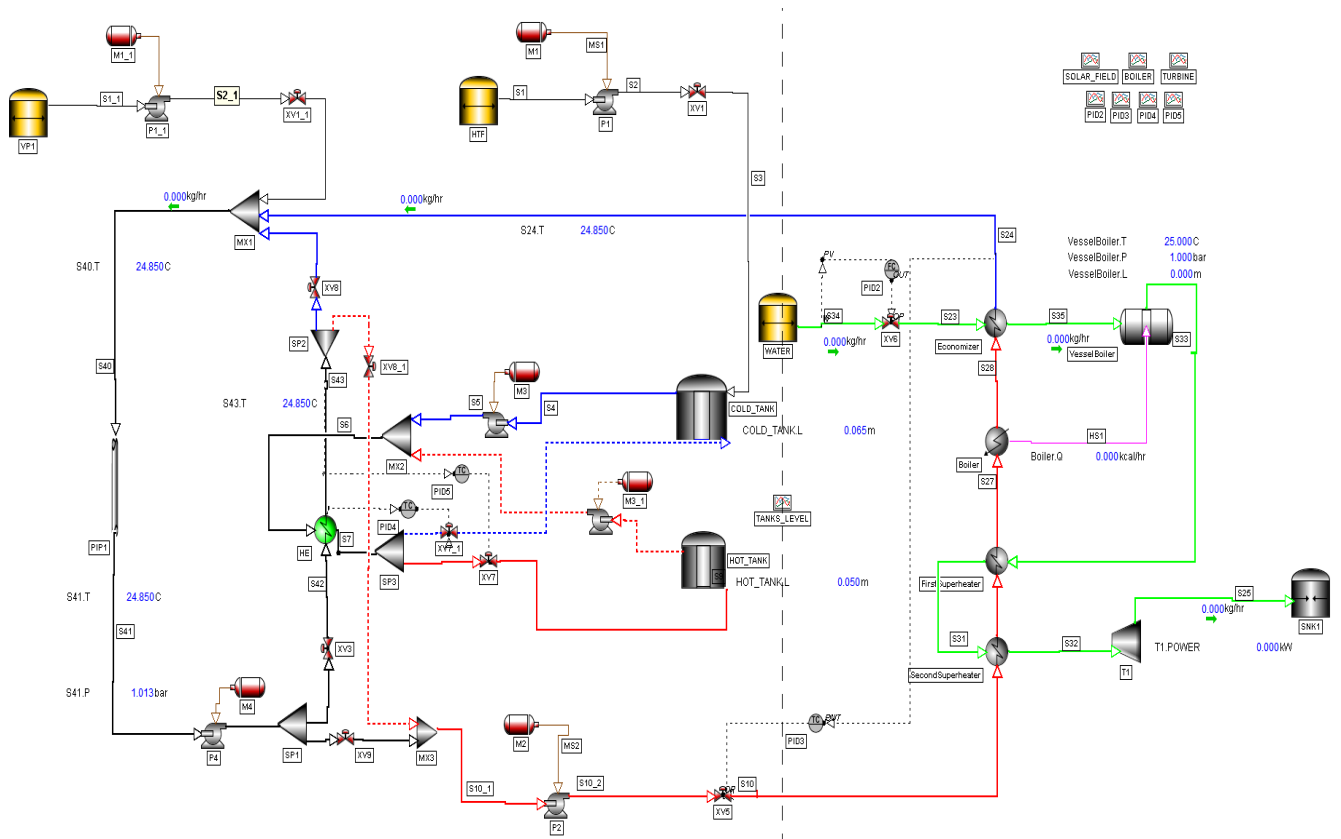


**Figure 3.18:** The control system of the ACSP plant with two-tank direct TES

The following table gives an overview of the parameters of the controllers used in the simulation.

**Table 3.7:** Parameters for the controllers (ACSP with two-tank indirect TES).

	PID2	PID3	PID4	PID5
Output	S34.W	S24.T	S43.T	S43.T
Manipulated variable	XV6.OP	XV5.OP	XV7_1.OP	XV7.OP
Action	Reverse	Reverse	Reverse	Reverse
Set point	60000 kg/hr	305°C	395°C	313°C
Proportional gain	0.1	0.1	0.2	0.2
Integral reset rate	0.1	0.1	0.1	0.1

### 3.2.2 Performance

The operation of the plant equipped with the control system described above, has to be tested. In order to do so, the same strategy will be followed, as in the case of the original ACSP plant simulation. A 24-hour scenario will be created in DYNsim and the behavior of the most important variables will be plotted and analyzed during the first minutes of the simulation but, also, during the sunrise, which is the strongest transient phenomenon that the plant has to face. The usual operation of the plant during night and day will, also, be commented. In this way, the following points can be achieved:

- Assessment of the control system used.
- Accurate and clear comparison between the two-tank direct and two-tank indirect TES technologies.
- Collection of useful information about the HTFs used.

The starting point of the simulation is at 20:30pm, right after sunset when the plant is ready to enter the night operation. The DNI reaching PIP1 (see Figure 3.18 on the facing page) is zero. The HOT\_TANK is filled up to 7.9 m with solar salt at 404°C while the level of the COLD\_TANK is 1.8 m, filled with solar salt of 280°C. The turbine's power output is zero and the transfer fluid Therminol VP-1 has just been inserted in the pipelines at a temperature of 265°C.

#### 24-hour operation of the plant

- The first minutes of the simulation (20:30pm - 21:00pm)

Following the approximation that the sun has just set at 20:30pm, from that point onwards and till the sunset only the dotted line of solar salt (see Figure 3.18 on the preceding page) will be working. Through this line, the solar salt moves from the HOT\_TANK to the COLD\_TANK. So, at the beginning of the simulation motor M3\_1 is activated and PID4 is set to auto mode. PID4 will be managing the opening of valve XV7\_1, adjusting in this way the flowrate of the hot solar salt inside the oil-salt heat exchanger. The transfer fluid Therminol VP-1 is pumped into the heat exchanger by activating motor M4 and opening valve XV3. Even though in the simulation it passes through the solar field (PIP1), the PIP1.QIMP is zero so theoretically the input and output solar field temperature of the fluid should be the same. At the output of the heat exchanger, the valve XV8 is closed while the XV8\_1 is open in order to force the hot Therminol VP-1 into the power block. Motor M2 is activated and the controllers PID3 and PID2 are set to auto mode.

The behavior of the controllers PID4 and PID3 during the first 30 minutes of the simulation is plotted in the Figures 3.19 on the following page and 3.20 on the next page, respectively.

At the beginning, the temperature of Therminol VP-1 at the outlet of the oil-salt heat exchanger is too low so PID4 opens up the valve XV7\_1 at 100% in order to let as much hot molten salt as possible enter the heat exchanger and raise S43.T.

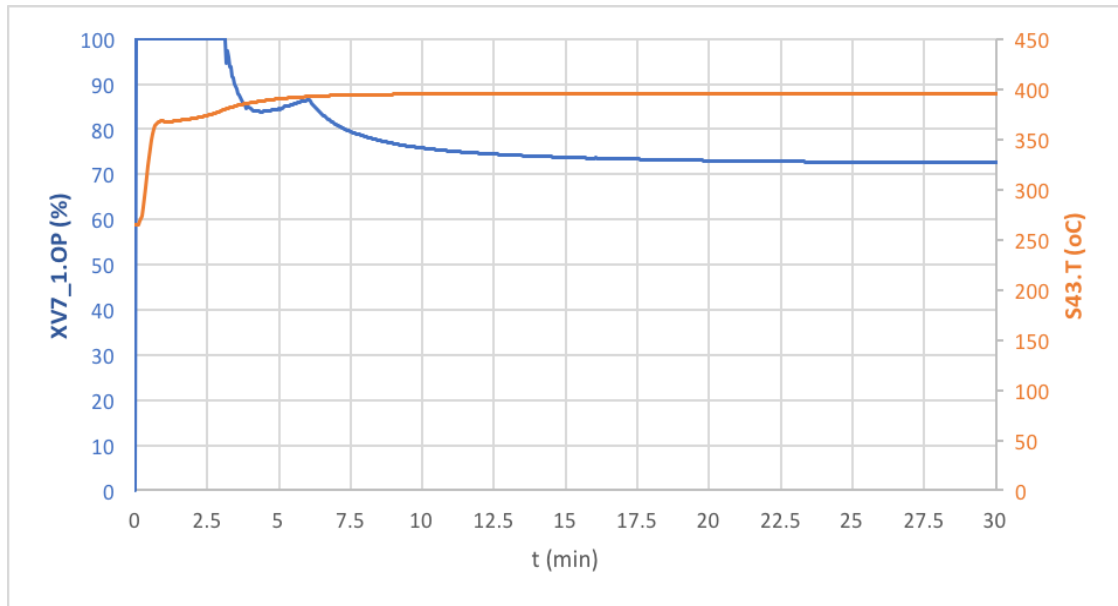


**Figure 3.19:** Controller PID4 during the first 30 minutes of the simulation

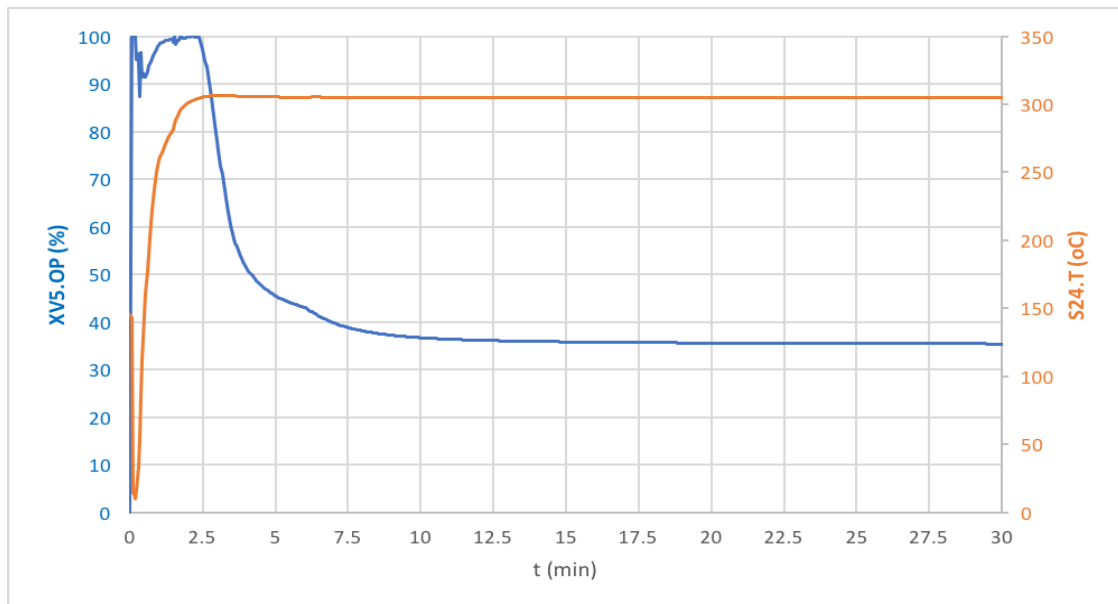


**Figure 3.20:** Controller PID3 during the first 30 minutes of the simulation

When the temperatures gets closer to the set point ( $t = 2.5\text{min}$ ), the PID4 regulates the opening of the valve and tries to reach the set point. Eventually the set point is reached after a small decrease and increase of the manipulated variable.

At the same time, PID3 is trying to control the temperature of the output of the power block (S24.T). At first, as already mentioned, S34.T is too low so the inlet temperature of Therminol VP-1 at the power block is not high enough in order to reach the set point at the outlet. This is why PID3 "commands" valve XV5 to open up at around 100%. The resulting high flow rate helps reaching the set point of S42.T after almost 2.5 min. Afterwards, the PID4 gradually closes the valve till 37% and manages to maintain the desired output temperature.

PID3 reaches its set point quickly, by imposing higher flow rates. But, it takes more time for PID4 to reach its set point. This is because the high temperature of the output of the power block (PID3) is not transferred quickly to the input of the heat exchanger. There is a time lag for the outlet temperature of the solar field (S41.T) to become equal to the temperature of the inlet stream (S40.T). So, in these very first minutes, the temperature of the stream reaching the heat exchanger is not high enough in order for the PID4 to get to the set point.

Of course, the point of interest of every simulation of the ACSP plant is the power output of the turbine. Its values for the first 30 minutes of the simulation are plotted in the following figure:

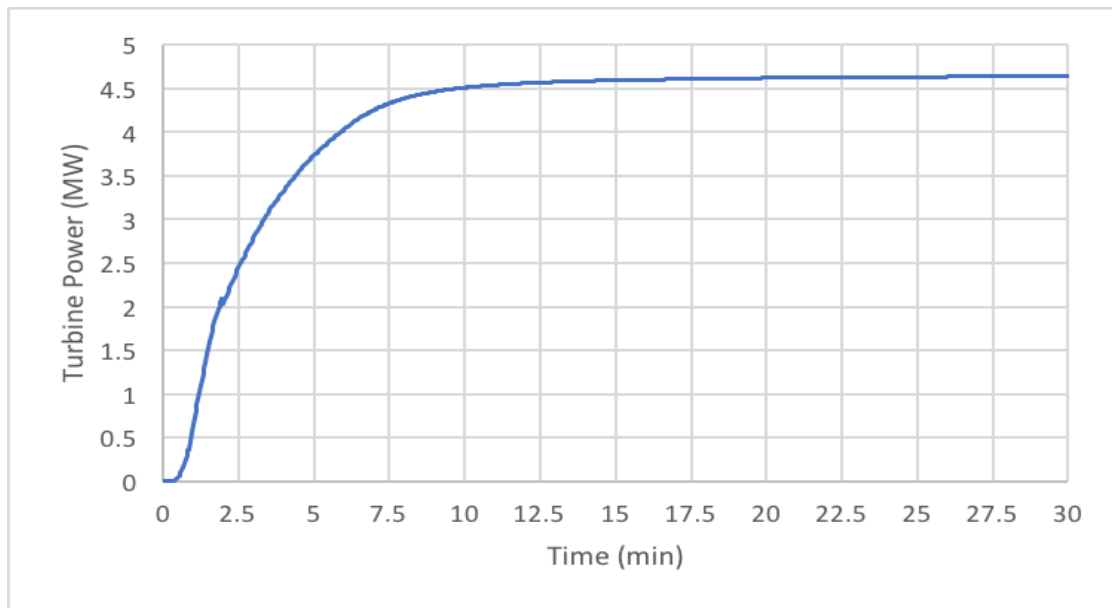


**Figure 3.21:** Power output during the first 30 minutes of the simulation

A quick increase at the power output can be observed, almost reaching the set point after just 7.5 minutes. This can be explained by looking at the temperature profile of the oil-salt heat exchanger outlet stream (Figure 3.19 on the facing page). This is the temperature at which Therminol VP-1 enters the power block and it is increasing constantly for the first 10 minutes of the simulation. Higher inlet power block temperature results to higher amounts of superheated steam, thus higher power production. The slope of the power output decreases significantly after the first 4 minutes because of the decreased flow rate entering the power block (see Figure 3.20 on the preceding page). It will be stabilized only when the opening of the valve XV5 remains constant.

It is really interesting how the monitored variables described above are all connected to each other. The behavior of the one cannot be explained without looking at how it affects and it is affected by the behavior of the others. And this is why each controller has to be designed carefully in order not to allow possible disturbances on a specific variable to affect the system, through this chain of interactions.

- Night operation

As it was commented, the controllers manage to reach their set points quite quickly, offering in that way an immediate stabilization of the operation of the system. Based on the simulation, during the night the values of the flow rates were almost constant thanks to the controllers, which they had already reached their set points in the first minutes of the simulation. In the meantime, the turbine increased a bit more its power output.

A screenshot of the flowsheet of the ACSP two-tank direct TES during the night operation (04:00 am) is presented in the following figure. The solid blue/red line connecting the COLD\_TANK and the HOT\_TANK during the day (see Figure 3.17 on page 66), has been "hidden" in the screenshot, because it is not in use and in order to make the scheme more understandable.

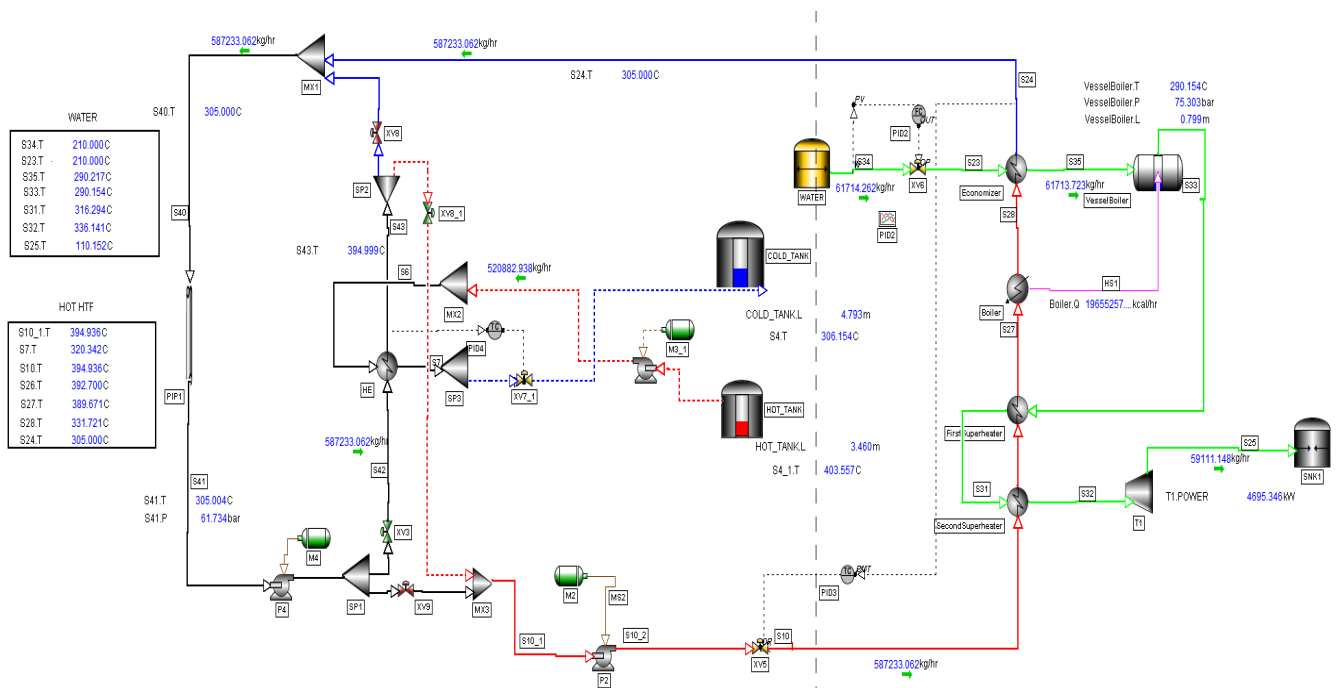


**Figure 3.22:** Operation of the ACSP plant with two-tank indirect storage during the night: flowsheet (04:00am)

Some comments on the operation of the plant during the night:

1. The plant continues to operate smoothly at night, under the set points of the controllers in use (see Table 3.7 on page 70). Therminol VP-1 enters the power block at 395°C and exits at 305°C. Also, the water flows at 61000 kg/hr, really close to the set point of the controller PID2.
2. The flowrate of the solar salt to the COLD\_TANK is 520000 kg/hr, which is higher than the corresponding flowrate in the case of the original two-tank direct ACSP plant. Due to the poor thermal conductivity of Therminol VP-1, a high flow rate of hot solar salt has to enter the oil-salt heat exchanger in order to manage to raise the temperature of Therminol VP-1. So, more solar



salt is needed during the night and this is why before the beginning of the simulation, the HOT\_TANK was filled up to 7.9 m, compared to the 5.7 m in the case of the simulation of the original plant. It is important to mention that the size of motors and pumps that circulate the solar salt remained the same in both cases, even if the flow rate is higher in the two-tank indirect TES.

3. Therminol VP-1 flows at approximately 587000 kg/hr. To do so, as it can be seen in the Table 3.6 on page 69, more powerful motors and pumps had to be used, always compared to the original solar salt plant.
4. The plant operates at a high pressure of almost 62 bar. This can be explained, partly, because of the high flow rates of the system. Assuming turbulent flow conditions, the pressure drop increases as the square of the flow rate. Also, the bigger size of the pumps affects the pressure drop. Probably the most important reason for the high operating pressure, though, is the fact that in this new plant configuration, the same Cv for the valves were used, just like in the case of the original plant (see Tables 3.6 on page 69 and 3.3 on page 52). So, by keeping the Cv constant and by increasing the flow rate, the pressure drop increases as it can be seen in Equation 4.3, which gives the mathematical definition of Cv.

- Sunrise (06:30am - 07:30am)

It is important to see how the control system and the plant behaves during the sunrise, which is the most important transient phenomenon to be faced. Following the same logic as in the case of the original ACSP plant, it is supposed that the sunrise lasts one hour in total, starting from 06:30am. During this time the operation of the whole plant changes. It is the transition from the night operation to the morning operation. The irradiation increases gradually and it is shown in the following Figure. The temperature of the fluid entering and exiting the solar field is, also, monitored and plotted.

At first, the DNI reaching the solar field is not high enough to raise the temperature of Therminol VP-1. This causes a drop both in the outlet and inlet temperature, of almost 50 degrees in 10 minutes. In this system, the temperature of the inlet solar field stream (S40) is connected to the outlet solar field stream (S41) in the following way. Higher outlet temperature (S41.T) results to higher temperature at the inlet and outlet of the heat exchanger for Therminol VP-1. The outlet stream of the heat exchanger is recycled back to the solar field, becoming the new inlet (S40.T). So, it is expected for the inlet and outlet temperatures of the solar field to follow a similar trend. After the first 10 minutes, the DNI is high enough to start raising the outlet temperature. Till the end of the sunrise, the outlet temperature keeps rising from 265°C to 405°C which is the desired temperature for the hot Therminol VP-1, close to its upper operative limit. The inlet solar field temperature, though, reaches its final value faster. It is important to be stated that this temperature is the result after mixing the outlet of the heat exchanger and the outlet of the power block at the mixer MX1.

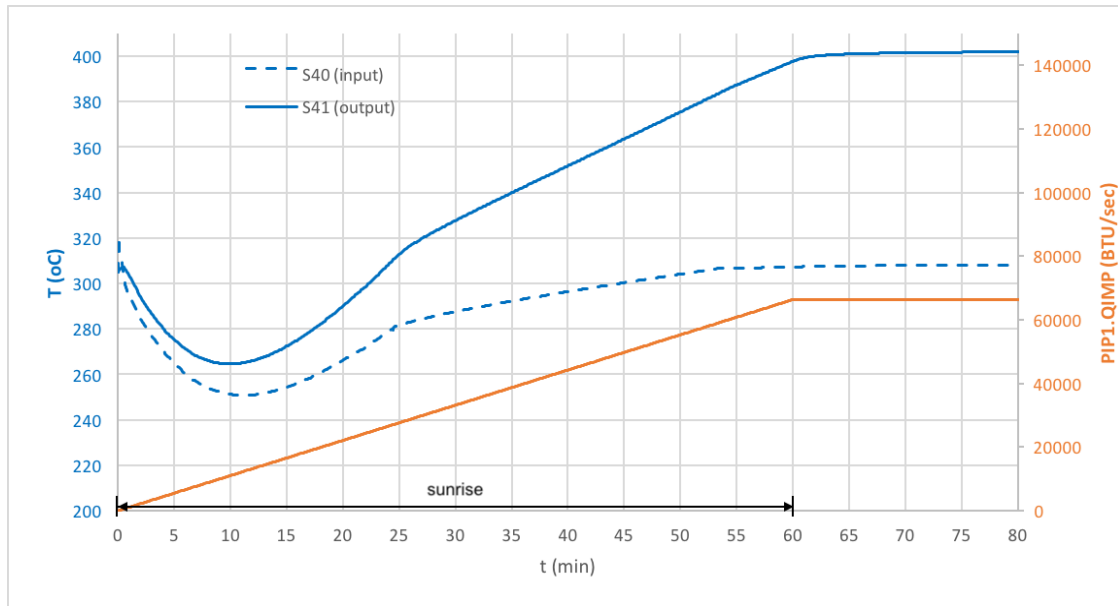


**Figure 3.23:** Indirect TES: Solar Field temperatures and DNI during sunrise

The behavior of the controller PID3 that regulates the outlet temperature of the power block by adjusting the inlet flow rate, is also plotted:

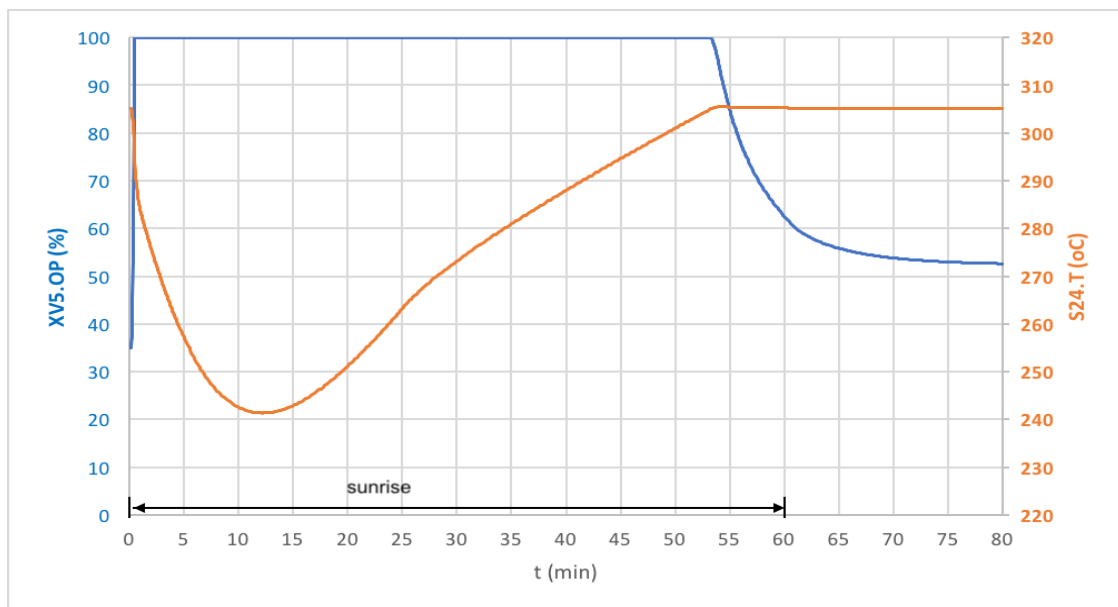


**Figure 3.24:** Indirect TES: Controller PID3 during sunrise

The low DNI at the first 10 minutes of the sunrise causes the controller to open up the valve XV5 at its maximum, because the temperature of the HTF reaching the power block is still low and it is not enough to achieve the set point of 305°C at the outlet of the power block. The valve remains fully open almost till the end of the sunrise. Only when the outlet power block temperature is close to the set point, the valve starts closing in order to keep the temperature constant. The temperature

initially drops and then gradually increases to reach, once again, the set point at the end of the sunrise.

Moving to the most important parameter of the plant, the power outlet, its trend during the sunrise can be seen in the following plot.

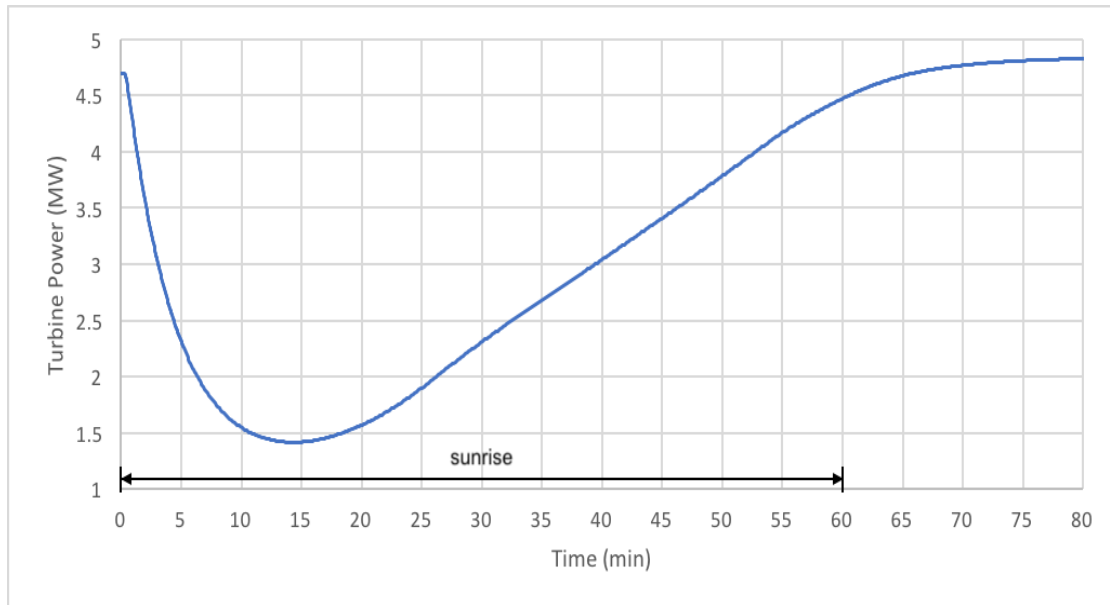


**Figure 3.25:** Indirect TES: Power output during sunrise

The low temperatures of Therminol VP-1 cause a drop to the power output of the turbine at the beginning. After 10-12 minutes, the temperature of the main streams start rising again and so does the power output. Its value keeps on increasing till the end of the sunrise, eventually reaching the desired value of 4.7 MW.

There are some interesting points to be made when comparing the sunrise transient between the original two-tank direct TES ACSP plant and the two-tank indirect TES configuration.

1. It is normal that in the beginning of the sunrise, when the DNI reaching the solar field is still low, the temperature of the working HTF will be affected. This effect of the low temperature is much more profound in the case of the two-tank indirect TES. As it can be seen in the three previous figures, the initial drop in the temperature of Therminol VP-1 is significant, and the same goes for the power output which is decreased noticeably in the first 10-15 minutes of the simulation. The reason behind this is the following: in the original two-tank direct configuration, the working fluid is pumped out of the hot tank in order to enter the power block (see Figure 3.10 on page 58). The first 10-15 minutes of the low DNI are not enough to affect significantly the temperature inside the hot tank, even if the fluid entering the hot tank is much colder compared to the fluid already inside it. On the other hand, in the case of the two-tank indirect TES, the working fluid that enters the power block comes directly from the outlet of the solar field. There is no

tank in-between to guarantee a high temperature even when the DNI is low. So, the low temperatures at the beginning of the sunrise affect the overall performance of the plant by limiting the power output.

2. In the original ACSP plant, it takes more time for the power output to get back to 4.7MW even if the initial drop is low. In the two-tank indirect TES the drop is much bigger but 10 minutes after the end of the sunrise the power output is 4.7MW.
3. An important advantage of the two-tank indirect TES is that a lower total DNI is used, probably thanks to the physical properties of Therminol VP-1 and its lower maximum operating temperature. This means that a satisfying result can be achieved, also, on a cloudy day.

- Day operation

A screenshot of the flowsheet of the two-tank indirect TES ACSP plant at 13:00pm is presented:

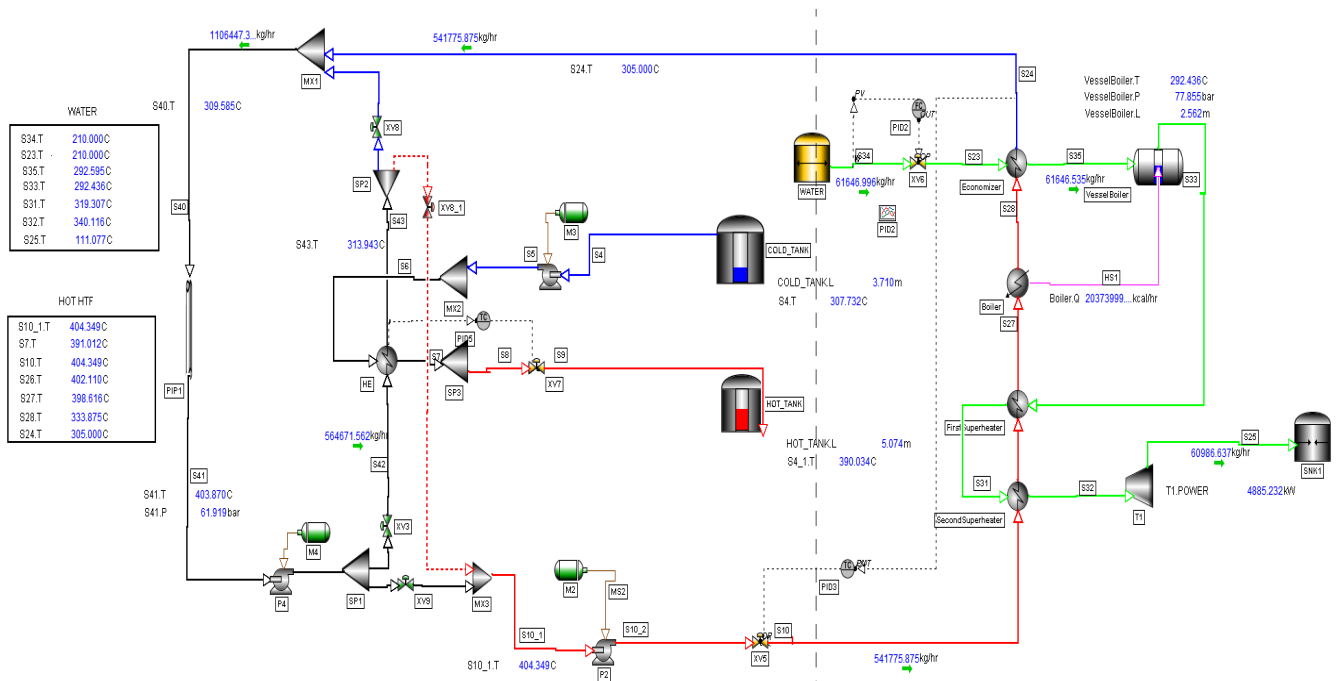


**Figure 3.26:** Indirect TES: Operation of the plant during the day (13:00pm)

The controllers have managed to maintain the set points. Therminol VP-1 is almost split in half in the splitter SP1 at a temperature of 403°C. One part goes to the heat exchanger in order to exchange energy with the solar salt and the other part goes to the power block. The outlets of these two routes are mixed at the mixer MX1 and they produce the new input stream of the solar field of around 310°C. The solar salt moves from the COLD\_TANK to the HOT\_TANK, reaching a temperature of 390°C.

This procedure will continue till the sunset when the plant will switch to the "night operation".

### 3.3 An innovative design

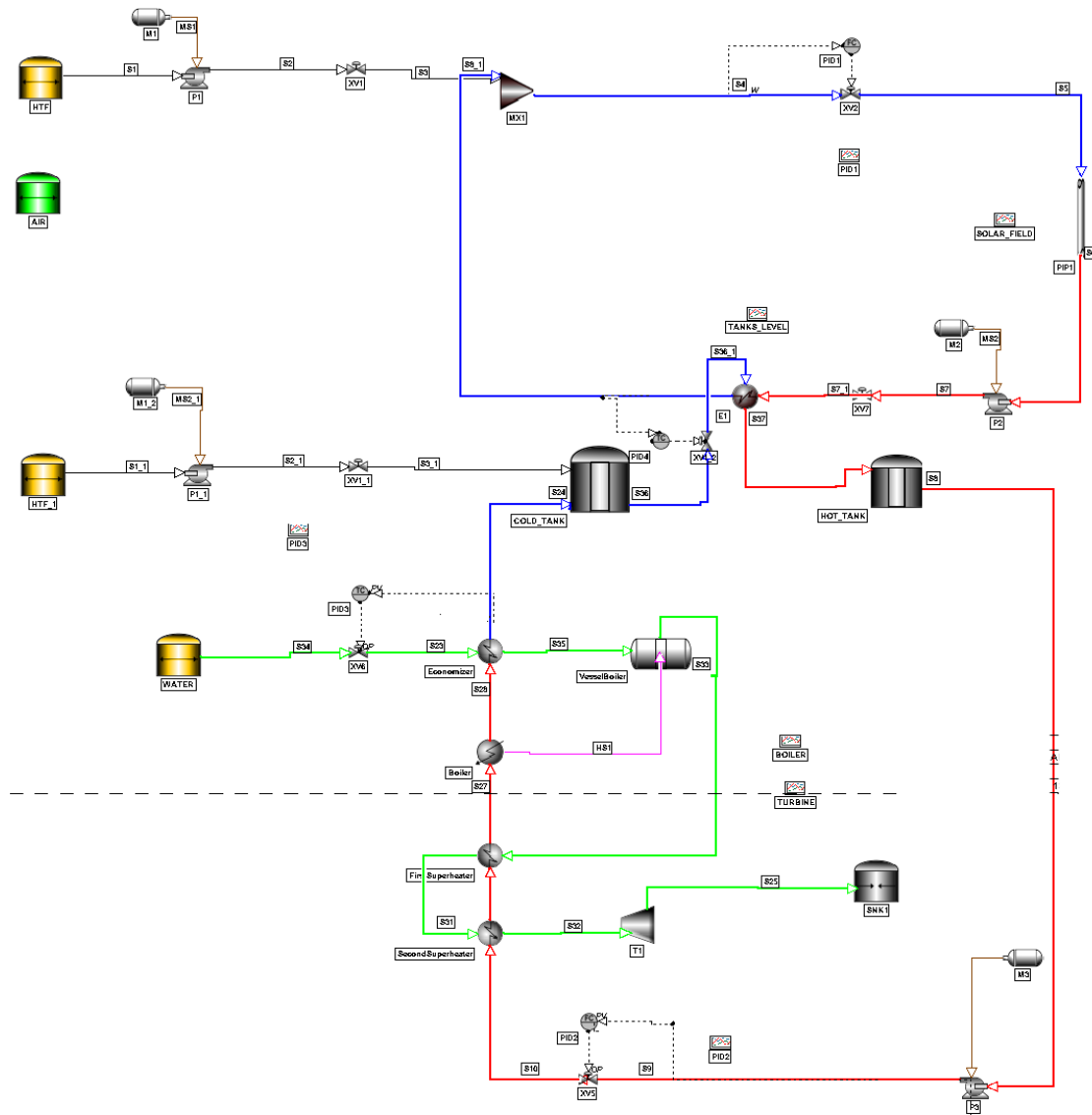


**Figure 3.27:** Indirect TES: An innovative design

This is an alternative interpretation of the two-tank indirect TES. The logic of operation is similar to the classic two-tank indirect TES, using the oil-salt heat exchanger as the main equipment of the plant, but the difference lies in the fact that the storage HTF is, also, the HTF that runs into the power block. More in details, during the day a HTF is loaded in the pipeline leading to the solar field. It passes through it and then enters the heat exchanger. There, it exchanges energy with the storage HTF, which comes from the COLD\_TANK. A part of the hot storage fluid enters the HOT\_TANK and the rest enters the power block for energy production. The cold HTF goes back to the solar field, from the output of the heat exchanger. During the night, the HOT\_TANK keeps providing hot HTF to the power block, so the turbine keeps on turning. From the output of the power block, cold HTF fills again the COLD\_TANK. The only problem of the structure

of this configuration is the storage of the working HTF during the night. It is not advisable to keep the HTF inside the pipeline during the night, so another tank could be possibly used to solve this problem. During the day, the HTF would be pumped out of the tank to restart the cycle.

This is a configuration that has not been studied in the bibliography and it could be a good choice for further research. Its control is simple and it uses less equipment than the original two-tank indirect system because there are not many splitters and mixers.

# Conclusions and Future Development

There are many ways to take advantage of the endless energy provided by the sun. The Concentrated Solar Power Plants is one of the most promising technologies. They offer high efficiency, low operating costs and good scale-up potential. There are many different categories of CSP plants that differ on the way that the solar power is concentrated. All of them have the same parts: the solar field where the solar radiation is concentrated and the power block where the electricity is produced. There is the possibility to store energy through the Thermal Energy Storage. Through the pipes of the plant, the Heat Transfer Fluid is flowing.

The different components of the plant offer many possibilities concerning the way of operation. In this thesis work an effort was made to investigate the dynamic behavior of an existing CSP plant (ACSP), under different HTFs, control and TES systems. The dynamic simulator DYNSIM was the computer program used for these purposes.

A control system was developed for the original configuration of the plant (two-tank direct TES with solar salt) and it was tested under the everyday transient phenomena that the plant has to face, such as the sunrise. Its performance was robust, helping the controller to reach the desired set points quickly. In this way, the control system guarantees the continuous steady performance of the plant.

In the above configuration, the HTF was changed. Therminol VP-1 was tested instead of the solar salt. The results were not satisfying. It was evident that it is not a good idea to use Therminol VP-1 as both the working and the storage fluid in a CSP plant. High flow rates are needed that automatically make the equipment significantly bigger, thus increasing the costs.

A completely new configuration was, also, tested for the ACSP plant. This time, the TES system was changed. By keeping the same tanks, a two-tank indirect TES system was tested. In this case, Therminol VP-1 was used as the working fluid and the solar salt as the storage fluid. The key point of the plant was the heat exchanger where energy is exchanged between the oil and the salt.

A robust control system of 4 PID controllers was developed, also, in this case offering really good results. In order to check the performance of the control system, the dynamic simulation was performed, always focusing on the strongest transient phenomena, such as the sunrise.

The dynamic simulation revealed some important differences between the two-tank direct and the two-tank indirect TES for the ACSP plant. First of all, the latter was affected more by the periods of low DNI. But, on the other hand, it was

able to work with lower total DNI and to reach the set points of the controllers more quickly. Generally higher flow rates are needed for the working fluid in the case of the two-tank indirect TES. Also, some small adjustments of the secondary equipment had to be made in the indirect configuration.

The dynamic simulations gave the possibility to see beyond the theoretical characteristics of the components of a CSP plant and test them under real life conditions.

Of course, other configurations for the ACSP plant can be tested and compared to the ones analyzed in this thesis work. The thermocline technology and the concept design presented in the last chapter, are suitable candidates.



# Acronyms

<b>IEA</b>	International Energy Agency
<b>CSP</b>	Concentrated Solar Power
<b>HTF</b>	Heat Transfer Fluid
<b>TES</b>	Thermal Energy Storage
<b>PTC</b>	Parabolic Trough Collector
<b>SPT</b>	Solar Power Tower
<b>LFR</b>	Linear Fresnel Reflector
<b>PDC</b>	Parabolic Dish Collector
<b>PV</b>	Photovoltaic
<b>SEGS</b>	Solana Generating Station
<b>LCOE</b>	Levelized Cost of Electricity
<b>DNI</b>	Direct Normal Irradiation
<b>FBS</b>	Fuel Backup System
<b>4E</b>	Energy Exergy Environmental Economic
<b>PCM</b>	Phase Change Material
<b>DSG</b>	Direct Steam Generation
<b>CFD</b>	Computational Fluid Dynamics
<b>OTS</b>	Operator Training Simulation
<b>ISCCS</b>	Integrated Solar Combined Cycle System
<b>ACSP</b>	Archimede Concentrated Solar Power Plant
<b>ODT</b>	1-octadecanethiol
<b>PID</b>	Proportional Integral Derivative



# Symbols

<b>MW</b>	Mega Watt
<b>KNO<sub>3</sub></b>	Potassium Nitrate
<b>NaNO<sub>3</sub></b>	Sodium Nitrate
<b>kW</b>	Kilo Watt
<b>MWh</b>	Mega Watt Hours
<b>hr</b>	Hour
<b>k/cp</b>	Thermal Diffusivity
<b>Q<sub>st</sub></b>	Heat Stored
<b>H</b>	Enthalpy
<b>K<sub>c</sub></b>	Gain
<b>C<sub>v</sub></b>	Valve Flow Coefficient
<b>SG</b>	Specific Gravity
<b>T<sub>m</sub></b>	Metling Temperature



# Bibliography

- [1] United Nations (UN). *Human Development Reports*. 2018. URL: <http://www.hdr.undp.org/en/2018-update>.
- [2] Enerdata. *Global Energy Statistical Yearbook*. 2018. URL: <https://yearbook.enerdata.net>.
- [3] International Energy Agency (IEA). *IEA Atlas of Energy*. 2016. URL: <http://energyatlas.iea.org/#!/tellmap/1378539487>.
- [4] Hannah Ritchie and Max Roser. “Fossil Fuels”. In: *Our World in Data* (2019). <https://ourworldindata.org/fossil-fuels>.
- [5] Charles H Eccleston and Frederic March. *Global environmental policy: concepts, principles, and practice*. CRC Press, 2010.
- [6] George W Crabtree and Nathan S Lewis. “Solar energy conversion”. In: *Physics today* 60.3 (2007), pp. 37–42.
- [7] HL Zhang et al. “Concentrated solar power plants: Review and design methodology”. In: *Renewable and sustainable energy reviews* 22 (2013), pp. 466–481.
- [8] Meriem Chaanaoui, Sébastien Vaudreuil, and Tijani Bounahmidi. “Benchmark of Concentrating Solar Power plants: historical, current and future technical and economic development”. In: *Procedia Computer Science* 83 (2016), pp. 782–789.
- [9] Ugo Pelay et al. “Thermal energy storage systems for concentrated solar power plants”. In: *Renewable and Sustainable Energy Reviews* 79 (2017), pp. 82–100.
- [10] Ramana G Reddy. *Molten salts: thermal energy storage and heat transfer media*. 2011.
- [11] Rafiqul Gani, Esben L Soerensen, and Jens Perregaard. “Design and analysis of chemical processes through DYNsIM”. In: *Industrial & engineering chemistry research* 31.1 (1992), pp. 244–254.
- [12] Md Tasbirul Islam et al. “A comprehensive review of state-of-the-art concentrating solar power (CSP) technologies: Current status and research trends”. In: *Renewable and Sustainable Energy Reviews* 91 (2018), pp. 987–1018.
- [13] K Vignarooban et al. “Heat transfer fluids for concentrating solar power systems—a review”. In: *Applied Energy* 146 (2015), pp. 383–396.
- [14] International Energy Agency (IEA). *Concentrated Solar Power (CSP) Roadmap*. 2010. URL: [https://www.iea.org/publications/freepublications/publication/csp\\_roadmap.pdf](https://www.iea.org/publications/freepublications/publication/csp_roadmap.pdf).

- [15] HELIOSCSP. *Concentrated Solar Power increasing cumulative global capacity more than 11 to just under 5.5 GW in 2018*. 2019. URL: <http://helioscsp.com/concentrated-solar-power-increasing-cumulative-global-capacity-more-than-11-to-just-under-5-5-gw-in-2018/>.
- [16] Ming Liu et al. “Review on concentrating solar power plants and new developments in high temperature thermal energy storage technologies”. In: *Renewable and Sustainable Energy Reviews* 53 (2016), pp. 1411–1432.
- [17] D Elzinga et al. “Energy technology perspectives 2015: mobilising innovation to accelerate climate action”. In: *Paris: International Energy Agency* (2015).
- [18] ESTELA Greenpeace. “SolarPACES, Solar thermal electricity global outlook 2016”. In: *Executive summary* (2016).
- [19] Soteris A Kalogirou. *Solar energy engineering: processes and systems*. Academic Press, 2013.
- [20] Giorgio Cau, Daniele Cocco, and Mario Petrollese. “Optimal energy management strategy for CSP-CPV integrated power plants with energy storage”. In: *Proceedings of the 28th International Conference on Efficiency, Cost, Optimization, Simulation and Environmental Impact of Energy Systems, Pau, France*. 2015.
- [21] Sarada Kuravi et al. “Thermal energy storage technologies and systems for concentrating solar power plants”. In: *Progress in Energy and Combustion Science* 39.4 (2013), pp. 285–319.
- [22] G Glatzmaier. *Summary Report for Concentrating Solar Power Thermal Storage Workshop: New Concepts and Materials for Thermal Energy Storage and Heat-Transfer Fluids, May 20, 2011*. Tech. rep. National Renewable Energy Lab.(NREL), Golden, CO (United States), 2011.
- [23] Wang Fuqiang et al. “Progress in concentrated solar power technology with parabolic trough collector system: a comprehensive review”. In: *Renewable and Sustainable Energy Reviews* 79 (2017), pp. 1314–1328.
- [24] Davide Ferruzza et al. “Start-up performance of parabolic trough concentrating solar power plants”. In: *AIP Conference Proceedings*. Vol. 1850. 1. AIP Publishing. 2017, p. 160008.
- [25] Soteris A Kalogirou. “Solar thermal collectors and applications”. In: *Progress in energy and combustion science* 30.3 (2004), pp. 231–295.
- [26] JD Nixon, PK Dey, and PA Davies. “Which is the best solar thermal collection technology for electricity generation in north-west India? Evaluation of options using the analytical hierarchy process”. In: *Energy* 35.12 (2010), pp. 5230–5240.
- [27] Juan Ignacio Burgaleta, Santiago Arias, and Diego Ramirez. “GemSolar, the first tower thermosolar commercial plant with molten salt storage”. In: *Proceedings of the SolarPACES 2011 conference on concentrating solar power and chemical energy systems, Granada, Spain*. 2011.

- [28] Antonio L Avila-Marin. “Volumetric receivers in solar thermal power plants with central receiver system technology: a review”. In: *Solar energy* 85.5 (2011), pp. 891–910.
- [29] RapTech. *Ivanpah Solar Electric Generating System*. 2014. URL: <http://www.raptech.it/ivanpah-solar-electric-generating-system/>.
- [30] Cristina Sierra and Alfonso J Vazquez. “High solar energy concentration with a Fresnel lens”. In: *Journal of materials science* 40.6 (2005), pp. 1339–1343.
- [31] Edmund Optics. *Advantages of Fresnel lenses*. 2014. URL: <https://www.edmundoptics.com/resources/application-notes/optics/advantages-of-fresnel-lenses/>.
- [32] World Solar Thermal Electricity Association. *Ivanpah Solar Electric Generating System*. 2015. URL: <http://www.stelaworld.org/linear-fresnel-reflectors/>.
- [33] Najla El Gharbi et al. “A comparative study between parabolic trough collector and linear Fresnel reflector technologies”. In: *Energy Procedia* 6 (2011), pp. 565–572.
- [34] Onur Taylan and Halil Berberoglu. “Fuel Production Using Concentrated Solar Energy”. In: *Application of Solar Energy*. IntechOpen, 2013.
- [35] VK Jebasingh and GM Joselin Herbert. “A review of solar parabolic trough collector”. In: *Renewable and Sustainable Energy Reviews* 54 (2016), pp. 1085–1091.
- [36] D Kearney et al. “Status of the SEGS plants”. In: *1991 Solar World Congress*. Elsevier. 1992, pp. 545–550.
- [37] The Center for Land Use Interpretation. *Kramer Junction Solar Electric Generating Station, California*. 2005. URL: <http://clui.org/ludb/site/kramer-junction-solar-electric-generating-station>.
- [38] NS Suresh et al. “Methodology for sizing the solar field for parabolic trough technology with thermal storage and hybridization”. In: *Solar Energy* 110 (2014), pp. 247–259.
- [39] TE Boukelia et al. “Investigation of solar parabolic trough power plants with and without integrated TES (thermal energy storage) and FBS (fuel backup system) using thermic oil and solar salt”. In: *Energy* 88 (2015), pp. 292–303.
- [40] Cristina Prieto et al. “Advanced thermal energy storage research in demo plants for commercial systems”. PhD thesis. Universitat de Lleida, 2016.
- [41] Yuan Tian and Chang-Ying Zhao. “A review of solar collectors and thermal energy storage in solar thermal applications”. In: *Applied energy* 104 (2013), pp. 538–553.
- [42] Eduard Oró et al. “Comparative life cycle assessment of thermal energy storage systems for solar power plants”. In: *Renewable Energy* 44 (2012), pp. 166–173.

- [43] Antoni Gil et al. “State of the art on high temperature thermal energy storage for power generation. Part 1—Concepts, materials and modellization”. In: *Renewable and Sustainable Energy Reviews* 14.1 (2010), pp. 31–55.
- [44] Cristina Prieto et al. “Review of technology: Thermochemical energy storage for concentrated solar power plants”. In: *Renewable and Sustainable Energy Reviews* 60 (2016), pp. 909–929.
- [45] Flavio Manenti and Zohreh Ravaghi-Ardebili. “Dynamic simulation of concentrating solar power plant and two-tanks direct thermal energy storage”. In: *Energy* 55 (2013), pp. 89–97.
- [46] Flavio Manenti et al. “Assessing thermal energy storage technologies of concentrating solar plants for the direct coupling with chemical processes. The case of solar-driven biomass gasification”. In: *Energy* 75 (2014), pp. 45–52.
- [47] Zohreh Ravaghi-Ardebili et al. “Assessment of direct thermal energy storage technologies for concentrating solar power plants”. In: *CHEMICAL ENGINEERING* 35 (2013).
- [48] Gerard Peiró et al. “Influence of the heat transfer fluid in a CSP plant molten salts charging process”. In: *Renewable energy* 113 (2017), pp. 148–158.
- [49] Termofluids. *STEScodes and LTEScodes. Optimizing the design and performance*. 2015. URL: <http://www.termofluids.com/products/stes-ltes/>.
- [50] Peiwen Li et al. “Similarity and generalized analysis of efficiencies of thermal energy storage systems”. In: *Renewable Energy* 39.1 (2012), pp. 388–402.
- [51] KS Reddy et al. “Performance investigation of single-tank thermocline storage systems for CSP plants”. In: *Solar energy* 144 (2017), pp. 740–749.
- [52] Scott Flueckiger, Zhen Yang, and Suresh V Garimella. “An integrated thermal and mechanical investigation of molten-salt thermocline energy storage”. In: *Applied Energy* 88.6 (2011), pp. 2098–2105.
- [53] James E Pacheco, Steven K Showalter, and William J Kolb. “Development of a molten-salt thermocline thermal storage system for parabolic trough plants”. In: *Journal of solar energy engineering* 124.2 (2002), pp. 153–159.
- [54] Kody M Powell and Thomas F Edgar. “An adaptive-grid model for dynamic simulation of thermocline thermal energy storage systems”. In: *Energy conversion and management* 76 (2013), pp. 865–873.
- [55] E Zarza Moya. “Parabolic-trough concentrating solar power (CSP) systems”. In: *Concentrating Solar Power Technology*. Elsevier, 2012, pp. 197–239.
- [56] Gilles Flamant et al. “A new heat transfer fluid for concentrating solar systems: Particle flow in tubes”. In: *Energy Procedia* 49 (2014), pp. 617–626.
- [57] Eastman. *Therminol VP-1 Heat Transfer Fluid: technical data sheet*. 2015. URL: <https://emnmktassets.blob.core.windows.net/therminol/>.
- [58] Qiang Peng et al. “High-temperature thermal stability of molten salt materials”. In: *International Journal of Energy Research* 32.12 (2008), pp. 1164–1174.



- [59] Xiaolei Li et al. “Dynamic simulation of two-tank indirect thermal energy storage system with molten salt”. In: *Renewable Energy* 113 (2017), pp. 1311–1319.
- [60] D Kearney et al. “Evaluation of a molten salt heat transfer fluid in a parabolic trough solar field”. In: *ASME Solar 2002: International Solar Energy Conference*. American Society of Mechanical Engineers. 2002, pp. 293–299.
- [61] David Kearney et al. “Assessment of a molten salt heat transfer fluid in a parabolic trough solar field”. In: *Journal of solar energy engineering* 125.2 (2003), pp. 170–176.
- [62] Alexander Bonk et al. “Advanced heat transfer fluids for direct molten salt line-focusing CSP plants”. In: *Progress in Energy and Combustion Science* 67 (2018), pp. 69–87.
- [63] J Spelling et al. “A high-efficiency solar thermal power plant using a dense particle suspension as the heat transfer fluid”. In: *Energy Procedia* 69 (2015), pp. 1160–1170.
- [64] A d’Entremont et al. “Modeling of a thermal energy storage system based on coupled metal hydrides (magnesium iron–sodium alanate) for concentrating solar power plants”. In: *International Journal of Hydrogen Energy* 42.35 (2017), pp. 22518–22529.
- [65] Evangelos Bellos, Zafar Said, and Christos Tzivanidis. “The use of nanofluids in solar concentrating technologies: a comprehensive review”. In: *Journal of cleaner production* 196 (2018), pp. 84–99.
- [66] Andrey Yasinskiy et al. “Dramatically enhanced thermal properties for TiO<sub>2</sub>-based nanofluids for being used as heat transfer fluids in concentrating solar power plants”. In: *Renewable energy* 119 (2018), pp. 809–819.
- [67] Roberto Gómez-Villarejo et al. “Towards the improvement of the global efficiency of concentrating solar power plants by using Pt-based nanofluids: The internal molecular structure effect”. In: *Applied energy* 228 (2018), pp. 2262–2274.
- [68] Omar Behar et al. “A review of integrated solar combined cycle system (ISCCS) with a parabolic trough technology”. In: *Renewable and Sustainable Energy Reviews* 39 (2014), pp. 223–250.
- [69] A Maccari et al. “Archimede Solar Energy molten salt parabolic trough demo plant: a step ahead towards the new frontiers of CSP”. In: *Energy Procedia* 69 (2015), pp. 1643–1651.
- [70] T Hirsch and A Khenissi. “A systematic comparison on power block efficiencies for CSP plants with direct steam generation”. In: *Energy Procedia* 49 (2014), pp. 1165–1176.
- [71] Archimede Solar Energy. *Archimede Concentrating Solar Energy Plant in Priolo Gargallo*. 2015. URL: [http://www.archimedesolarenergy.it/reference\\_project\\_1.htm](http://www.archimedesolarenergy.it/reference_project_1.htm).

- [72] Mark Matzopoulos. “Dynamic process modeling: Combining models and experimental data to solve industrial problems”. In: *Process systems engineering* 7 (2011), pp. 1–33.
- [73] Francisco J. Da Silva. *Dynamic Process Simulation: When do we really need it?* 2015. URL: <http://processecology.com/articles/dynamic-process-simulation-when-do-we-really-need-it>.
- [74] Sergio Aquenza and L Ferraro. “Dynamic Simulation: a Tool for Advanced Design and Operating Behaviour Prediction”. In: *Chemical Engineering Transactions* 57 (2017), pp. 1015–1020.
- [75] George P Richardson, Alexander L Pugh, et al. *Introduction to system dynamics modeling with DYNAMO*. Vol. 48. MIT press Cambridge, MA, 1981.
- [76] William Luyben. *Plantwide dynamic simulators in chemical processing and control*. CRC Press, 2002.
- [77] GF List and HA List. *DYNSIM, a software package for computer-aided railroad equipment design projects*. Tech. rep. 1983.
- [78] Richard C Dorf and Robert H Bishop. *Modern control systems*. Pearson, 2011.
- [79] George Stephanopoulos. *Chemical process control: an introduction to theory and practice*. 1984.
- [80] Gene F Franklin et al. *Feedback control of dynamic systems*. Vol. 3. Addison-Wesley Reading, MA, 1994.
- [81] Haojie Xu et al. “Transient model and characteristics of parabolic-trough solar collectors: Molten salt vs. synthetic oil”. In: *Solar Energy* 182 (2019), pp. 182–193.
- [82] A Buscemi et al. “Concrete thermal energy storage for linear Fresnel collectors: Exploiting the South Mediterranean’s solar potential for agri-food processes”. In: *Energy Conversion and Management* 166 (2018), pp. 719–734.
- [83] Belen Munoz-Sanchez et al. “Rheology of Solar-Salt based nanofluids for concentrated solar power. Influence of the salt purity, nanoparticle concentration, temperature and rheometer geometry”. In: *Solar Energy Materials and Solar Cells* 176 (2018), pp. 357–373.
- [84] Elisa I Martin et al. “Unraveling the role of the base fluid arrangement in metal-nanofluids used to enhance heat transfer in concentrating solar power plants”. In: *Journal of Molecular Liquids* 252 (2018), pp. 271–278.